

ISTANBUL TECHNICAL UNIVERSITY ★ GRADUATE SCHOOL OF SCIENCE
ENGINEERING AND TECHNOLOGY

**AERODYNAMIC AND PERFORMANCE ANALYSIS OF HELICOPTER
ROTOR BLADE MORPHING CONCEPTS IN HOVER**



M.Sc. THESIS

Hüseyin URAL

Department of Aeronautical and Aerospace Engineering

Aeronautical and Aerospace Engineering Programme

MAY 2019

ISTANBUL TECHNICAL UNIVERSITY ★ GRADUATE SCHOOL OF SCIENCE
ENGINEERING AND TECHNOLOGY

**AERODYNAMIC AND PERFORMANCE ANALYSIS OF HELICOPTER
ROTOR BLADE MORPHING CONCEPTS IN HOVER**

M.Sc. THESIS

**Hüseyin URAL
(511161125)**

Department of Aeronautical and Aerospace Engineering

Aeronautical and Aerospace Engineering Programme

Thesis Advisor: Assist. Prof. Dr. Özge ÖZDEMİR

MAY 2019

ISTANBUL TEKNİK ÜNİVERSİTESİ ★ FEN BİLİMLERİ ENSTİTÜSÜ

**HELİKOPTER ŞEKİL DEĞİŞTİRME KONSEPTLERİNİN ASKIDA KALMA
UÇUSU SIRASINDA AERODİNAMİK VE PERFORMANS AÇISINDAN
İNCELENMESİ**

YÜKSEK LİSANS TEZİ

**Hüseyin URAL
(511161125)**

Uçak ve Uzay Mühendisliği Anabilim Dalı

Uçak ve Uzay Mühendisliği Programı

Tez Danışmanı: Assist. Prof. Dr. Özge ÖZDEMİR

MAYIS 2019

Hüseyin Ural, a M.Sc. student of İTÜ Graduate School of Science Engineering and Technology student ID 511161125, successfully defended the thesis/dissertation entitled “AERODYNAMIC AND PERFORMANCE ANALYSIS OF HELICOPTER ROTOR BLADE MORPHING CONCEPTS IN HOVER”, which he prepared after fulfilling the requirements specified in the associated legislations, before the jury whose signatures are below.

Thesis Advisor : **Dr. Özge ÖZDEMİR**
İstanbul Technical University

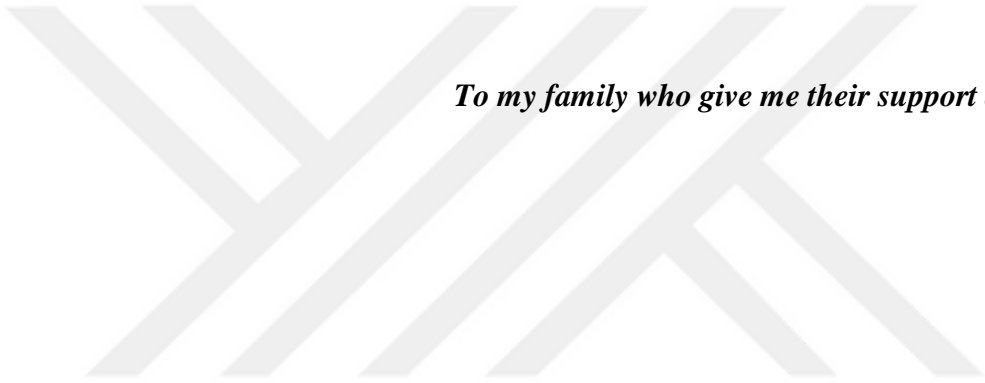
Jury Members : **Prof. Dr. Metin Orhan KAYA**
İstanbul Technical University

Assist. Prof Dr. Baha ZAFER
İstanbul University

Dr. Özge Özdemir
İstanbul Technical University

Date of Submission : 03 May 2019
Date of Defense : 12 June 2019





To my family who give me their support all the time



FOREWORD

This study is a thesis study of Department of Aeronautical and Aerospace Engineering, Aeronautical and Aerospace Engineering Programme. In this work, active twist and trailing edge flap systems are studied as an on blade actuation systems and aerodynamic and performance characteristics of these systems are examined.

I want to thank to my thesis advisor Assist. Prof. Dr. Özge Özdemir and TUSAŞ for all their support about this thesis. Finally I want to thank my family for their support for not only the time during my thesis but also my whole life.

May 2019

Hüseyin URAL

(Aircraft Engineer & Research Assistant)

TABLE OF CONTENTS

	<u>Page</u>
FOREWORD	ix
TABLE OF CONTENTS	xi
ABBREVIATIONS	xiii
LIST OF TABLES	xv
LIST OF FIGURES	xvii
SUMMARY	xix
ÖZET	xxi
1. INTRODUCTION	1
1.1 Hover Flight Aerodynamics	1
1.2 Morphing Concepts	3
1.2.1 Helicopter blade morphing	4
1.2.2 Trailing edge flaps	10
1.2.3 Active blade twist	13
1.3 Purpose and Road Map	15
2. AERODYNAMIC FORMULATIONS	17
2.1 Momentum Theory	17
2.1.1 Applying conservation laws	18
2.2 Blade Element Theory	20
2.3 Blade Element Momentum Theory	25
2.4 Prandtl Tip Loss Correction	28
3. AERODYNAMIC PERFORMANCE PARAMETERS	31
3.1 Geometry Effects	31
3.2 Blade Twist Characteristics	31
3.3 Blade Taper Characteristics	33
3.4 Flapped Blade Characteristics	36
4. NUMERICAL IMPLEMENTATION	41
4.1 Rotor Specifications	41
4.2 Look Up Table and Xfoil	41
4.2.1 Blade section airfoil polars	43
4.2.2 Cla calculation for more specificity	45
4.3 Matlab Code Structure	48
5. CONCLUSIONS AND RECOMMENDATIONS	51
5.1 Aerodynamic Properties of the Morphing Blade Concepts	51
5.1.1 Flapped blade aerodynamic results	51
5.1.1.1 One flap (tip)	51
5.1.1.2 One flap (middle)	53
5.1.1.3 One flap (root)	55
5.1.1.4 Two flap (tip, middle)	57
5.1.1.5 Two flap (middle, root)	59
5.1.1.6 Three flap (tip, middle, root)	61
5.1.1.7 Linear blade twist	63

5.2 Performance Properties of the Morphing Blade Concepts	66
5.2.1 Flapped blade results	66
5.2.2 Twisted blade performance results	67
5.3 Conclusions of Aerodynamic and Performance Calculations	69
5.4 Future Work.....	70
REFERENCES	71
CURRICULUM VITAE.....	73



ABBREVIATIONS

TE	: Trailing Edge
BET	: Blade Element Theory
BEMT	: Blade Element Momentum Theory
MT	: Momentum Theory
MIT	: Massachusetts Institute of Technology
HHC	: High harmonic Control
IBC	: Individual Blade Control
SABRE	: Shape Adaptive Blade for Rotorcraft Efficiency
SMART	: Smart Material Actuated Rotor Technology
AoA	: Angle of Attack
FM	: Figure of Merit
CFD	: Computational Fluid Dynamics



LIST OF TABLES

	<u>Page</u>
Table 4.1 : Rotor blade specifications.....	41
Table 5.1 : 1 Flap (Tip) with different flap deflection angles at 4 deg collective	52
Table 5.2 : 1 Flap (Tip) with different flap deflection angles at 10 deg collective ...	52
Table 5.3 : 1 Flap (Middle) with different flap deflection angles at 4 deg collective	54
Table 5.4 : 1 Flap (Middle) with different flap deflection angles at 10 deg collective	54
Table 5.5 : 1 Flap (Root) with different flap deflection angles at 4 deg collective ...	56
Table 5.6 : 1 Flap (Root) with different flap deflection angles at 10 deg collective .	56
Table 5.7 : 2 Flap (Tip, Middle) with different flap deflection angles at 4 deg collective.....	58
Table 5.8 : 2 Flap (Tip, Middle) with different flap deflection angles at 10 deg collective.....	58
Table 5.9 : 2 Flap (Middle, Root) with different flap deflection angles at 4 deg collective.....	60
Table 5.10 : 2 Flap (Middle, Root) with different flap deflection angles at 10 deg collective.....	60
Table 5.11 : 2 Flap (Tip, Middle, Root) with different flap deflection angles at 4 deg collective.....	62
Table 5.12 : 2 Flap (Tip, Middle, Root) with different flap deflection angles at 10 deg collective	62
Table 5.13 : Lineer twist with different twist rate values at 4 deg collective	64
Table 5.14 : Lineer twist with different twist rate values at 10 deg collective.....	65
Table 5.15 : Same Disk Loading with Different Flap Concepsts Performance Comparison.....	66
Table 5.16 : Same Disk Loading with Different Twist Ratios Performance Comparison.....	68



LIST OF FIGURES

	<u>Page</u>
Figure 1.1 : Complications over the helicopter rotor (Krishnan, 2017)	1
Figure 1.2 : Hover flight overview (Leishman, 2006)	2
Figure 1.3 : Rotor blade angles (Johnson, 1994)	3
Figure 1.4 : Why we need morphing systems? Answer chart (Weisshaar, 2013)	4
Figure 1.5 : Helicopter blade all morphing approaches (Miller & Narkiewicz, n.d) ..	5
Figure 1.6 : Swashplate system representation	6
Figure 1.7 : Cyclic pitch control of the swashplate	7
Figure 1.8 : Rotor system that represents viable morphing concepts (Rauleder et al, 2018)	8
Figure 1.9 : Swashplateless rotor system concept (Miller & Narkiewicz, n.d)	9
Figure 1.10 : Helicopter performance enhancement and vibration reduction concepts	10
Figure 1.11 : Trailing edge flaps of Karman Helicopter	11
Figure 1.12 : Whirl tower test of trailing edge flap system	12
Figure 1.13 : Trailing edge flap with piezostack actuators for model rotor blades ...	13
Figure 1.14 : Piezoceramic crystal orientation on the blade	14
Figure 1.15 : Piezoelectric actuated active twist rotor blade	14
Figure 2.1 : Flow velocity gradient over rotor disk (Leishmann, 2006)	18
Figure 2.2 : Top view of the blade element (Leishman, 2006)	21
Figure 2.3 : Side view of the blade element (Leishman, 2006)	22
Figure 2.4 : Top view of the rotor annulus (Leishman, 2006)	26
Figure 2.5 : Side view of the rotor annulus (Leishman, 2006)	27
Figure 2.6 : Lift distribution over the blade with and without tip loss (Leishman, 2006)	29
Figure 2.7 : Sectional thrust gradient value with and without tip loss (Leishman, 2006)	30
Figure 3.1 : Ideally twisted blade and linear approximation over the r	32
Figure 3.2 : Local inflow characteristics with the change of blade twist	33
Figure 3.3 : Optimum and linear taper over the rotor blade (Johnson, 1994; Leishman, 2006)	36
Figure 3.4 : Effect of plan flap to airfoil polars (Anderson, 2009)	37
Figure 3.5 : Sectional flap effectiveness with different range of flap deflections	38
Figure 3.6 : Flap effectiveness due to flap cord divided by blade cord (Abbot & Doenhoff, 1958)	39
Figure 3.7 : 15 deg deflected 20% cord flapped blade Naca 0012 Xfoil	40
Figure 3.8 : Vectorial Cp values of 20% flapped blade at 10 degree collective	40
Figure 4.1 : Xfoil Naca 0012 at Re = 400000	42
Figure 4.2 : Xfoil Naca 0012 at Re = 400000, pressure coefficient vectors	42
Figure 4.3 : Rotor blade that divided 6 sections	44
Figure 4.4 : Polar values of 1. and 7. sections	44
Figure 4.5 : Lift distribution over the rotor blade using BET calculation	45

Figure 4.6 : Sectional polar values for all sections	46
Figure 4.7 : Different Cla values for different pitch angles at a specific section.....	47
Figure 4.8 : The drag polars for all the section	48
Figure 4.9 : Matlab Code Flow Chart.....	49
Figure 5.1 : 1 Flap (Tip) deflection Effect on Sectional Thrust.....	51
Figure 5.2 : 1 Flap (Tip) deflection Effect on Sectional Thrust 0-10 deg deflection	52
Figure 5.3 : 1 Flap (Tip) Deflection Effect on Sectional Induced Inflow Ratio	53
Figure 5.4 : 1 Flap (Middle) deflection Effect on Sectional Thrust	53
Figure 5.5 : 1 Flap (Middle) deflection Effect on Sectional Thrust 0-10 deg flap deflection.....	54
Figure 5.6 : 1 Flap (Middle) deflection Effect on Sectional Inflow Ratio	55
Figure 5.7 : 1 Flap (Root) deflection Effect on Sectional Thrust	55
Figure 5.8 : 1 Flap (Root) deflection Effect on Sectional Thrust 0-10 deg flap deflection.....	56
Figure 5.9 : 1 Flap (Root) deflection Effect on Sectional Inflow Ratio	57
Figure 5.10 : 2 Flap (Tip, Middle) deflection Effect on Sectional Thrust.....	57
Figure 5.11 : 2 Flap (Tip, Middle) deflection Effect on Sectional Thrust 0-10 deg flap deflection.....	58
Figure 5.12 : 2 Flap (Tip, Middle) deflection Effect on Sectional Inflow Ratio	59
Figure 5.13 : 2 Flap (Middle, Root) deflection Effect on Sectional Thrust.....	59
Figure 5.14 : 2 Flap (Middle, Root) deflection Effect on Sectional Thrust 0-10 deg flap deflection.....	60
Figure 5.15 : 2 Flap (Middle, Root) deflection Effect on Sectional Inflow Ratio	61
Figure 5.16 : 3 Flap (Tip, Middle, Root) deflection Effect on Sectional Thrust	61
Figure 5.17 : 2 Flap (Tip, Middle, Root) deflection Effect on Sectional Thrust 0-10 deg flap deflection	62
Figure 5.18 : 3 Flap (Tip, Middle, Root) deflection Effect on Sectional Inflow Ratio	63
Figure 5.19 : Lineer Twist Effect on Sectional Thrust at 4deg Collective	63
Figure 5.20 : Lineer Twist Effect on Sectional Thrust at 10deg Collective	64
Figure 5.21 : Lineer Twist Effect on Sectional Inflow Ratio at 10deg Collective....	65
Figure 5.22 : Same Disk Loading with Different Flap Concepsts Thrust Variation.	66
Figure 5.23 : Same Disk Loading with Different Flap Concepts Inflow Variations	67
Figure 5.24 : Same Disk Loading with Different Twist Ratio.....	67
Figure 5.25 : Same Disk Loading with Different Twist Ratios Inflow Variations ...	68

AERODYNAMIC AND PERFORMANCE ANALYSIS OF HELICOPTER ROTOR BLADE MORPHING CONCEPTS IN HOVER

SUMMARY

Helicopter has a very complicated aerodynamic environment. Because, it creates lift, thrust in the forward flight and control inputs via only rotor system. This high demand from rotor system makes the aerodynamic environment of the helicopter quite complicated. Generally this complications effects the aerodynamic performane of helicopter, lead to produce vibrations and high noise levels. This type of problems can be solve at least partiall by producing the helicopter blade specific to that flight environment. However, if the flight conditions cahenge during the flight, moderate design can not help us, because a design of the vehicle can not be done to satisfy two contradicting condition. Morphing systems are thought that they can help us to solve this type of problems. Mainly, morphing blade means that blade shape is changed to be optimum at different flight conditions. Of course to know this type optimum conditions firsts, we need to know the more optimised conditions that can be reached with morphing systems like in hover. If we specifically examine the conditions like this, after that we got a database that includes the answer of which type of blade shape that is transitivised by morphing system is more optimum for that solution. Furthermore, the optimum condition is needed to know because, morphing system tries to change the blade to make it more optimum.

There are numerous morphing concepts but active blade twist and TE flap concepts are the concepts that are investigated in this thesis in aerodynamics and performance perspectives.

The main focus of this thesis is to develop a computer code that can calcuates the rotor blade aerodynamic properties and performance parameters. Blade twist and airfiol shape can effect the rotor aerodynamics and performance. Airfoil shape change can be applied to the rotor with trailing edge flap system. In the thesis blade twist and TE flap effects on the helicopter aerodynamics and performance are examined using the MATLAB code that is written originally.

The rotor blade that specifically examimed in the thesis is the blade that is used in the rotor hover performance testing in our Rotorcraft Technology Laboratory.

The code was written using BET and BEMT. Blade sectional induced inflow ratio is found using BEMT. The sectional thrust and power values found using BET. In the BET calculations every section is assumed to have no mutual effects. Thus, every section of the blade are calculated discretely. Of course, through the tip portion this assumptions does not work because of the tip vortices. To model tip vortices effects on the blade, Prandtl's correction factor used. At the end, BET needs 2-D aerodynamics of the bladde sections. At this point Xfoil programme that is created by Mark Dreala from MIT is used to calculate the 2-D viscous blade polars. These values are found using every blades corresponding Re numbers. From these values look up

table is created in excel file. While calculation of every blade section code opens the specific page of the excel an inport the values into the matlab to carry on the calculations.



HELİKOPTER ŞEKİL DEĞİŞTİRME KONSEPTLERİNİN ASKIDA KALMA UÇUŞU SIRASINDA AERODİNAMİK VE PERFORMANS AÇISINDAN İNCELENMESİ

ÖZET

Helikopter hem ileri uçuş hem de dikey kalkış ve iniş yapması bakımından kendine has bir kullanım alanı sunar. Ancak hem dikey kalkış hem ileri uçuş yapması gerekmesi nedeni ile, aerodinamik ve dinamik olarak bir hayli karmaşık bir yapıya sahip olmaktadır. Bu karmaşık aerodinamik yapı özellikle helicopter rotorunun dönüşünden kaynaklanmaktadır. Helikopter rotoru aracın ileri uçuk hızına gerek kalmadan taşıma yaratabilmesi için dönüş hareketi yapmaktadır. Ancak tek görevi bu da değildir. Helikopter rotoru sabit kanatlı uçakların ayrı ayrı sistemlerle gerçekleştirdiği uçuş sırasındaki gereklilikleri rotor yapısı ile gerçekleştirmektedir. Bu gereklilikler ise taşıma oluşturma, ileri uçuş sırasında itki üretme ve pilot kontrolleridir. Bu üç gerekliliği aynı anda gerçekleştirmek rotor üzerinde bir hayli karmaşık bir aerodinamik yapı oluşmasını sağlar. Bu karmaşık aerodinamik yapı helicopter aerodinamiği, performansı ve kontrolü üzerinde büyük etkiye sahiptir.

Bu karmaşık aerodinamik yapı neticesinde helicopter pallerinin control edilmesi ve daha efektif çalışması önemli bir unsur olmaktadır. Aslında belli bir tasarım koşuluna göre nasıl daha efektif bir pal geometrisi tasarlanacağı matematiksel olarak gösterilmekte ve uygulanmaktadır. Bu tasarımlar pala geometrisi üzerinde burulma ve TAPER, kanat profili üzerinde de firar kenarı flabı pala geometrisini daha efektif hale getirecek konseptlerdir. Helikopter rotorunun hangi konseptler kullanıldığında hangi uçuş şartlarında nasıl tepkiler verdiği ve elde edilen performanslar araştırılmalıdır. Çünkü, farklı uçuş koşullarında bu performansların bilinmesi demek helikopterin uçuşu sırasında pal şeklinin nasıl değişmesi gerekeceğinin öngörülmesi anlamına gelmektedir.

Şekil değiştiren pala konseptleri günümüzde değişen uçuş şartlarında helicopter palinin daha iyi adapte olmasını ve uçuş boyunca daha optimum performansa yakın şekilde çalışmasını sağlamaya yöneliktir.

Bu sistemler genel anlamıyla kontrol yöntemleri adı altında incelersek. Kontrol yöntemleri yüksek harmonic kontrol (HHC) ve tekil pala kontrolü (IBC) olmak üzere 2 ye ayrılabilir. HHC sistemi tüm swashplate'in yukarı aşağı hareket ederek tüm pallere aynı anda etkimesi şeklinde kullanılan bir yöntemdir. IBC ise her palin kendi içinde ayrı ayrı control girdileri ile kontrol edilmesi mantığına dayanır. Standart kullanımında kontrol çubuklarına uygulanan kontrol girdileri ile çalışan bir sistemdir. Ancak akıllı malzemelerin de kullanımı ile IBC sistemine aktif burulma ve aktif kaçış kenarı flabı olmak üzere iki farklı control yöntemi daha eklenmiştir.

Aktif yöntemlerin kullanılması sonucu hover uçuşu sırasında elde edilecek olan performans artışı etkisini görmek için aerodinamik modelleme yapılmıştır. Bu modelleme yapılırken momentum teorisini, pala elemanı teorisini, pala elemanı momentum teorisini kullanılmıştır. Pala elemanı teorisinde palanın her bir kanat kesiti ayrı ayrı ve birbirine etkisi yokmuş gibi kabul edilerek modellenir. Sonuç olarak her pala kesitinin tek tek itki ve güç değerleri elde edilebilir. Bu hesaplar yapılırken 2 boyutlu kesitin etkin hücum açısı değerini bulmak önem taşır. Etkin hücum açısı değeri palanın kesitinin geometric hücum açısından indüklenmiş içakış açısının çıkarılması ile oluşur. Helikopter rotoru çalışırken üstündeki havayı alıp rotor diskinden geçirerek aşağı doğru atar bu nedenle de bir indüklenmiş akış oluşur. Bu akış palın etkin hücum açısının azalması yönünde bir sonuç doğurur. Burada iç akışın hesaplanması pala elemanı teorisini için büyük önem taşımaktadır. Bu hesaplar ise radial olarak pala elemanı momentum teorisini ile yapılır. Her pala kesiti için açılar tek tek bulunur. Bu açılar pala kesitinin aerodinamik katsayılarının bulunması için önem taşır. Katsayılar bulunduktan sonra pala geometrisi de belli ise hesaplar yapılabilir.

Pala elemanı teorisini kullanabilmek için helicopter palasını bellisayıda elemana bölmek ve her elemanın geometrik ve aerodinamik özellikleri kullanılarak hesaplama yapılmalıdır. Geometrik özellikler yapılan hesaplarda girdi olarak verileceğinden bizim için önemli olan nokta incelenen pala kesitinin taşıma ve sürüklenme katsayıları ile indüklenmiş hız hesabı için taşıma eğrisi eğiminin bilinmesidir. Hesapları basitleştirmek adına taşıma katsayısı direk olarak hücum açısı ile taşıma eğrisi eğimi çarpımı şeklinde elde edilebilir. Bu hesabı yapmak için önceden bir taşıma eğrisi eğimi belirlemek gereklidir. Ayrıca sürüklenme için ise tüm pala için yaklaşık sabit bir değer alınabilir. Bu şekilde yapılan hesaplar pala üzerindeki aerodinamik etkileri genel çerçevede halinde verebilir.

Ancak, biz daha iyi ve gerçeğe yakın sonuçlar istiyoruz. Bunun için öncelikle pala elemanı teorisinin 2 boyutlu hesabından kaynaklanan bir hata giderilmelidir. Bu hata pala ucuna doğru kendini gösteren ve girdap etkisi ile pal ucundaki taşıma değerini ani şekilde sıfıra götüren kanat ucu kayıplarıdır. Bu 3 boyutun etkisidir ve hesaplara bir düzeltme faktörü yardımı ile eklenir. Bu faktöre Prandtl düzeltme faktörü denir. Bu faktörün kullanılmasının yanında hesapları daha fazla gerçeğe yaklaştırmak için 2 boyutlu aerodinamik katsayıların daha yüksek doğruluk payında bulunması gereklidir. Bunun için öncelikle indüklenmiş akış hesabında kullanılan taşıma eğrisi eğiminin her pala elemanı için ayrıca her elemanın farklı geometric hücum açıları için bulunmalıdır. Her pala elemanı için aerodinamik ortam farklı Re sayılarına sahip oldukları için C_L her eleman için değişiklik gösterecektir. Ayrıca düşük Re da taşıma eğrisi eğimi 4-5 dereceden sonra değişkenlik gösterir. Bu farklılık nedeni ile aynı pala elemanı içinde sabit bir C_L kabul etmek yerine bunu geometric hücum açısı ile bu hücum açısının denk geldiği C_L değerinin karşılık geldiği nokta ile sıfır taşıma noktası arasındaki eğim olarak almak hesaplamalarda daha yüksek bir hassasiyete ulaşmamızı sağlayacaktır.

Yukarıda bahsedilen hesapları yapabilmek için her pala elemanı için C_L ve C_D nin hücum açısı ile değişimi bilinmelidir. Bunun için 2 boyutlu kanat profile çözücüsü olan Xfoil programı kullanılmış ve her pala elemanı için o elemanın taşıma kaybı yaşadığı noktayı birkaç derece geçene kadar 0.5'er derecelik artımlarla katsayı değerleri bulunmuştur. Burada taşıma kaybından sonra hesapları yapmamamızın nedeni elde edilen verilere polinom uydururken polinomun yeterli doğrulukta elde edilememesidir. Buna taşıma kaybı sonrası kanat profili karakteristiğinin ani şekilde

değişmesi neden olur. Bu şekilde her pala elemanı için bir excel sayfasına veriler yazılmıştır.

Aerodinamik modelleme aşamasında teorik kısımdan sonra hesaplamaların yapılması için MATLAB programı kullanılmıştır. Program girdileri arasında ortam şartları, palanın geometrik verileri ve önceden hazırlanmış excel verileri vardır. Program her pala elemanı için köke en yakın noktadan başlar ve uca kadar tek tek her eleman için itki, güç ve bunların katsayı değerlerini bulur. Her eleman için bu değerler 2 boyuttadır. Bulunan değerleri 3 boyuta taşımak için her bir eleman üzerinde bulunan değer eleman açıklığıyla çarpılır.

Kullanılan kodda standart dikdörtgen pal, ideal ve lineer burulmalı pal ve özellikleri değiştirilebilir şekilde flap yöntemleri modellenenmektedir. Bu şekilde farklı aktif yöntemlerin pal aerodinamiği ve performansı üzerinde nasıl bir etkiye sahip olduğu elde edilebilir.

Helikopter pallerinin performans değerlendirilmesi verim ölçüsü (FM) değerlerinin eşit disk yüklemesinde ($\frac{C_T}{\sigma}$) karşılaştırılması sonucu elde edilebilir. Eşit disk yüklemesine sahip rotorlar arasında verim ölçüsü değeri yüksek olan pala geometrisi daha efektiftir. Yapılan hesaplamalarda burulmasız pala, lineer burulmalı pala ve ideal burulmalı pala ile aktif flap konseptli palalar için verim ölçüsü değerleri hesaplanmış ve sonuçlar değerlendirilmiştir.



1. INTRODUCTION

1.1 Hover Flight Aerodynamics

Numerous aerodynamic problems occur at helicopter rotor. These problems need to be understood deeply to develop solid comprehension about helicopter. There are some approaches about aerodynamic problems which are analytic theories, numerical modeling and experimentation. These three approaches go hand in hand to examine and understand the helicopter aerodynamics. What makes the helicopter rotor quite complicated is that it requires to provide all three aircraft functions which are separated in fixed wing aircrafts. These complications create numerous aerodynamic problems (see Figure 1.1) over the helicopter rotor.

These 3 functions that an aircraft needs to perform, vertical lift force to counter the weight, propulsive force to move forward and control the attitude and position of the aircraft in three dimensions. Unlike the fixed wing aircraft, helicopter rotor needs to provide these three functions altogether only with a rotor system. Thus, the control of these functions can not be separated from each other.

3

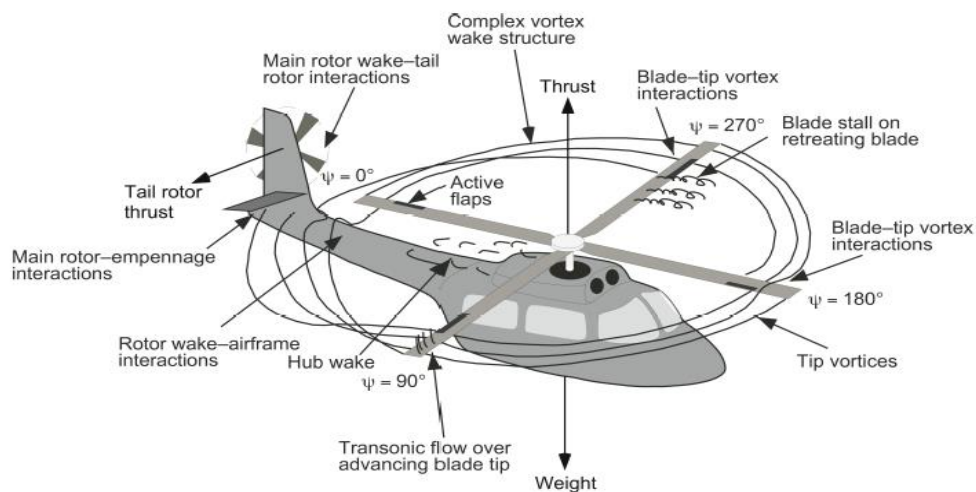


Figure 1.1 : Complications over the helicopter rotor (Krishnan, 2017)

The helicopter rotor rotates to provide thrust force, which means that all sections of the blade has same angular velocity and different linear velocity. Linear velocity of each section equals to radial distance of the section from root of the blade times angular velocity. This creates a linear varying linear velocity distribution over the blade (see Figure 1.2). This all means that lifting capability of a blade is related to local parameters like local AoA and local dynamic pressure.

Azimuth angle defines the position of blades over the rotor disc. In hovering flight it has no effect on the blade speed.

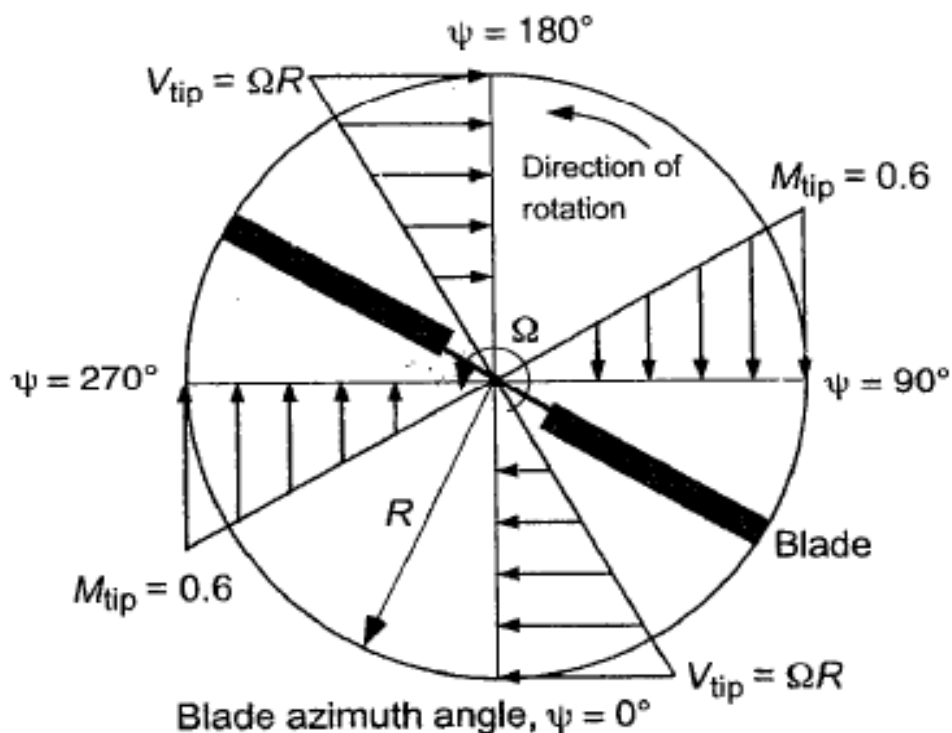


Figure 1.2 : Hover flight overview(Leishman, 2006)

The blade motion and the angles of rotations are important to know. Because we are dealing with the blade twist in this thesis, pitch angle and its variation over the blade is especially important. The Figure 1.3 shows all three degrees of freedom of a rotor blade. Those are flap(β), lag(ζ), and pitch(θ) angles (Johnson, 1994).

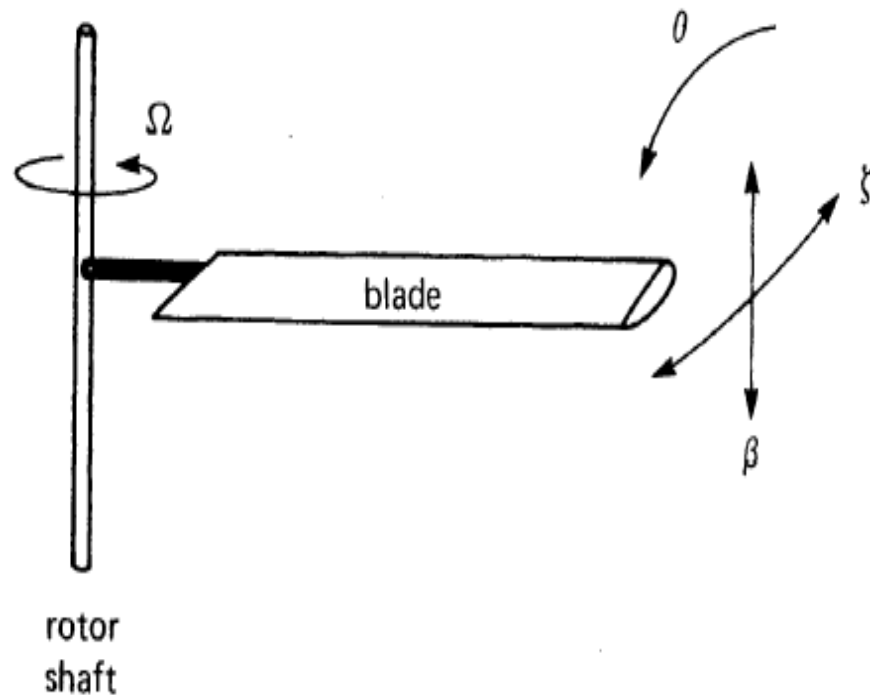


Figure 1.3 : Rotor blade angles (Johnson, 1994)

1.2 Morphing Concepts

Morphing means for an aircraft or any other vehicle that changing the geometrical shape to adapt the environment that differs through operation. For aviation perspectives, fixed wing aircrafts and helicopters can have a lot of benefit this type of shape shifting. There are 2 reason for applying the morphing on an air vehicle. Those are to adapt both high and low speed flight conditions and to be able to control the flight in different conditions (Weisshaar, 2013).

Efficient, adaptive and multipoint words came to mind when defining the morphing concepts.

To simplify the mechanical system, reduce the weight and make the aircraft more energy efficient means that efficiency. To be able to meet the requirements of contradictory environment means multipoint. Adaptability means that in the case of the use of the aircraft in unpalanned manner morphing system provides flexibility and adjustibility.

The real question is that why do we need a morphing system? There are three main reasons for morphing (see Figure 1.4). Multi-ability, evolution and survivability.

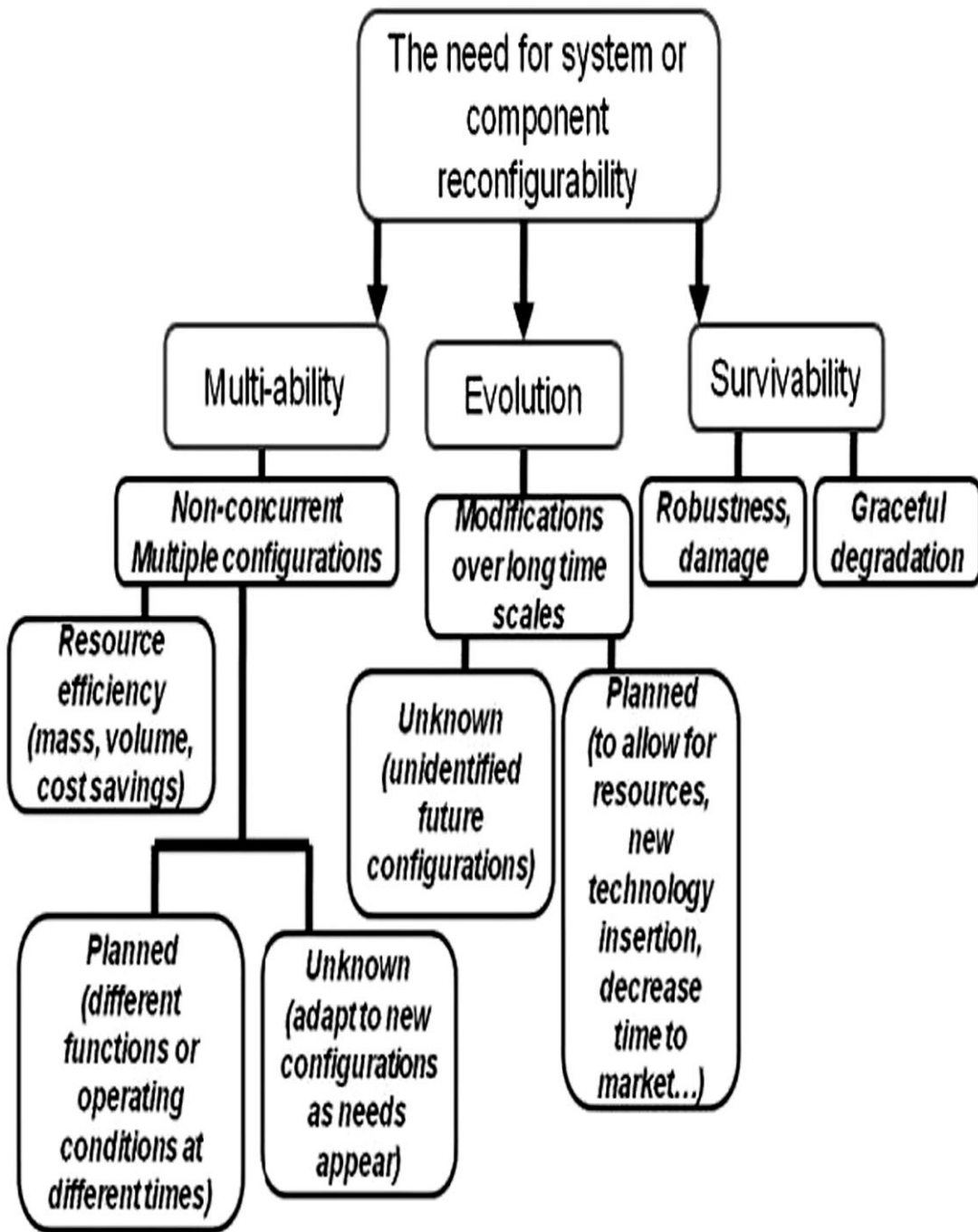


Figure 1.4 : Why we need morphing systems? Answer chart (Weisshaar, 2013)

1.2.1 Helicopter blade morphing

Helicopter has somewhat more complex aerodynamic environment than fixed wing aircraft. Thus, to conserve the stable flight condition for helicopter is challenging. Although the most simple flight condition is hover, rotor faced with the velocity difference through the radial direction. In forward flight, there is an azimuth effect as well.

There are numerous concepts that can change the rotor behaviour. These concepts are described in the Figure 1.5.

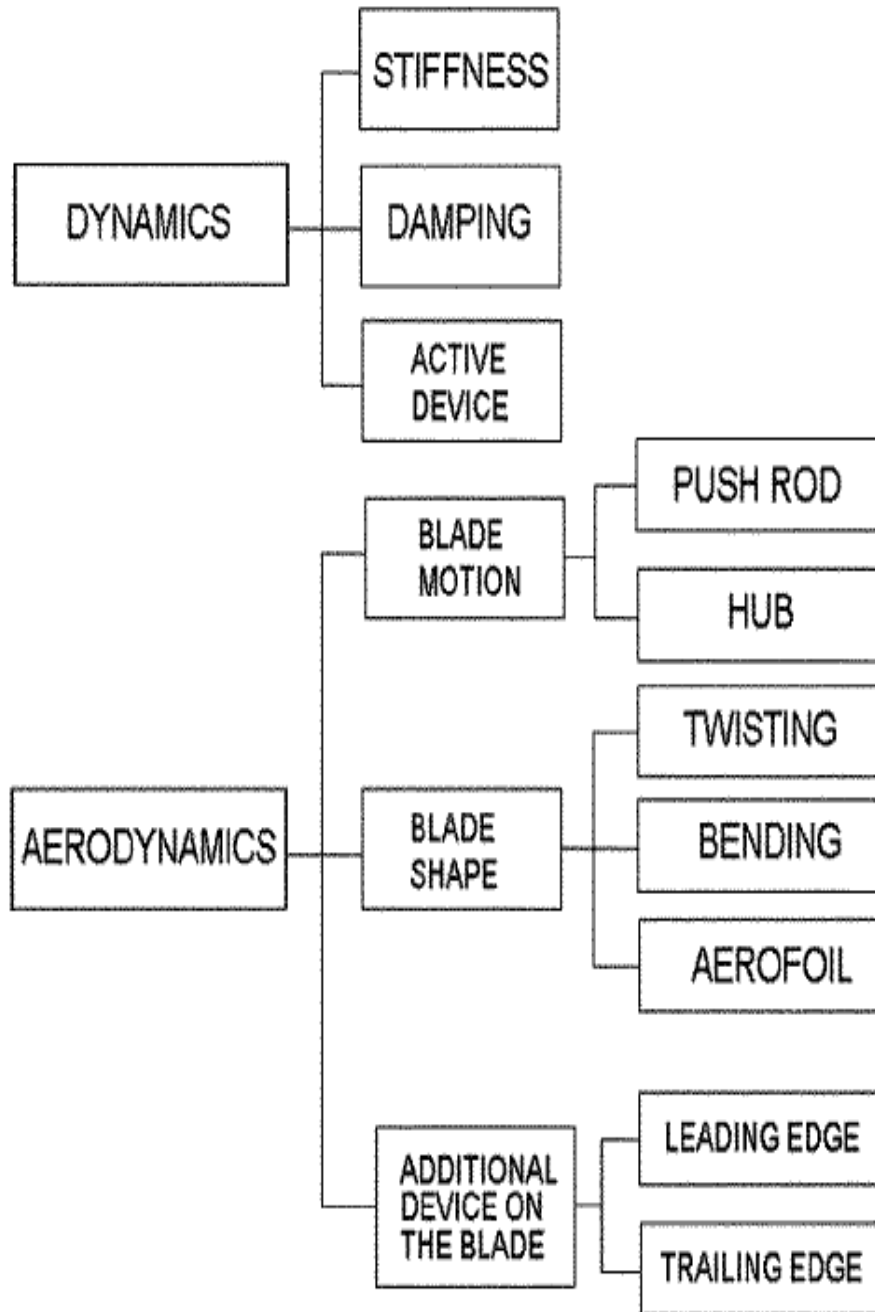


Figure 1.5 : Helicopter blade all morphing approaches (Miller & Narkiewicz, n.d)

To control the helicopter the classical approach is to use swashplate system. This system control the blades azimuthally by changing blade pitch through the rotor disk but it is not the optimum one. Also, fix geometry of blade is not an optimal approach

because the optimal geometry requirement for blade are changing with the different environment. Vibration is another issue about helicopter blades. Increased asymmetrical loading over over the rotor disk and blade tip shocks are two of the many reasons of blade vibration. The helicopter swashplate system is shown in the Figure 1.6.

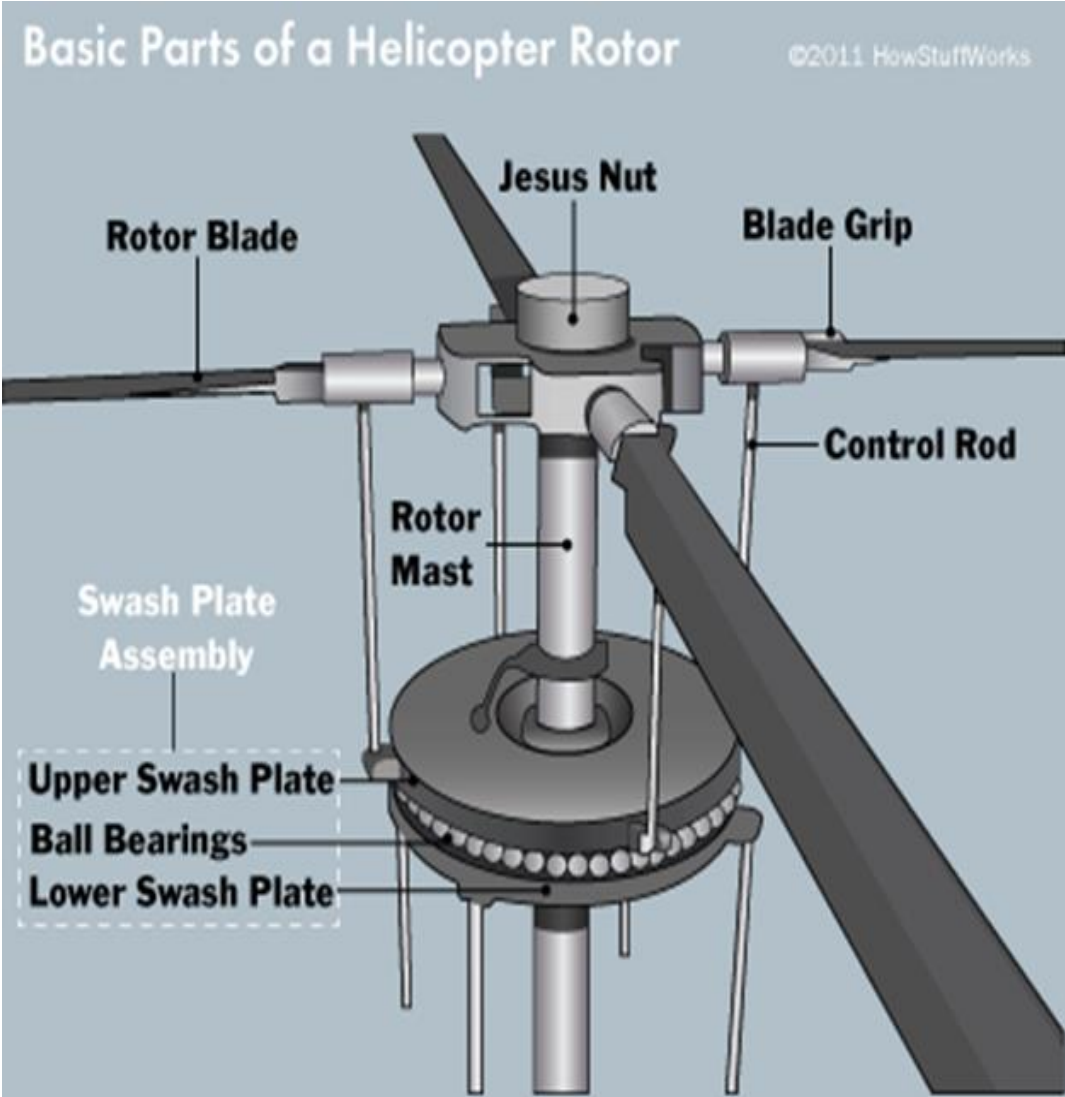


Figure 1.6 : Swashplate system representation

Swashplate system is capable of giving the blade collective and cyclic pitch inputs. Swashplate has control rods that connects to the rotor root to give control inputs. When swashplate is up then all the blade pitch angles are increases. This situation means collective pitch input. The cyclic input is given to the system when swashplate is tilted which creates different pitch angle azimuthally over the rotor disk. The cyclic pitch case is shown in the Figure 1.7.

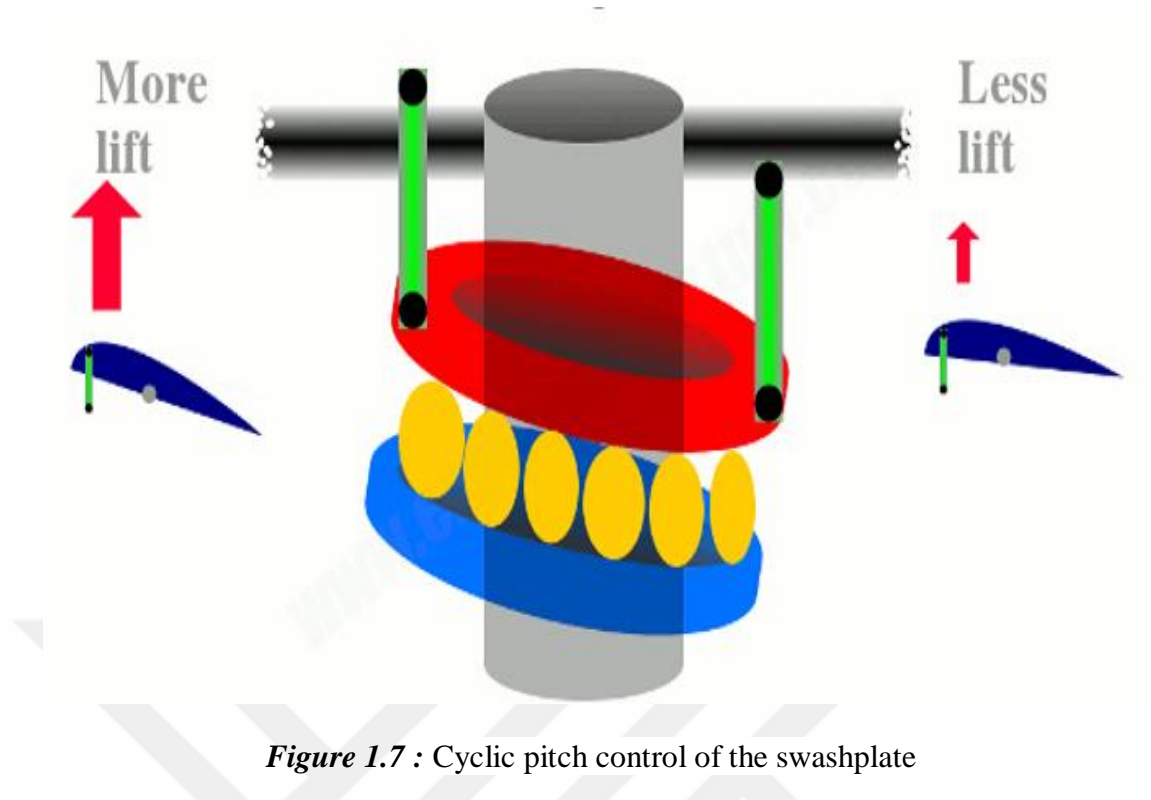


Figure 1.7 : Cyclic pitch control of the swashplate

However, swashplate can not control blade radially and can not control the blade geometry also it creates drag force in the flight. Morphing systems are thought as a replacement or at least mechanism that enhance the performance of the rotor.

There are two possible ways to make blades more adaptive when the time dependency is our concern. . Those are quasi-static and dynamic control. Quasi-static means function of flight condition. Dynamic adaptive is about the azimuth angle. There is a direct planform change for quasi static condition like twist, chord, chamber and span of the blades. Dynamic adaptation has $N-1$, N , $N+1/\text{rev}$ inputs into the rotor system. This type of control is done by HHC or IBC systems. In the thesis we are dealing with the quasi-static morphing. This means that for different flight conditions, morphing system tries to make rotor blade geometry optimum.

A concept multi morph helicopter is shown in the Figure 1.8. Morphing concept that are shown on the helicopter is assessed in the Project called SABRE - Shape Adaptive Blades for Rotorcraft Efficiency (Rauleder et al, 2018).

When it is about the optimise the flight properties, reducing the noise and vibration levels, active control systems seems most promising rotor control application. The most common use of the active control systems is as an actuator. They can be put on the blade to change geometry or pitch angles (Wilbur et al, 2018).

Active control systems include HHC, IBC and smart rotor blade systems. High harmonic control (HHC) is about giving higher than 1/rev inputs for changing collective blade pitch angle. Individual blade control (IBC) system works like HHC with one main difference. In IBC every blade can be given different input. Lastly, smart rotor systems use smart materials to produce blade control inputs or adapting the blade shape according to current flight conditions. The difference of smart rotors is that they do not need a swashplate system to control the blade. They have their actuators on the blade (Miller & Narkiewicz, n.d).

Active TE flap and twist concepts are the most studied morphing concepts for helicopter rotors (see Figure 1.9, Figure 1.10). Both two tries to redistribute the induced inflow over the blade to make performance enhancement or vibration reduction.



Figure 1.8 : Rotor system that represents viable morphing concepts (Rauleder et al, 2018)

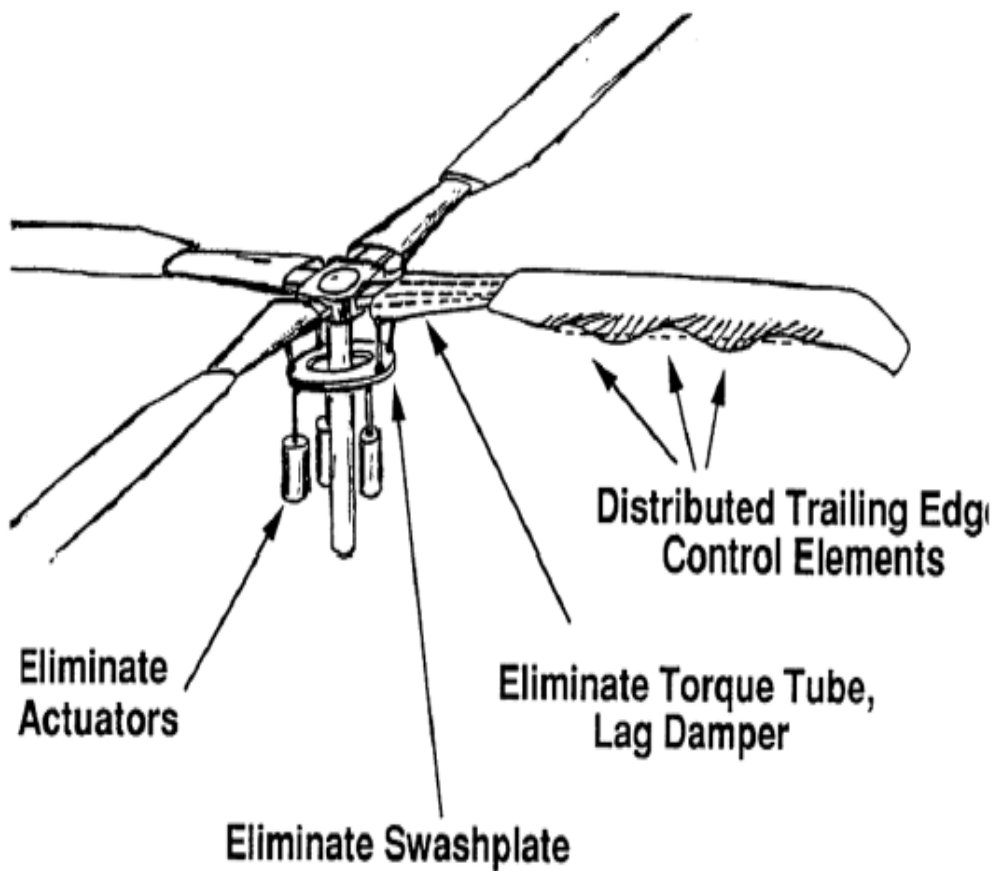
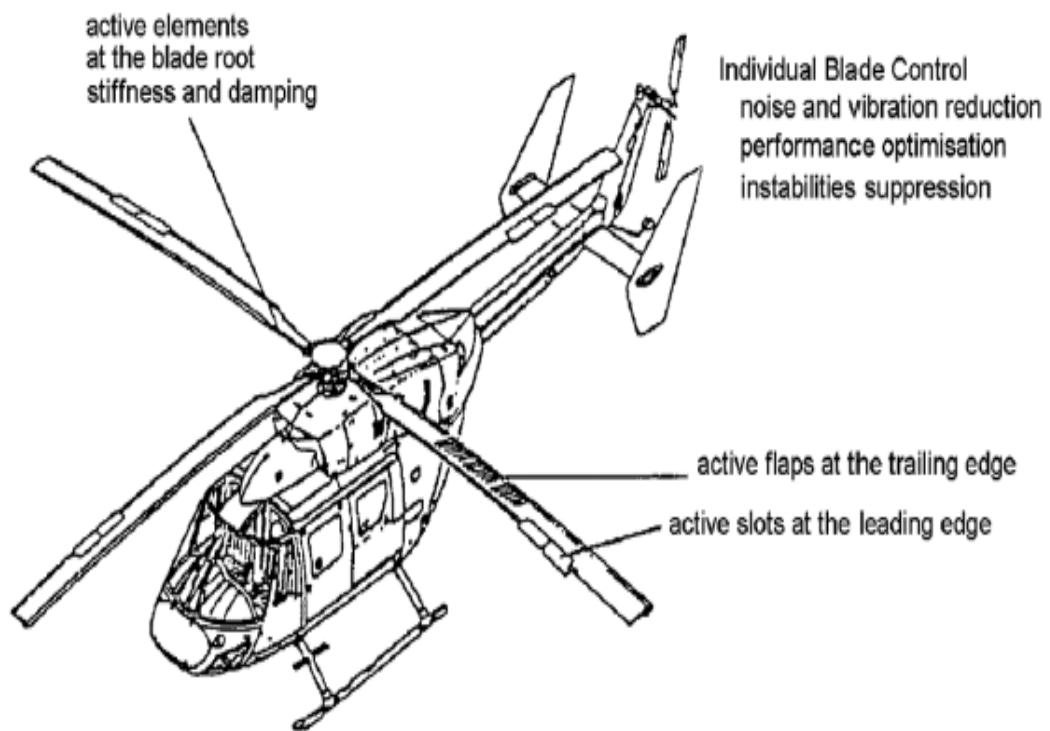


Figure 1.9 : Swashplateless rotor system concept (Miller & Narkiewicz, n.d)

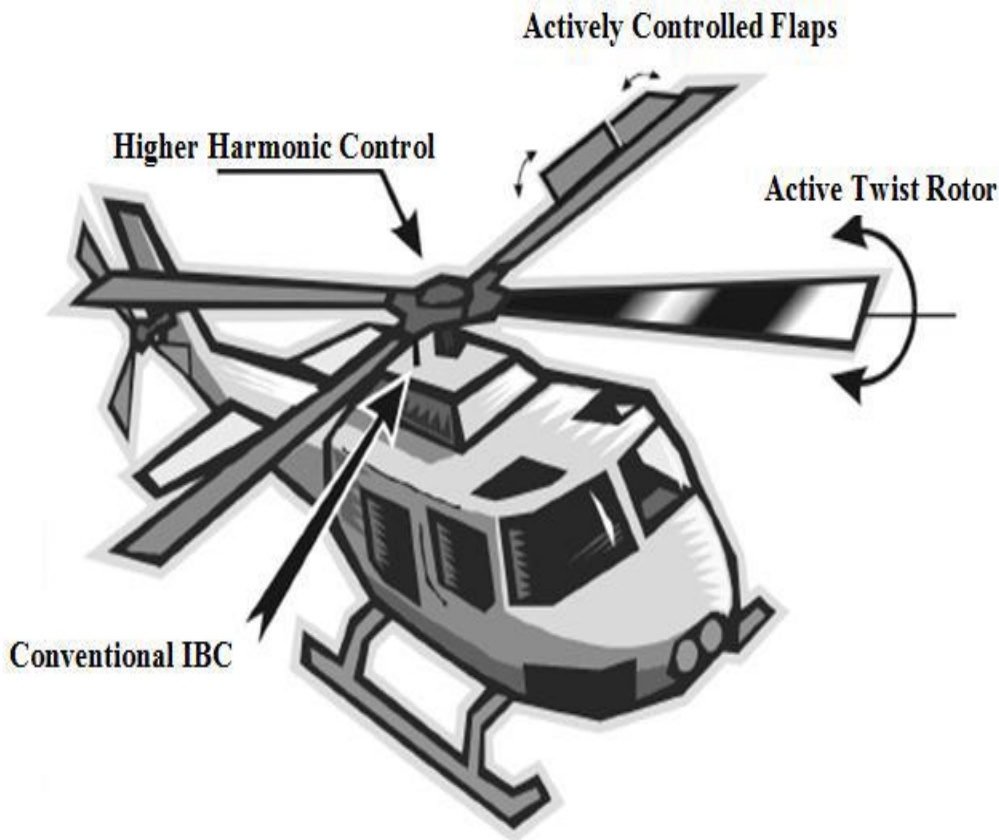


Figure 1.10 : Helicopter performance enhancement and vibration reduction concepts

1.2.2 Trailing edge flaps

Helicopter blade morphing has a long history beginning with the prototype Kaman K-125 helicopter in 1947. The K-125 used servo flaps. As shown in the Figure 1.11. There are relatively big flaps near the 75% chord can be seen easily. However, servo flaps have some drawbacks which are drag produced by the system components. State of art helicopter trailing edge flap designs are focusing on the plain flap systems. There are studies about the vibration reduction and performance enhancement (Wilbur et al, 2018)

Plain flap is the one that is used in helicopter rotor as a morphing concept. In the Figure 1.12 there is a blade that has a trailing edge flap system in a whirl tower testing of the SMART active flap rotor. Smart material actuated rotor technology system uses piezoelectric materials as an actuator to control the trailing edge flaps. Results show 80% vibration reduction and 10dB noise reduction and 10% thrust increment from baseline thrust.

Chopra and Koratkar has a study over froude scale blades. In this study, they achieve flap deflection of 8° at 900 rpm and 5/rev. This creates 10% thrust increment at 6° collective (Koratkar & Chopra, 2000).



Figure 1.11 : Trailing edge flaps of Karman Helicopter

Walz and Chopra creates a teoretical formulations to get the system aerodynamic response. At this study, actuator design is main purpose. Thus, flap hinge moment calculations are the important results in this study. After that appropriate atuator design can be made using these analytic results (Walz & Chopra, 1994).

Chopra and Spencer tested a rotor blade with Naca 0012 profile. Span of the flap is 8 in and cord is 20% of the blade cord. Results show that the real flap deflection angle is smaller than the calculated one (Spencer & Chopra, 1996).

There is another study at the University of Maryland. The study examine the TE flaps for vibration reduction and performance improvement. For hover performance they got performance improvement from using TE flaps (Ravichandran, Chopra, Wake, & Hein, 2013).

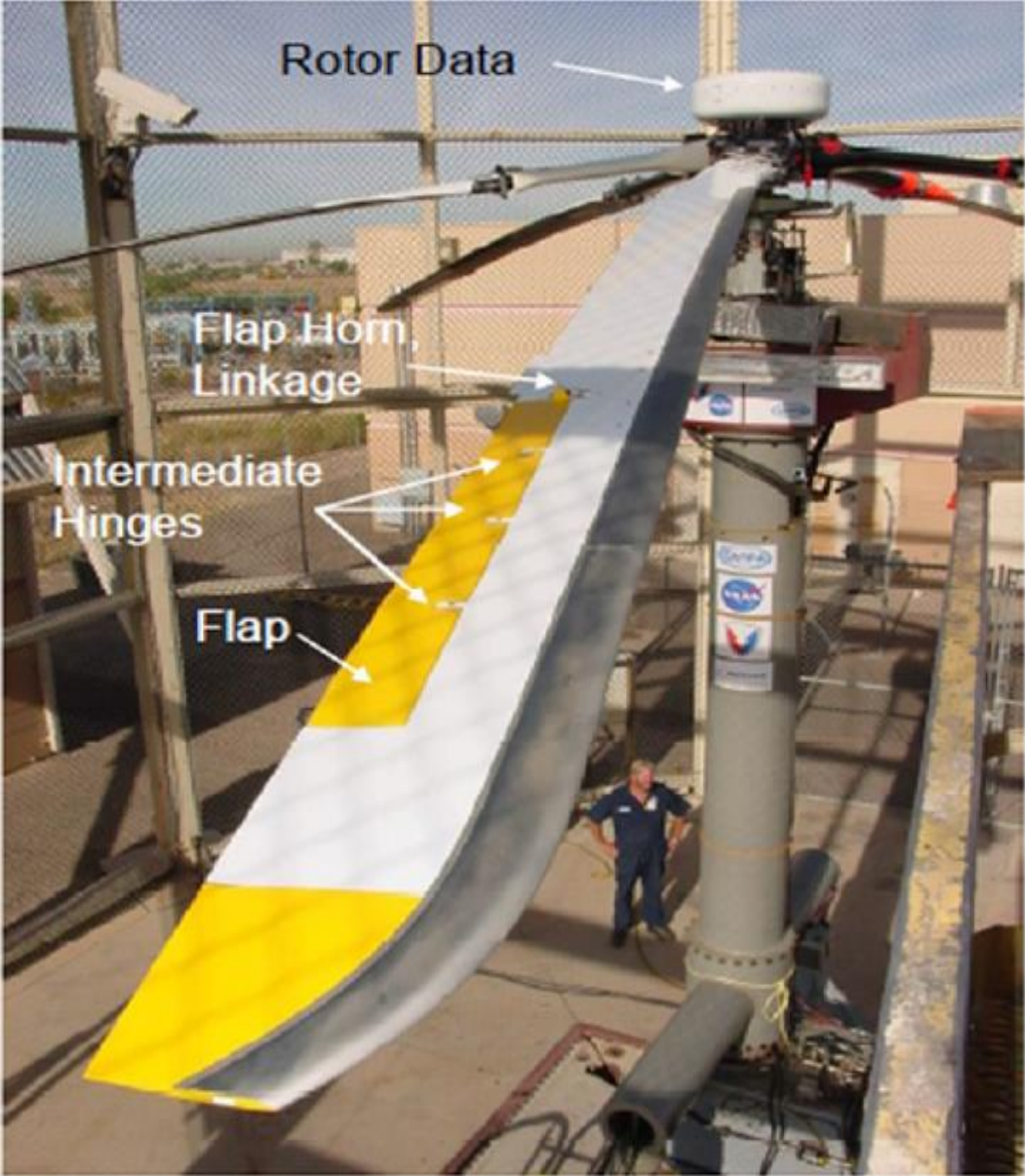


Figure 1.12 : Whirl tower test of trailing edge flap system

In the Figure 1.13, active trailing edge flap system can be seen for model scale rotor blade. TE flaps are actuated with the piezostack actuators.

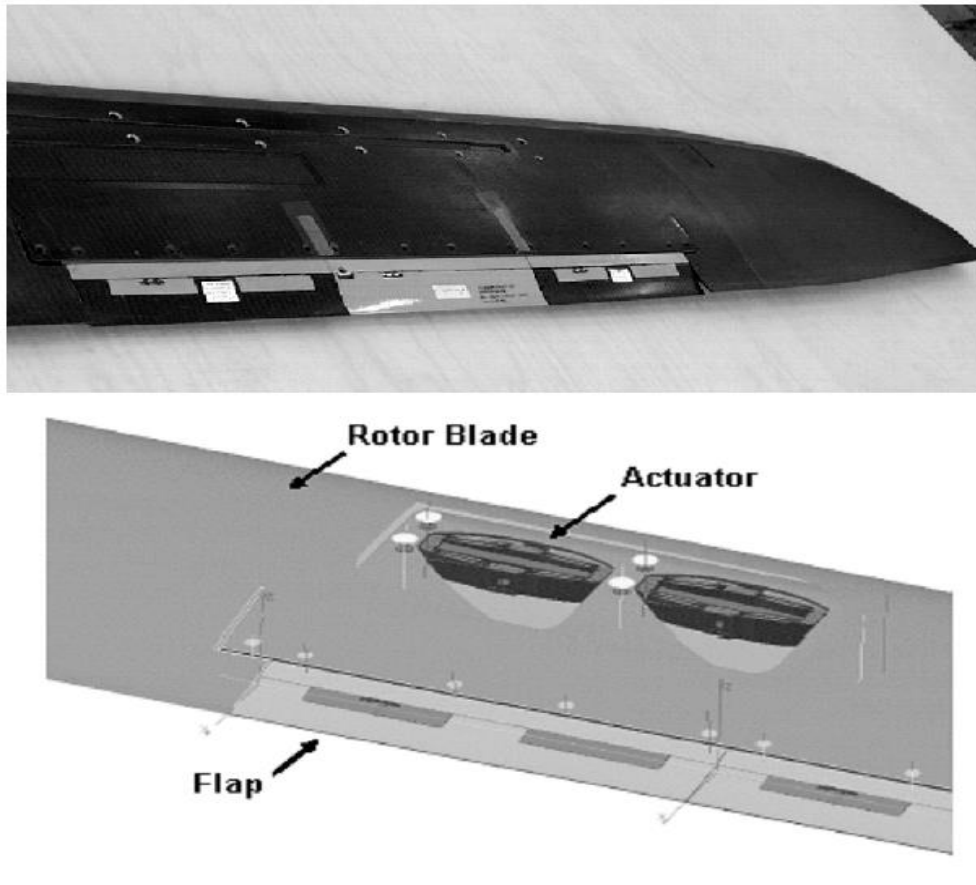


Figure 1.13 : Trailing edge flap with piezostack actuators for model rotor blades

1.2.3 Active blade twist

Active flap system has two ways to control rotor system forces with increased lift by deflected flap and with increasing torsional moment by twisting the beam elastically. However, this is not the only way to produce active control system. Active blade twist with on blade actuations can perform this type of need. Active blade twist can be acquired by quasi static and dynmaic. As we said before we are dealing with the quasi static situation. Furthermore, there are some studies about quasi static twist changing and its effect on the vibration and performance (Wilbur et al, 2018).

Actually there are extensive research on the field of active twist control of the rotor blade. Chen and Chopra apply the piezoceramic actuators under the skin of the blade and the 45⁰ piezo material lay up seemed the most effective way to twist a rotor blade (Chen & Chopra, 1997).

Figure 1.14 and Figure 1.15 shows that blade twist prosedure. This blade is actuated by piezoelectric ceramics that is put into the blade.

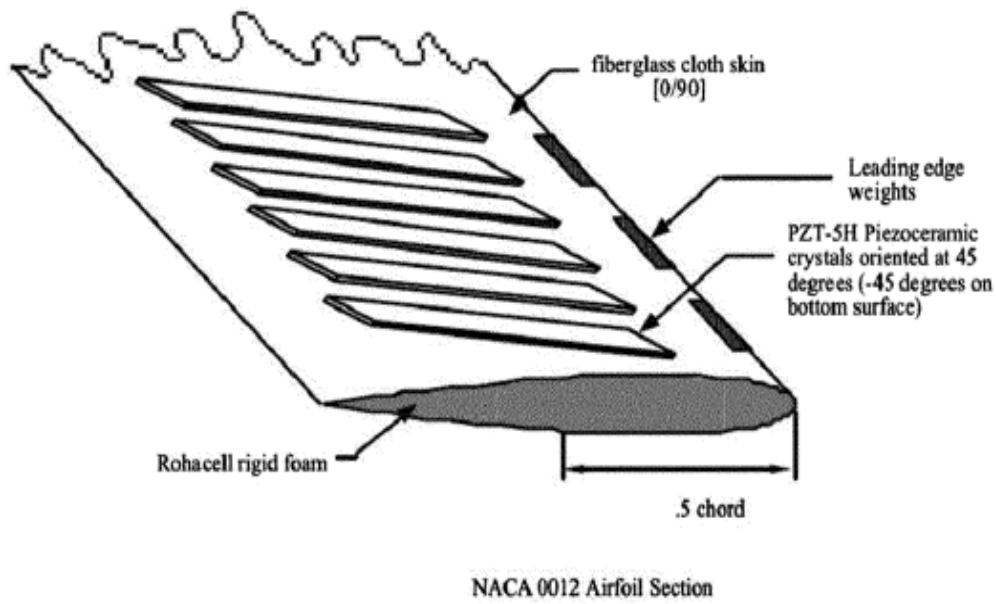


Figure 1.14 : Piezoceramic crystal orientation on the blade

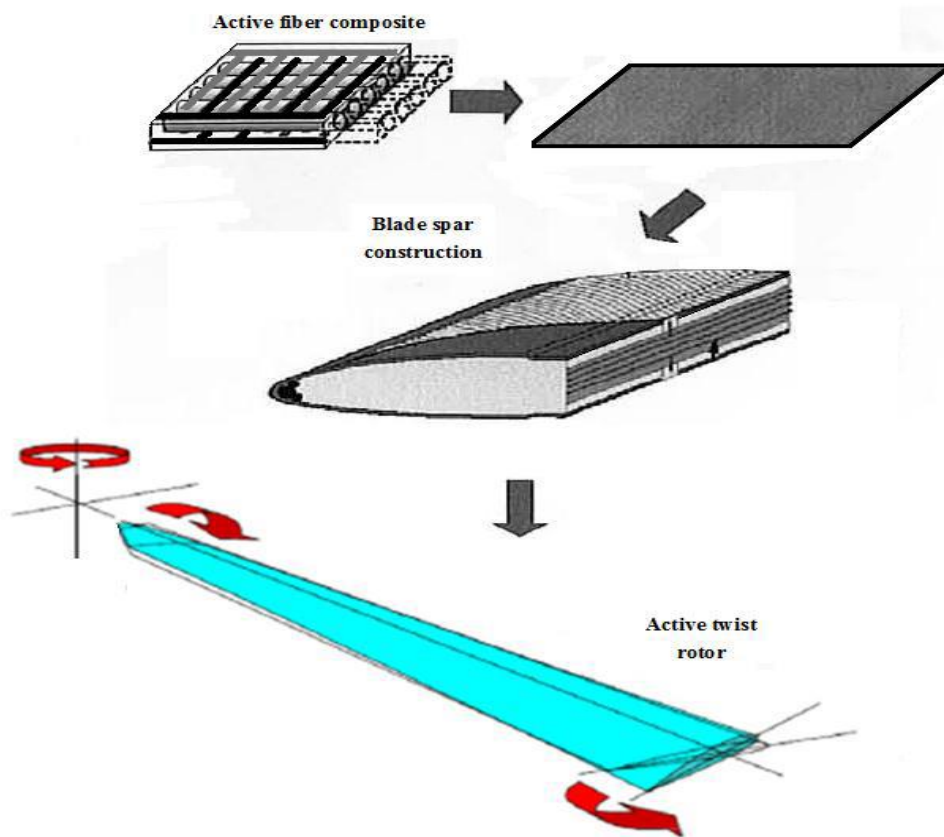


Figure 1.15 : Piezoelectric actuated active twist rotor blade

1.3 Purpose and Road Map

The main focus of this thesis is to develop a computer code that can calculate the rotor blade aerodynamic properties and performance parameters. Blade twist and airfoil shape change affects the rotor aerodynamics and performance. The TE flap system can be used to change the airfoil camber and deflects the airfoil polar characteristics. In the thesis blade twist and TE flap effects on the helicopter aerodynamics and performance are examined using the MATLAB code that is written originally.

The code was written using BET and BEMT. Blade sectional induced inflow ratio is found using BEMT. The sectional thrust and power values found using BET. In the BET calculations every section is assumed to have no mutual effects. Thus, every section of the blade are calculated discretely. This means that blade BET assumes all the blade has 2-D aerodynamics. However, this approach fails near the tip portion of the blade where 3-D effect are rather dominant. To model tip vortices effects on the blade, Prandtl's correction factor used.

The solution is conducted using 2-D aerodynamic properties and Prandtl corrections. To specifically know the airfoil properties Xfoil programme that is created by Mark Drela from MIT is used assuming that the flow is viscous (Mueller, T. J. (Ed.), 1989). These values are found using every blades corresponding Re numbers. From these values look up table is created in excel file. While calculation of every blade section, code opens the specific page of the excel and import the values into the matlab to carry on the calculations. At the end of the calculations, besides of sectional thrust and power values, FM values are found for different disk loading values.



2. AERODYNAMIC FORMULATIONS

2.1 Momentum Theory

The helicopter must operate hover, climb, descent or forward flight. All these flight regimes have different characteristics. In hover and descent there is no forward speed to disturb the flow over the rotor disc. In this case there is only an axial flow over the rotor disc which means that the flow is axisymmetric over the rotor disc. Moreover, in hovering flight there is no axial velocity component of flow over the rotor disc. This time there is only induced inflow velocity.

In hover condition flow is axisymmetric over the rotor disc and presumably easier to calculate analytically. In the Figure 2.1, there is shown velocity field of rotor flow in hover condition.

In hover conditions the lift is axisymmetric. This means that same conditions apply to the blade regardless of its azimuthal position. In Figure 2.1, there are some aspects to consider. Although, there is a pressure jump over the rotor disk, there are no velocity jumps, velocity is increased smoothly through the far wake. The blade tip vortices trace down and create a slipstream boundary.

Now, the physical characteristics of hovering flow are apparent. Let's apply the conservation laws to the control volume surrounding the rotor and the wake. In the modeling three conservation laws are applied to the rotor and its flow field. Momentum theory calculations can be used to calculate only the thrust and power for the whole system. The details of the flow field can not be calculated. Rankine (1865) was the person who first developed this approach to analyse the marine propellers. After some time W.Froude (1878) developed the theory. However, Froude approached the rotor disk as elementary rings rather than the whole. There is a one big assumption in both theories which is the rotor disk is infinitesimally thin actuator disk and only produces pressure jump over the flow passing through it.

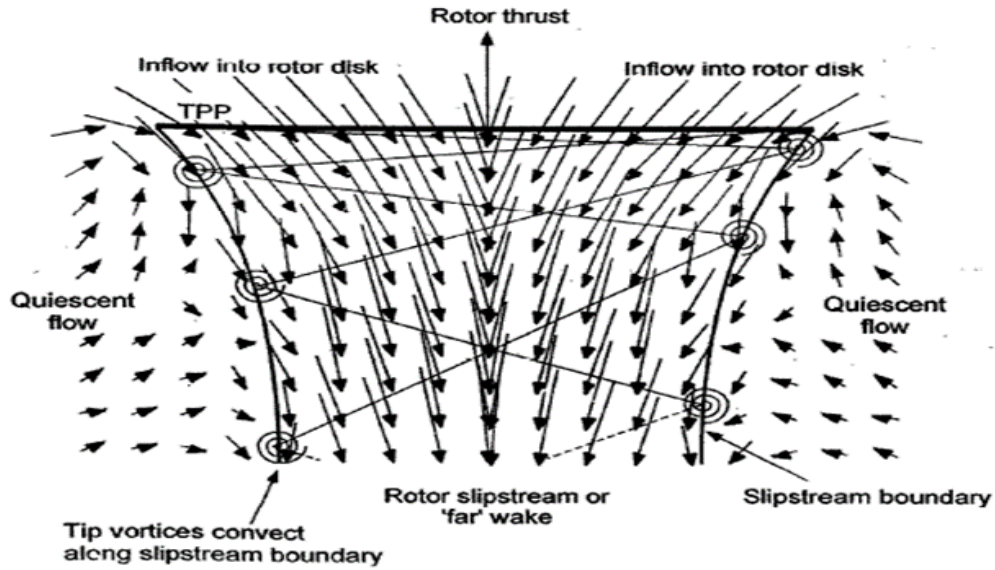


Figure 2.1 : Flow velocity gradient over rotor disk (Leishmann, 2006)

While approaching to the problem, some assumptions about flow field around the rotor disk are needed to be made beforehand. There are four assumptions, the flow is one dimensional, quasi-steady, incompressible and inviscid. Of course, all these assumptions have its own meaning. To assume the flow both incompressible and inviscid means that there is no viscous shear between fluid elements which results that induced losses are the only reason for all rotor losses. Moreover, assuming that the flow is quasi-steady means that the flow properties does not change over time for at a point. Lastly, one-dimensional flow means that flow properties are only changing the axial direction over the rotor disk.

Conservation laws includes mass, momentum and energy conservation. These are applied to the control volume which surrounds the rotor and wake structure. Lets show control volume as \vec{S} .

2.1.1 Applying conservation laws

Conservation of mass assumes than in and out of the flow from control volume is equal to each other. This relationship is shown in (2.1). \vec{V} is the local velocity and ρ is the density of the fluid.

$$\iint_S \rho \vec{V} d\vec{S} = 0 \quad (2.1)$$

If we remember the assumption about flow that it is quasi-steady and consider conservation of mass, its conclude that mass flow rate is constant in control volume.

$$\iint_S \rho \vec{V} d\vec{S} = \dot{m} \quad (2.2)$$

$$\dot{m} = \rho A_\infty w = \rho A_2 v_i = \rho A v_i \quad (2.3)$$

Conservation of momentum means that net force on the flow in the control volume is equal to rate of the momentum change with time in that control volume. The relationship can be written like in equation (2.5).

$$\vec{F} = \iint_S \rho d\vec{S} + \iint_S (\rho \vec{V} d\vec{S}) \vec{V} \quad (2.5)$$

$$T = \dot{m} w \quad (2.6)$$

The conservation energy means that work done on the fluid results the kinetic energy increase in to the control volume.

$$W = \iint_S \frac{1}{2} (\rho \vec{V} d\vec{S}) |\vec{V}|^2 \quad (2.7)$$

$$T v_i = \frac{1}{2} \dot{m} w^2 \quad (2.8)$$

$$v_i = \frac{1}{2} w \quad (2.9)$$

Induced velocity is and important parameter for rotor calculations because it effects induced losses. From the conservation of momentum induced velocity can be found using equations (2.3), (2.6) and (2.9)

$$T = 2\rho A v_i^2 \quad (2.10)$$

$$v_i = \sqrt{\frac{T}{2\rho A}} \quad (2.11)$$

Now the relation between thrust coefficient and induced inflow ratio can be written after finding inflow velocity.

Thrust coefficient, induced inflow ratio and tip speed equations are (2.12), (2.13) and (2.14), respectively.

$$C_T = \frac{T}{\rho A V_{tip}^2} \quad (2.12)$$

$$\lambda_i = \frac{v_i}{V_{tip}} \quad (2.13)$$

$$V_{tip} = \Omega R \quad (2.14)$$

Using the equations (2.12), (2.13) and (2.14), induced inflow ratio can be written in equation (2.15),

$$\lambda_i = \sqrt{\frac{C_T}{2}} \quad (2.15)$$

Because of the structure of the momentum theory, radial variation of the flow over the rotor disk can not be modeled. Thus, the induced inflow ratio is assumed to be same all over the rotor disk. This is the most important assumption and not quite correlate the actual flow physics (Leishman, 2006).

2.2 Blade Element Theory

Blade element analysis can help to estimate radial and azimuthal differences over the rotor disk. In the blade element analysis 2-D aerodynamics are assumed over the blade. However, to add 3-D effects tip loss and other factors that is found empirically can be applied in formulations to model. BET can give informations while designing the blade geometry like blade twist, the planform distribution and airfoil shape because using BET sectional blade characteristics can be examined. After these sectional characteristics is found, they can be integrated or numerically added to each other over

the blade to find the overall rotor performances. Overall rotor performances means that thrust and power of the selected rotor.

In the analysis of BET, blade sections are idealized as 2-D airfoils. Thus, there is no effect from one airfoil to another. However, there is a nonuniform induced inflow effect across the blade. To calculate induced inflow some assumptions can be made like uniform or linear distribution of induced velocity.

Flow environment and aerodynamic forces at blade element on the rotor is shown in Figure 2.2, 2.3. It is assumed the aerodynamic forces is created by only the effect of AoA and velocity of the rotor. As its said before there is no mutual effects of airfoils. Thus, the radial velocity component can be ignored when calculating aerodynamic forces on the blade.

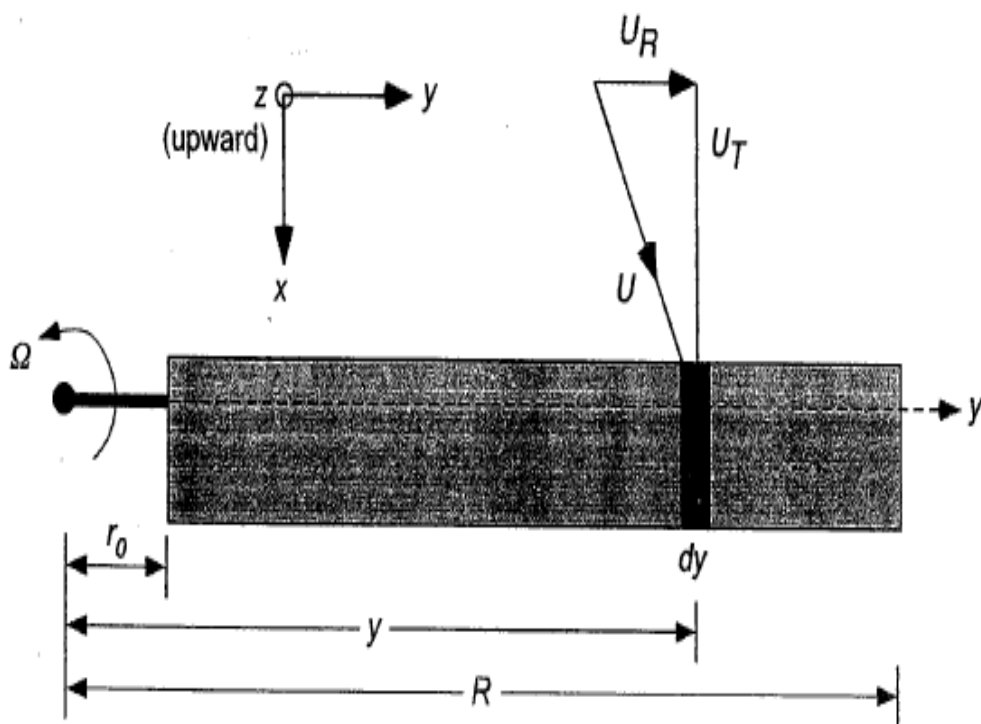


Figure 2.2 : Top view of the blade element (Leishman, 2006)

The inflow angle of attack, ϕ is dependent on induced velocity of the blade section. The inflow changes the direction of the flow over the blade section resulting effective AoA change. Also, induced velocity alters the direction of the lift force and create induced drag over the blade.

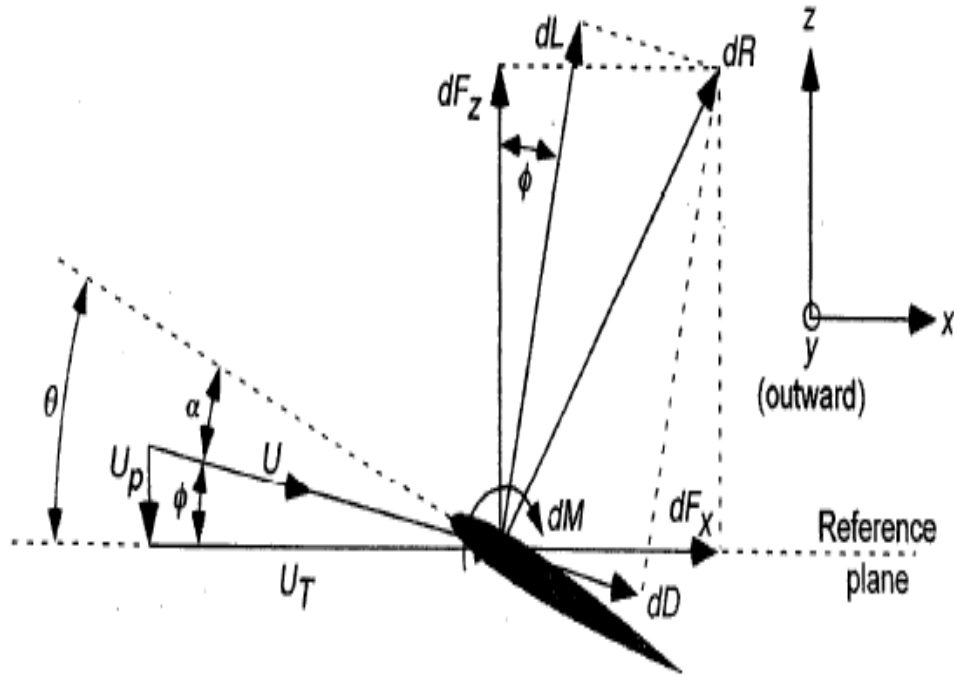


Figure 2.3 : Side view of the blade element (Leishman, 2006)

In BET calculation, analysis is about 2-D aerodynamics of blade sections which means that there are two velocity component perpendicular to each other (see Figure 2.2). One is the in-plane component which results from the rotation of the blade, $U_T = \Omega y$. The other component is perpendicular component to the rotor disk which results from the induced inflow. This component called induced velocity, $U_p = v_i$. Furthermore, there is a correlation between velocities like,

$$U = \sqrt{U_T^2 + U_p^2} \quad (2.16)$$

As seen in the Figure 2.3 there are some parameters to define and correlate each other. There are three angles and each of them has different meaning. α means effective angle of attack, θ means geometric pitch angle of the blade section and ϕ means induced inflow angle.

$$\alpha = \theta - \phi \quad (2.17)$$

Inflow angle has a correlation with tangential and perpendicular velocity component of blade section,

$$\phi = \tan^{-1}\left(\frac{U_p}{U_T}\right) \quad (2.18)$$

If small angle assumption is used, which is viable than,

$$\phi = \frac{U_p}{U_T} \quad (2.19)$$

The relationship between angles be like,

$$\alpha = \theta - \frac{U_p}{U_T} \quad (2.20)$$

The sectional lift (dL) and drag (dD) force can be written using basic aerodynamic relationships. Sectional lift and drag forces are perpendicular to each other. And they act upon the direction of the resultant velocity, U . dL is perpendicular and dD is parallel to it.

$$dL = \frac{1}{2}\rho U^2 c C_l dy \quad (2.21)$$

$$dD = \frac{1}{2}\rho U^2 c C_d dy \quad (2.22)$$

C_l and C_d are sectional lift and drag coefficients of blade. C is the sectional blade cord and U is sectional blade velocity.

Blade thrust, torque and power values can be found using above equations. But, first the perpendicular and parallel forces needed to be found. These forces are identified by reference plane. dF_z is perpendicular and dF_x is parallel to reference plane. They can identify using lift and drag forces of the section.

$$dF_z = dL \cos\phi - dD \sin\phi \quad (2.23)$$

$$dF_x = dL \sin\phi + dD \cos\phi \quad (2.24)$$

Now using this relations, where y is the distance of the blade section from the rotation axis and N_b is the number of blades.

$$dT = N_b dF_z \quad (2.25)$$

$$dQ = N_b dF_x y \quad (2.26)$$

$$dP = N_b dF_x \Omega y \quad (2.27)$$

The most general form of sectional thrust, torque and power is

Whith the small angle assumption of ϕ ,

$$dT = N_b dL \quad (2.28)$$

$$dQ = N_b (dL \sin\phi + dD \cos\phi) y \quad (2.29)$$

$$dP = N_b (dL \sin\phi + dD \cos\phi) \Omega y \quad (2.30)$$

The nondimensional quantities are going to be used later on to specify the rotor properties and compare different rotors. Thus, C_T, C_P and C_Q should be found. To calculate nondimensional quantities lengths are divided with R and velocities are divided by ΩR .

Besides the sectional coefficients, induced inflow ratio can be written using nondimensional parameters.

$$\lambda = \frac{v_i}{\Omega R} = \frac{v_i}{\Omega y} \left(\frac{\Omega y}{\Omega R} \right) = \frac{U_p}{U_T} \left(\frac{y}{R} \right) = \phi r \quad (2.31)$$

The coefficients can be written as,

$$dC_T = \frac{dT}{\rho A (\Omega R)^2} \quad (2.32a)$$

$$dC_T = \frac{N_b dL}{\rho A (\Omega R)^2} = \frac{N_b \left(\frac{1}{2} \rho U_T^2 c C_l dy \right)}{\rho \pi R^2 (\Omega R)^2} \quad (2.32b)$$

As written before, the velocity and length are divided with R and ΩR .

$$dC_T = \frac{1}{2} \left(\frac{N_b c}{\pi R} \right) C_l \left(\frac{y}{R} \right)^2 d \left(\frac{y}{R} \right) \quad (2.33a)$$

$$dC_T = \frac{1}{2} \left(\frac{N_b c}{\pi R} \right) C_l r^2 dr \quad (2.33b)$$

There is an important quantity that is called solidity. It is the ratio of the rotor blade area to rotor disk area.

$$\sigma = \frac{\text{Blade area}}{\text{Disk area}} = \frac{A_b}{A} = \frac{N_b c R}{\pi R^2} = \frac{N_b c}{\pi R} \quad (2.34)$$

Rotor sectional thrust coefficient is now become

$$dC_T = \frac{1}{2} \sigma C_l r^2 dr \quad (2.35)$$

Using the same logic above, power and torque coefficients can be found. In nondimensional form they can be written as equals.

$$\begin{aligned} dC_Q \equiv dC_P &= \frac{dQ}{\rho A (\Omega R)^2 R} = \frac{N_b (\phi dL + dD) y}{\rho \pi R^2 (\Omega R)^2 R} \\ &= \frac{1}{2} \left(\frac{N_b c}{\pi R} \right) (\phi C_l + C_d) r^3 dr \end{aligned} \quad (2.36a)$$

$$dC_Q \equiv dC_P = \frac{1}{2} \sigma (\phi C_l + C_d) r^3 dr \quad (2.36b)$$

Torque and power coefficient include profile and induced part of the calculations. To show this induced inflow equation, equation (2.31), is used,

$$dC_P = \frac{1}{2} \sigma \phi C_l r^3 dr + \frac{1}{2} \sigma C_d r^3 dr \quad (2.37a)$$

$$dC_P = \frac{1}{2} \sigma \lambda C_l r^2 dr + \frac{1}{2} \sigma C_d r^3 dr \quad (2.37b)$$

$$dC_P = dC_{P_i} + dC_{P_0} \quad (2.37c)$$

dC_{P_i} represents the induced power and dC_{P_0} represents the profile power part. (Leishman, 2006)

2.3 Blade Element Momentum Theory

Blade element momentum theory is an hybrid model to apply helicopter hover calculations. Gustafson and Gessow was the first scientists who introduce this theory. Basic methodology is to combine the momentum theory and blade element theory approaches. This combined theory has the power to calculate the inflow distribution radiolly over the helicopter blade which is quite handy property that momentum and blade element approaches could not have.

Momentum theory assumes uniform inflow and blade element theory uses this results in the calculations. The reminder for the assumption, $\lambda_i = \sqrt{\frac{C_T}{2}}$, in equation (2.15).

BEMT for momentum theory part uses differential momentum theory that is introduced by Froude for propeller analysis in axial motion. Like the theories before, this theory also has some assumptions. According to this theory, to calculate the particular distance from rotation axis, conservation laws are applied to the rotor annulus (see Figure 2.4, Figure 2.5). The annulus can be defined as actuator ring that has distance y form rotation axis and has thickness dy . Also, no annulus has an effect to another one. Every annulus threated as individual without any outside effect.

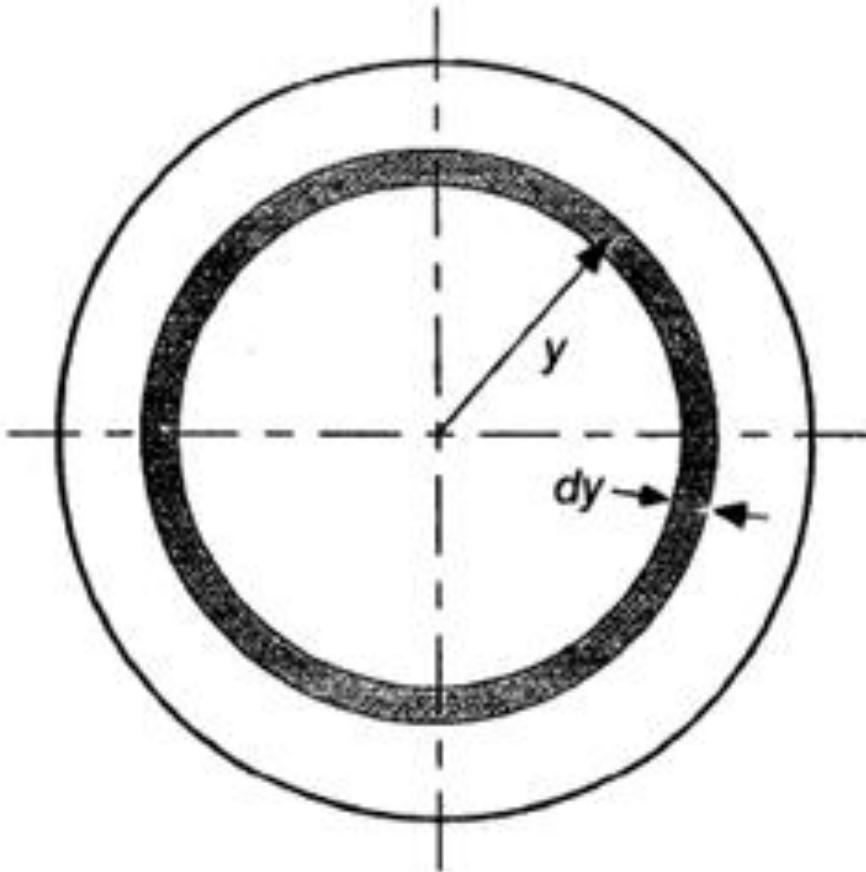


Figure 2.4 : Top view of the rotor annulus(Leishman, 2006)

In 1-D momentum theory, only total thrust and power estimates could be made. However, when differential momentum theory is used, every annulus models the one section of blade in hover, which means that the theory models the flow in 2-D. Still, the basis of the theory is to use mass flow rate to calculate the incremental thrust. To calculate mass flow rate, annular area is needed. The area can be identified as $dA=2\pi ydy$. In the equations $\lambda_i=\lambda$, because all the calculations are conducted for hover conditions. Using equations (2.13) and (2.16), equation (2.38) can be found.

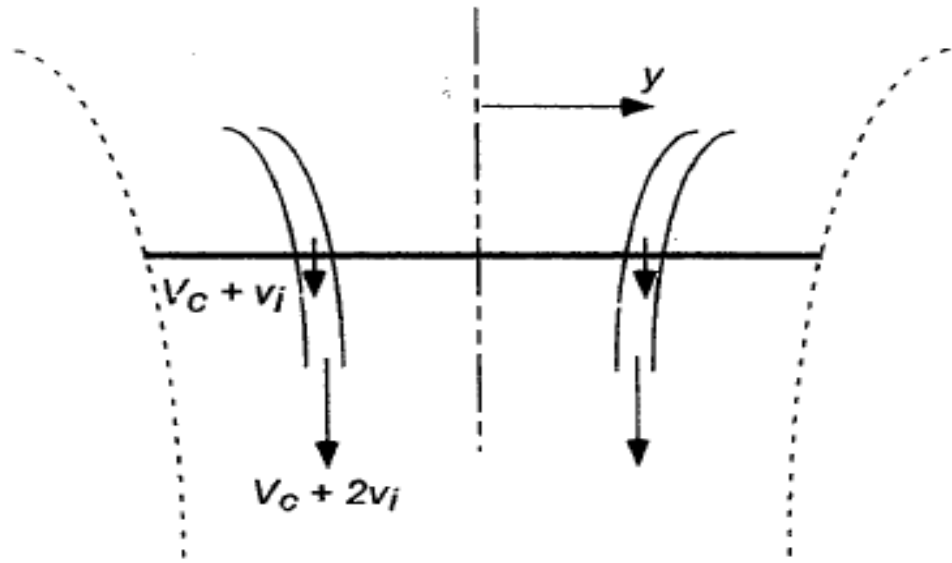


Figure 2.5 : Side view of the rotor annulus (Leishman, 2006)

$$T = 4\pi\rho v_i^2 y dy \quad (2.38)$$

Equation (1.38) is used to calculate dC_T ,

$$dC_T = \frac{dT}{\rho A(\Omega R)^2} = \frac{4\pi\rho v_i^2 y dy}{\rho A(\Omega R)^2} \quad (2.39a)$$

$$dC_T = 4\lambda^2 r dr \quad (2.39b)$$

The induced power is,

$$dC_{P_i} = \lambda dC_T = 4\lambda^3 r dr \quad (2.40)$$

The purpose of the differential momentum theory calculations is to find inflow distribution radially. To achieve this equation the circulation theory of lift which is found using BET and momentum theory of lift which is found using differential momentum theory are come up to each other. In equations (2.35) and (2.39b) thrust coefficients that are found these two theory is given.

Before writing the final equation sectional lift coefficient is needed to be written more open form.

$$C_l = C_{l_\alpha} \alpha \quad (2.41)$$

$$\phi = \frac{\lambda}{r} \quad (2.42)$$

$$C_l = C_{l_a} \left(\theta - \frac{\lambda}{r} \right) \quad (2.43)$$

C_{l_a} value is lift curve slope for the airfoil of the blade section.

Let's write the thrust coefficient equations (2.35) and (2.39b) as equal to each other and use equation (2.43).

$$\frac{1}{2} \sigma C_{l_a} (\theta r^2 - \lambda r) = 4\lambda^2 r \quad (2.44)$$

Now the solution of the quadratic equation for induced inflow ratio for hover case,

$$\lambda(r) = \frac{\sigma C_{l_a}}{16} \left(\sqrt{1 + \frac{32}{\sigma C_{l_a}} \theta r} - 1 \right) \quad (2.45)$$

Induced inflow for hover case can be bound to four parameters. Those are solidity, lift curve slope, sectional pitch angle and sectional non dimensional radial distance. Moreover, induced inflow ratio can be found according to radial location of blade section, which means that it is not uniform. To find nonuniform induced inflow ratio is important because it represents the flow physics better (Johnson, 1994; Leishman, 2006).

2.4 Prandtl Tip Loss Correction

Every theory that is examined before has some drawbacks and some correction factors needed to be added to properly model the flow physics over the rotor disc in hover. Momentum theory is disabled to calculate sectional properties using BET and 2-D flow, sectional properties of flow can be calculated. However, BET lacks of modeling the induced inflow ratio over the rotor disk. Thus, BEMT approach is used. Now, BEMT is a 2-D flow approach because of that, 3-D effects can not be modeled, but it is needed at some point. Especially, near the blade tips BEMT approach without any corrections has some deviation from real flow physics. Thus, to improve the modeling formulation for converging the reality better, vortex theory calculations are used and some correction factors are added to the BEMT calculations (Johnson, 1994; Leishman, 2006).

The Figure 2.6 shows the radial distribution of blade sectional lift calculation using BEMT with and without tip loss correction. It is obvious that tip loss correction is a handy tool to model the real flow physics better.

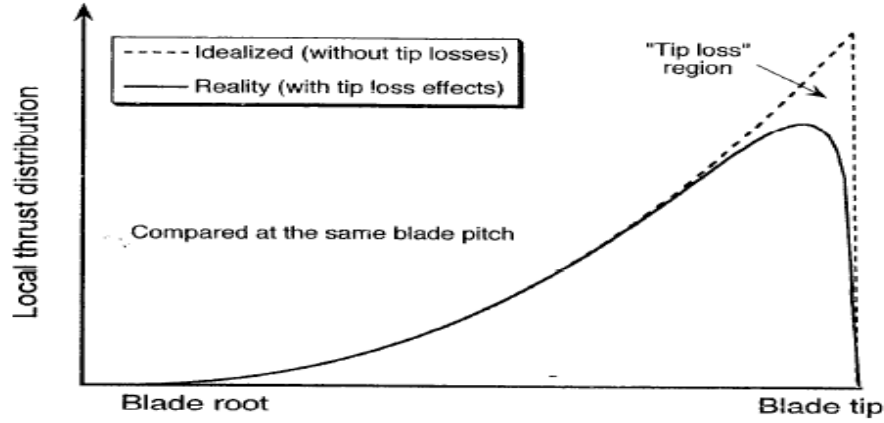


Figure 2.6 : Lift distribution over the blade with and without tip loss (Leishman, 2006)

Prandtl gives a formulation about tip loss correction. Because of the assumptions that made in the theories, MT, BET and BEMT can only model the airflow in 2-D. But there are some point over the rotor disk that flow is more of a 3-D flow and needs a treatment as such. The tip loss correction that Prandtl gives provide this 3-D effect near the blade tip.

$$F = \left(\frac{2}{\pi}\right) \cos^{-1}(\exp(-f)) \quad (2.46)$$

$$f = \frac{N_b}{2} \left(\frac{1-r}{\lambda}\right) \quad (2.47)$$

These F value is added to the C_T value of differential momentum theory result. After that, C_T from BET is equating to find the analytical form of induced inflow radially over the blade.

$$dC_T = 4F\lambda^2 r dr \quad (2.48)$$

If the equations (2.35) and (2.48) is equal, the final analytical form of induced inflow ratio becomes,

$$\lambda(r) = \frac{\sigma C_{l_a}}{16F} \left(\sqrt{1 + \frac{32F}{\sigma C_{l_a}} \theta r} - 1 \right) \quad (2.49)$$

The blade thrust gradient calculation sectionally over the blade at $C_T = 0.008$ with and without Prandtl's correction is shown in Figure 2.7. After the 90 percent the flow begins to drop and reach the value of zero at the blade tip (Johnson, 1994; Leishman, 2006).

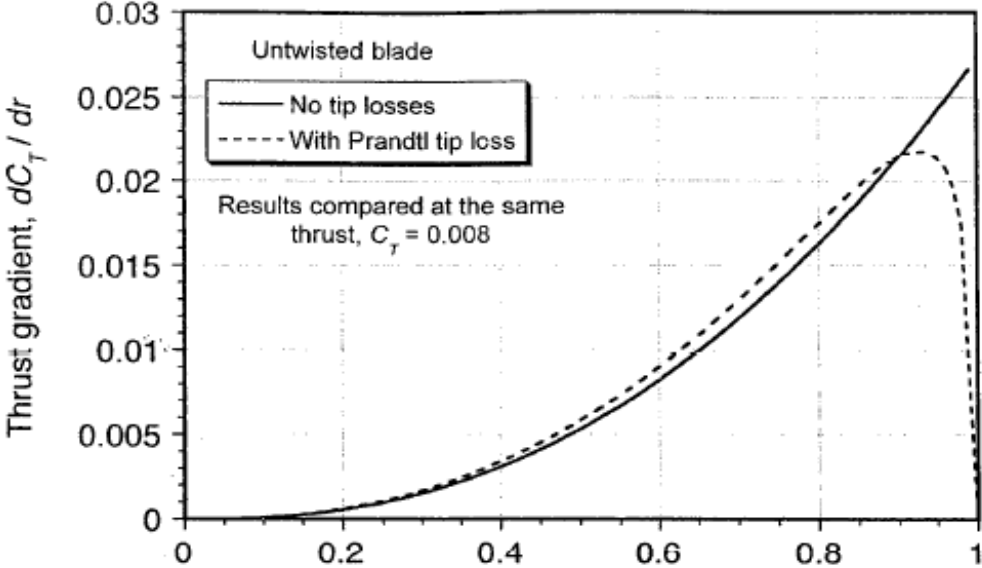


Figure 2.7 : Sectional thrust gradient value with and without tip loss (Leishman, 2006)

3. AERODYNAMIC PERFORMANCE PARAMETERS

3.1 Geometry Effects

While examining the blade geometry there are three main concepts to make the blade geometry more optimized for aerodynamics. These concepts are rotor blade twist, taper and trailing edge flap. All these three can be used to make the induced inflow more uniform over the rotor blade which is an optimum induced power condition. There are also one more power loss component for rotor blade which is profile power which is about the drag of the blade. Power coefficient includes both induced and profile power.

$$C_p = C_{p_i} + C_{p_o} \quad (3.1)$$

Twist and taper is a geometrical shape of the blade. Twisted means that the sectional angle of attack of the rotor blade changes over the blade. Tapered means that the chord length changes over the rotor blade (Johnson, 1994; Leishman, 2006).

However trailing edge flap concept is different from other two because it generally is used as an active blade concept. Flap concept is used to change the aerodynamic characteristics of a blade section. The effect of it depends on the flap features (Abbot & Doenhoff, 1958).

3.2 Blade Twist Characteristics

The twist means that the pitch angle of the blade is changing from one blade section to another. If the blade is produced with its own twist it is called pre-twist. Moreover, there is an active twist concept which means that blade geometry is changing in flight to adopt the changing conditions of the flight.

Blade twist is a concept that is used to optimize the blade aerodynamic performance. It is used to modify the induced inflow over the blade to make it more uniform. The ideal and most effective form of induced inflow is to be uniform over the blade. However, this can be achieved

with ideal blade twist. With the assumption of uniform inflow, ideal twist equation can be derived using BEMT (Johnson, 1994; Leishman, 2006).

There are four different variables in the induced inflow equation (see (). Solidity, lift curve slope, sectional pitch angle and percent of radial location of blade section. If the blade is rectangular and has same blade airfoil over the entire blade than σ and C_{l_a} is constant. To make the $\lambda(r)$ uniform than $\theta(r)r$ value needed to be constant over the blade. The constant value is the tip pitch angle of the blade.

$$\theta(r)r = \theta_{tip} \quad (3.2)$$

$$\theta(r) = \frac{\theta_{tip}}{r} \quad (3.3)$$

If the pitch angle equation is examined it can be seen that as r decreases angle of attack of the sections near the root increases rapidly. This phenomena can also be seen in the Figure 3.1. Actually, infinite blade sectional AoA is not possible. However, there is a portion of the blade that is not produce lift. This portion is the distance from the center of the rotor hub to the starting point of the blade lifting section. It is called root cut out. Because of this portion $\theta(r)$ can not go infinity and the sectional pitch angle distribution over the blade is somewhat aggrivable.

However, as seen Figure 3.1 the twist of the rotor blade through the root of the blede is increasing hyperbolicly. The more important part of helicopter blade is near the tip reigion because most of the lift produced there. Using linear twist distribution can be a good approach to reach more optimum aerodynamic condition over the blade with less production complications.

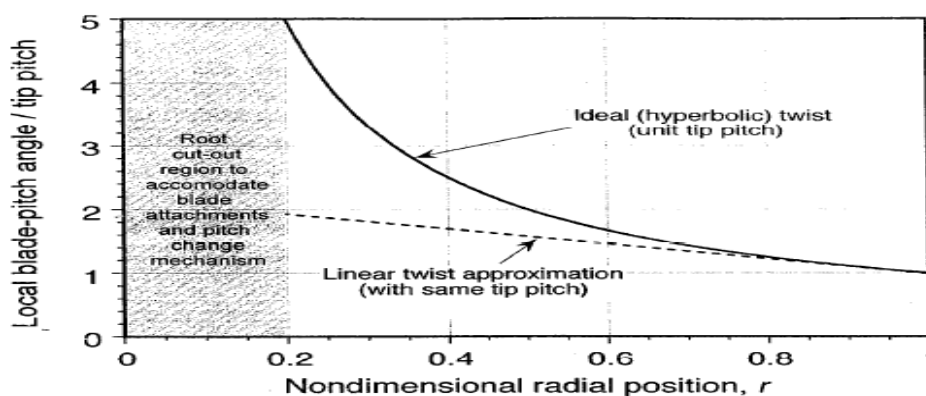


Figure 3.1 : Ideally twisted blade and linear approximation over the r

Linear twist means that the pitch angle is changing over the blade linearly. θ_0 means the pitch angle at the root, θ_{tw} is twist rate and it is negative value and $\theta(r)$ is the sectional pitch angle. The linear distribution of pitch angle is shown in the Figure 3.1.

$$\theta(r) = \theta_0 + r\theta_{tw} \quad (3.4)$$

Even though linear lift distribution can not make the inflow uniform, it makes it more uniform over the blade. In the Figure 3.2, there are 4 blade twist cases are plotted against the local induced inflow ratio (Johnson, 1994; Leishman, 2006).

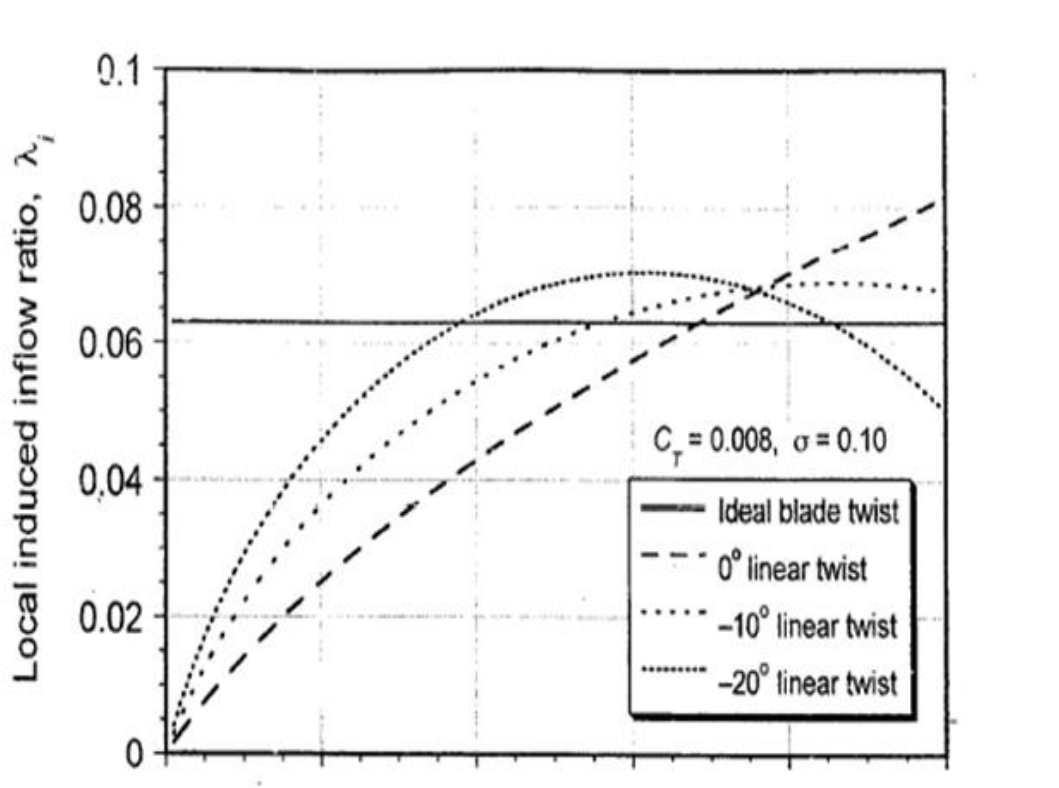


Figure 3.2 : Local inflow characteristics with the change of blade twist

3.3 Blade Taper Characteristics

Blade twist is used to minimize the induced power but the power over the helicopter rotor has two parts. C_{P_i} is the induced power and as seen from the equation. Induced power means that the power needed to produce rotor blade thrust. C_{P_0} is the profile power and as seen from the equation. Profile power is the power needed to overcome the blade drag force while operating.

$$dC_{P_i} = \frac{1}{2} \sigma \lambda C_l r^2 dr \quad (3.5)$$

$$dC_{P_o} = \frac{1}{2} \sigma C_d r^3 dr \quad (3.6)$$

The optimum rotor concept is a rotor geometry that makes the total power C_P minimum while making C_{P_i} and C_{P_o} minimum individually. There is a trivial solution to the problem which is the total power being equal to zero. However, there are one more constraint for this problem. While C_P is minimum C_T needs to be as big as possible. This is an optimisation problem and the solution can be found looking to the 2-D aerodynamics of airfoils.

It is also known that for optimum induced power inflow ratio needs to be uniform. What about profile power? For optimum value of profile power every blade section needs to have effective angle of attack that gives the best $\frac{L}{D}$. Maximum point of the $\frac{C_l}{C_d} - \alpha$ graph is the optimum point. In the graph below this situation is shown for naca0012 for different Reynolds numbers. If the airfoil section operates an effective AoA value that makes that section has maximum $\frac{C_l}{C_d}$, the pitch angle of the section is optimum value for that blade. If every section is operated at maximum $\frac{C_l}{C_d}$ value, this means the optimum hovering rotor is achieved.

Let's make the calculations of the helicopter blade geometrical needs to operate at optimum condition. The situations that affect the blade geometry is pitch angle of the every section of the helicopter blade. Thus, the sectional blade pitch angle is the important parameter to be dealt with when making optimum rotor calculations.

Now, it is known that to reach the optimum rotor performance two power factors needed to be optimum. However, the main problem is which rotor geometry makes this possible? To clarify this question, the conditions were specified as C_{P_i} and C_{P_o} is minimum. To make induced power optimum uniform inflow is needed. If momentum theory is remembered as seen in equation (2.15), inflow was assumed uniform and the result was in regard to thrust coefficient.

Thrust coefficient value can be found using BET. BET result is dependent on the blade geometric characteristics. Thus, to use the BET to calculate the thrust coefficient makes it easy to bound the geometry of the blade to the rotor aerodynamic characteristics. It is shown in equation (2.35).

If equation (2.42) and (3.7) are used,

$$\theta(r) = \frac{\theta_{tip}}{r} \quad (3.7)$$

$$C_l = C_{l_a} \left(\frac{\theta_{tip}}{r} - \frac{\lambda}{r} \right) \quad (3.8)$$

Also, there is another assumption for optimum blade, the assumption is every airfoil section of the blade operates at its optimum angle which gives the maximum value of $\frac{C_l}{C_d}$. This angle can be assumed to be α_{opt} . The thrust coefficient becomes,

$$C_l = C_{l_a} \alpha_{opt} \quad (3.9)$$

After specify the optimum angle of the blade, induced inflow can be calculated using BEMT approach. Let's use equations (2.44) and (3.9) to calculate the induced inflow equation for optimum blade,

$$\lambda = \sqrt{\frac{\sigma C_{l_a} \alpha_{opt} r}{8}} \quad (3.10)$$

Assumption was inflow to be uniform. Thus, σr needs to be uniform over the blade because C_{l_a} and α_{opt} are uniform. In this case solidity should be examined in detailed. Solidity is the blade area divided by rotor disk area.

$$\sigma r = \frac{N_b c r}{\pi R} \quad (3.11)$$

Blade number and radius is constant in the equations. Thus, only solution to make solidity constant is to make $c r$ constant in equation (3.11). As a result equations (3.12) and (3.13) is found.

$$c(r) = \frac{c_{tip}}{r} \quad (3.12)$$

$$\sigma(r) = \frac{\sigma_{tip}}{r} \quad (3.13)$$

This means that blade cord is changing over the blade section. This type of geometry is called ideal taper. Taper of the blade means that the cord length of the some portion of the blade is not equal the other portions. However, ideal tapered is not the only way to make the blade tapered.

Generally there is a linear tapered blades, taper of this type of blade identified with the ratio between the tip and root cord of the blade. The optimum and linear tapered blade is shown in the Figure 3.3 (Johnson, 1994; Leishman, 2006).

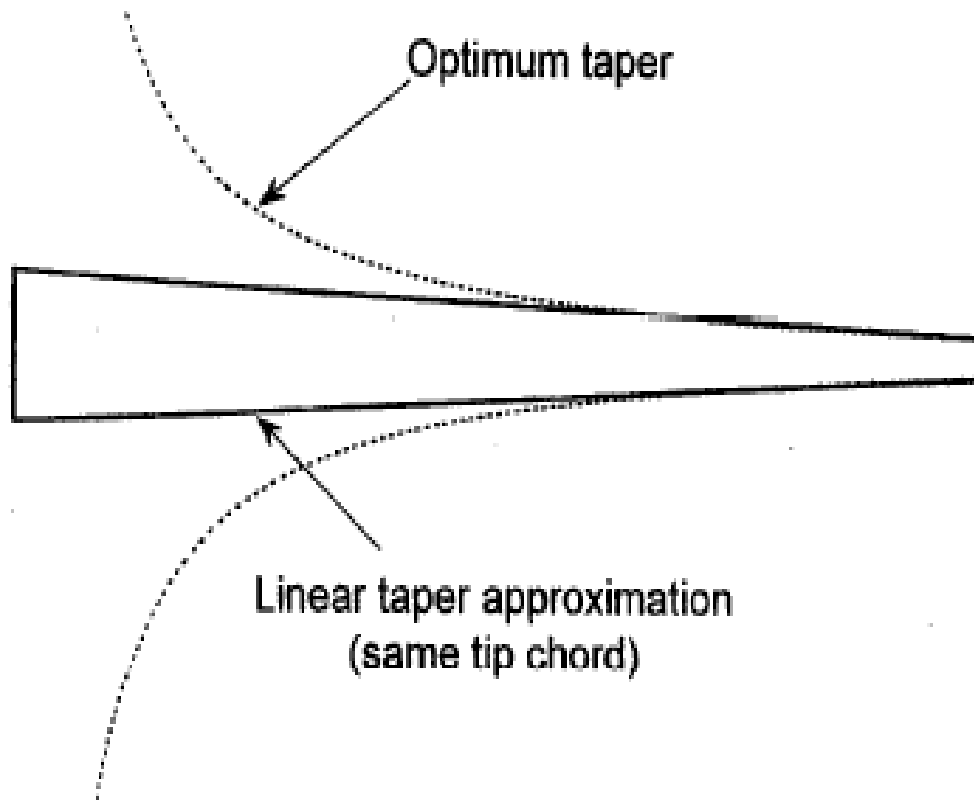


Figure 3.3 : Optimum and linear taper over the rotor blade (Johnson, 1994; Leishman, 2006)

3.4 Flapped Blade Characteristics

There are different types of flap like plain, slotted, split and external. The reason to use them is to change the blade geometry of the wing or blade section to change the airfoil characteristic or to control the aircraft or rotorcraft motion. Flap section is doing this by producing higher lift with the same airfoil section (Abbot & Doenhoff, 1958). When the flap deflected downward, which is a positive direction for flap deflection, it actually effects the airfoil chamber. It can be seen by thin airfoil theory that zero lift angle become more negative with the flap deflection. Although, maximum point of lift coefficient is met lower angle of attack, maximum value is getting bigger with more deflected flap. In the Figure 3.4, shows that affect.

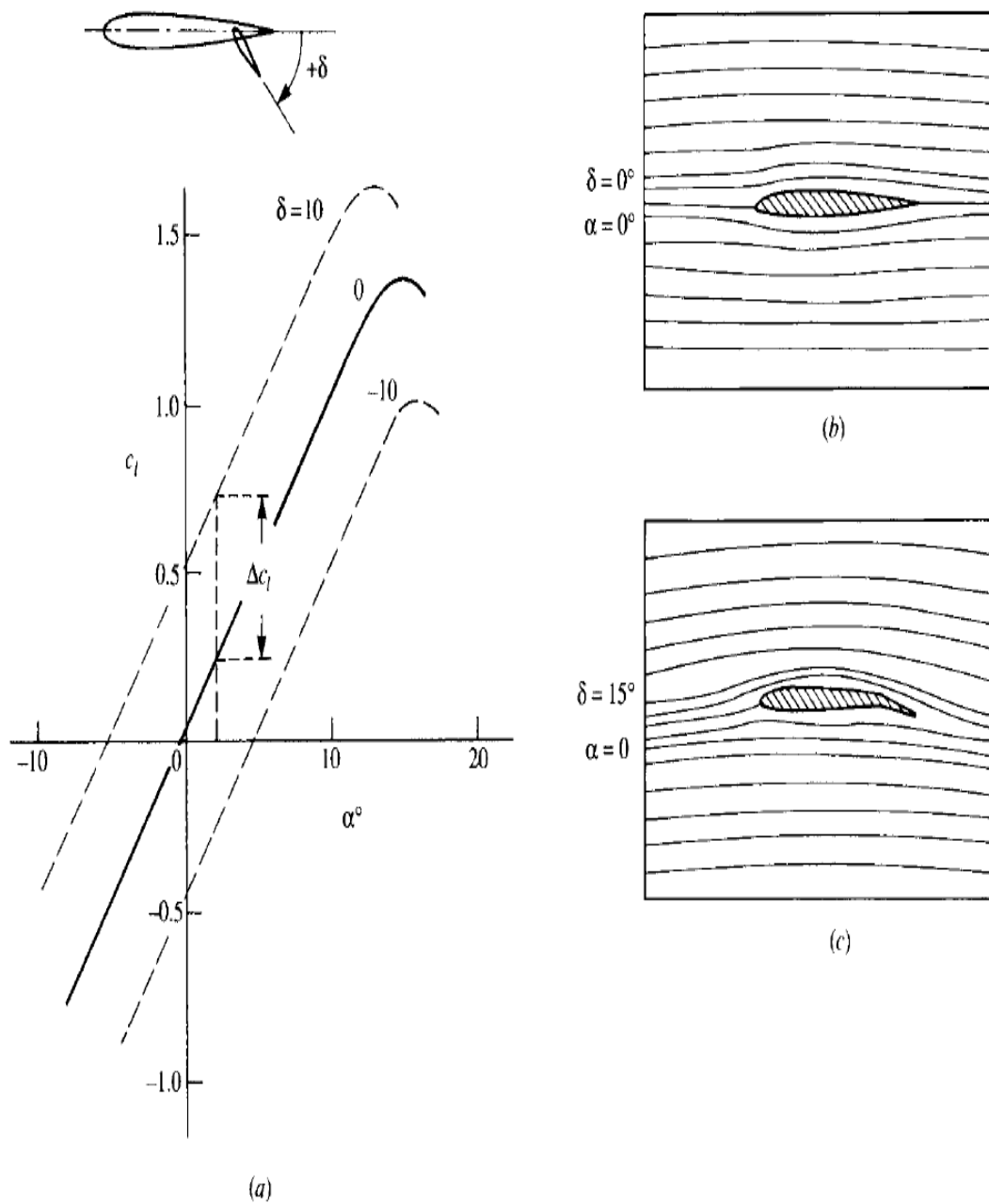
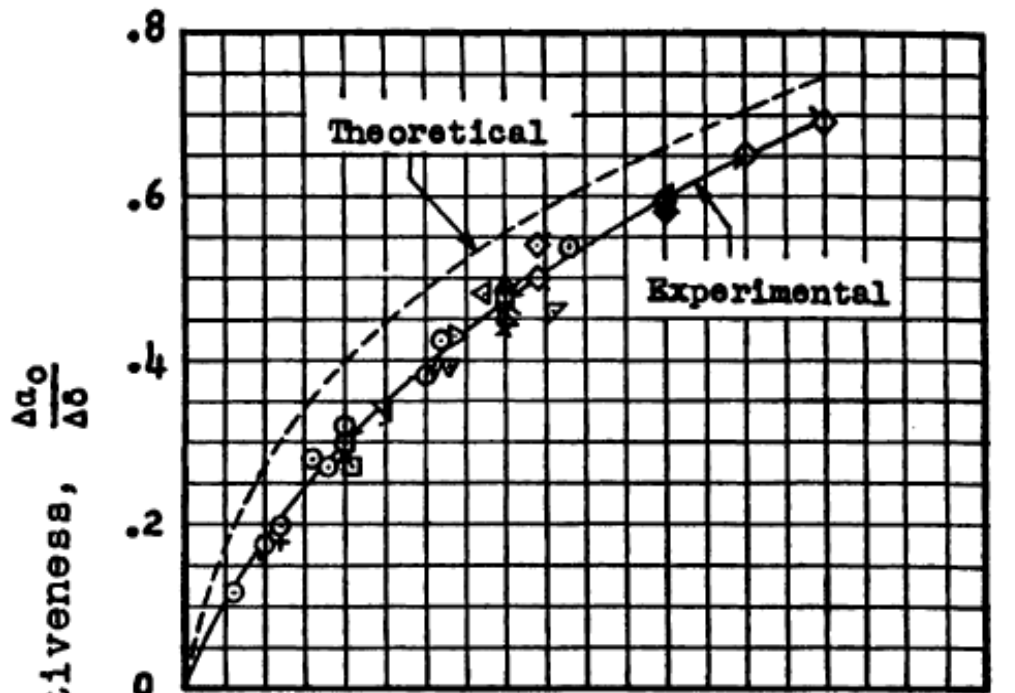


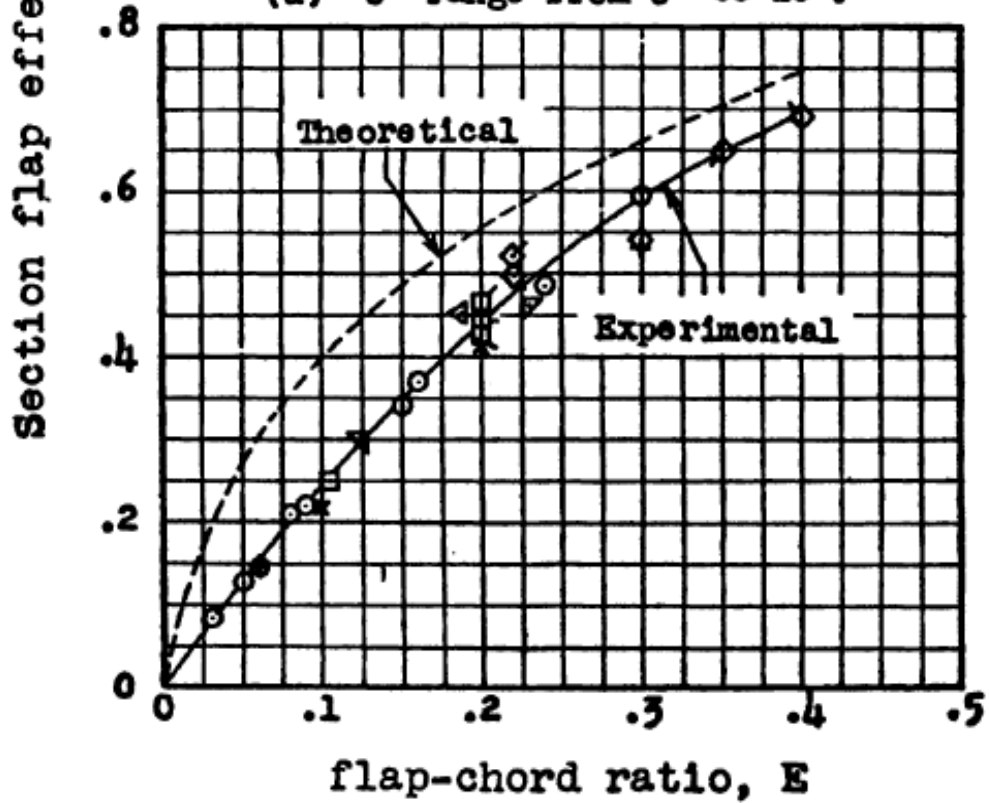
Figure 3.4 : Effect of plan flap to airfoil polars (Anderson, 2009)

There is a concept that has significant amount of importance about trailing edge flap which is called flap effectiveness. Flap effectiveness is the rate of change of zero lift angle of the applied section of the rotor blade or wing section opposed to flap deflection angle.

The Figure 3.5 shows the experimental and theoretical values of the flap effectiveness for different range of flap deflection angles.



(a) δ range from 0° to 10° .



(b) δ range from 0° to 20° .

Figure 3.5 : Sectional flap effectiveness with different range of flap deflections

To calculate the flapped section aerodynamic characteristics, the flap effectiveness is needed to be included to the formulation of BEMT. The value that affected by the flap deflection is effective angle of attack value of the section. Actually, the value of maximum C_l and the α of corresponding to that value is changing. This enables the flapped sections of the rotor blade to have more $C_{l_{max}}$ value in less angle of attack.

While adding the flap effectiveness into the equation (2.49), pitch angle value is cahnging and the value of change of zero lift angle is added to the added to the pitch angle value. $\frac{\Delta\alpha_0}{\Delta\delta} \delta$ is the flap effectiveness value. This value is needed to be put near to the pitch angle value in to the calculations. This value increases the blade pitch angle with the value of $\frac{\Delta\alpha_0}{\Delta\delta} \delta$. The value of flap effectiveness is found using Figure 3.6.

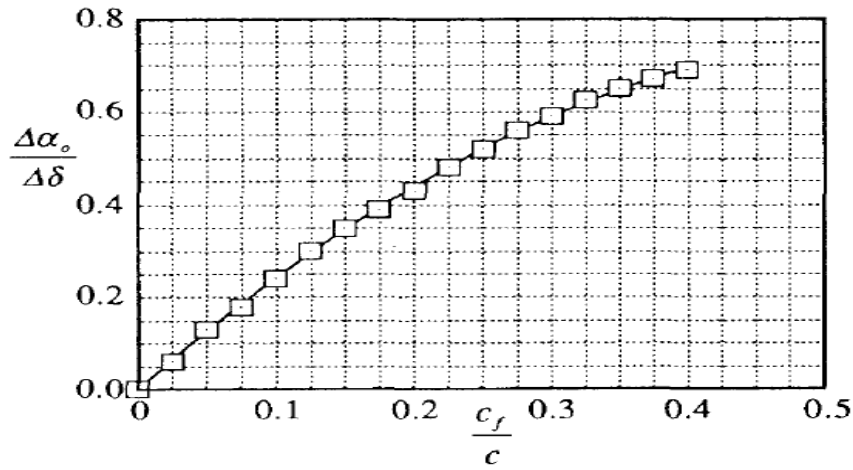


Figure 3.6 : Flap effectiveness due to flap cord divided by blade cord (Abbot & Doenhoff, 1958)

If the curve fitting is applied to the values in the Figure 3.6, the equations we get is,

$$\frac{\Delta\alpha_0}{\Delta\delta} = -0.002192 + 2.669 \frac{c_f}{c} - 2.323 \frac{c_f^2}{c} \quad (3.14)$$

$$\alpha = \theta + \frac{\Delta\alpha_0}{\Delta\delta} \delta - \phi \quad (3.15)$$

$$C_l = C_{l_a} \left(\theta + \frac{\Delta\alpha_0}{\Delta\delta} \delta - \frac{\lambda}{r} \right) \quad (3.16)$$

$$\lambda(r) = \frac{\sigma C_{l_a}}{16} \left(\sqrt{1 + \frac{32}{\sigma C_{l_a}} \left(\theta(r) + \frac{\Delta\alpha_0}{\Delta\delta} \delta \right) r} - 1 \right) \quad (3.17)$$

Above equations can be used to calculate the flapped blade sectional lift and power calculations (Abbot & Doenhoff, 1958; Johnson, 1994; Leishman, 2006; Walz & Chopra, 1994).

Even if there is a flap effectiveness value that we have. In the calculations, airfoils with deflected flap polar are found using Xfoil program to get more reliable values. In the Figure 3.7, the trailing edge flapped blade geometry is shown and in the Figure 3.8 Cp values are shown for the flapped airfoil. These photos were taken from Xfoil programme.

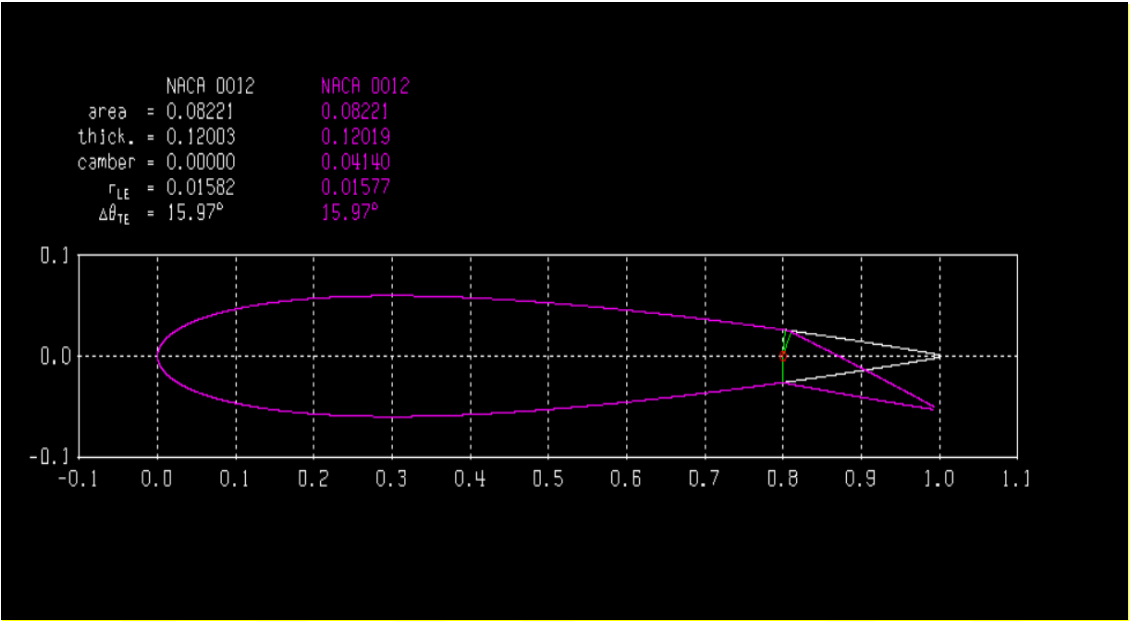


Figure 3.7 : 15 deg deflected 20% cord flapped blade Naca 0012 Xfoil

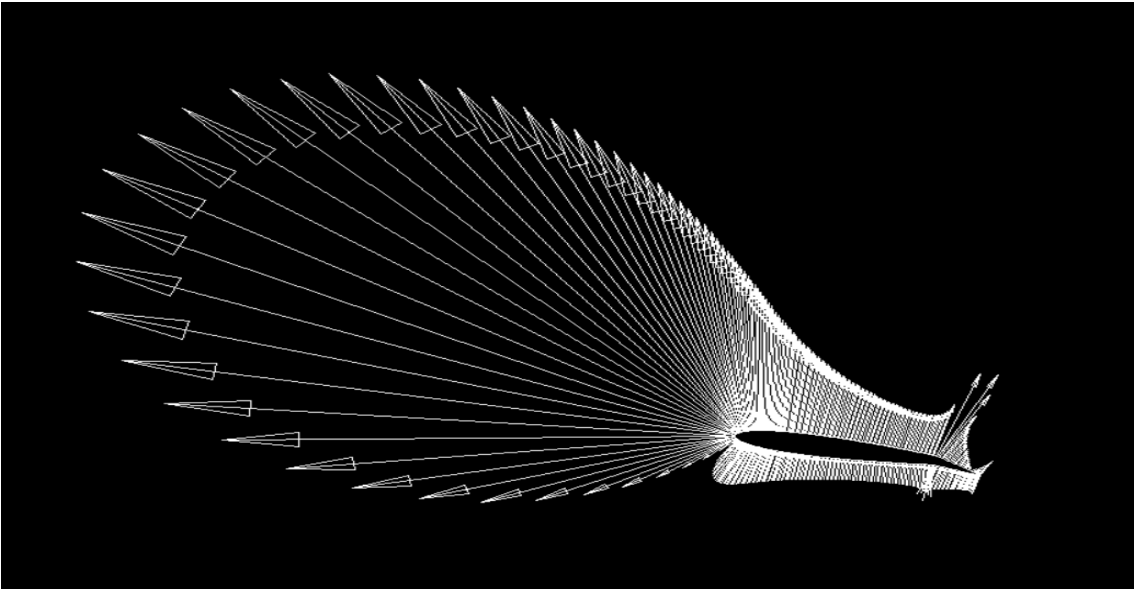


Figure 3.8 : Vectoral Cp values of 20% flapped blade at 10 degree collective

4. NUMERICAL IMPEMENTATION

We give the necessary information about the aerodynamic theories and helicopter morphign blade techniques. Now its time to implement existing theories and morphing blade ideas to the computer code.

4.1 Rotor Specifications

The rotor blade is a test blade that is used in our rotorcraft technology laboratory to make hover testing on. Blade charecteristics are selected through scaling and the dimensions of the room that is used to conduct the tests are the limiting factors.

Rotor blade specifications are listed in the Table 4.1.

Table 4.1 : Rotor blade specifications

Specification of Blade	Corresponding Value
Blade Profile	Naca 0012
Blade radius (m)	0.7
Root cut out (m)	0.1
Blade cord (m)	0.06
Number of blades	4
Solidity	0.0935
Rpm	1500

4.2 Look Up Table and Xfoil

Xfoil is a program which developed by MIT professor Mark Drela (Mueller, T. J. (Ed.), 1989). It is a 2-D airfoil solver using panel method to calculate the aerodynamic parameters. It can be used to find selected airfoil polars. It can also calculate for viscous and inviscid flow cases. For viscous cases the reynolds number and mach

number can be input of the program. Program found these parameters by finding the pressure distribution of airfoil.

In the Figure 4.1 and Figure 4.2, pressure coefficient is shown for the upper and lower part of the airfoil. Calculations are conducted with $\alpha = 5^\circ$, $Re = 400000$ and the airfoil profile was Naca 0012.

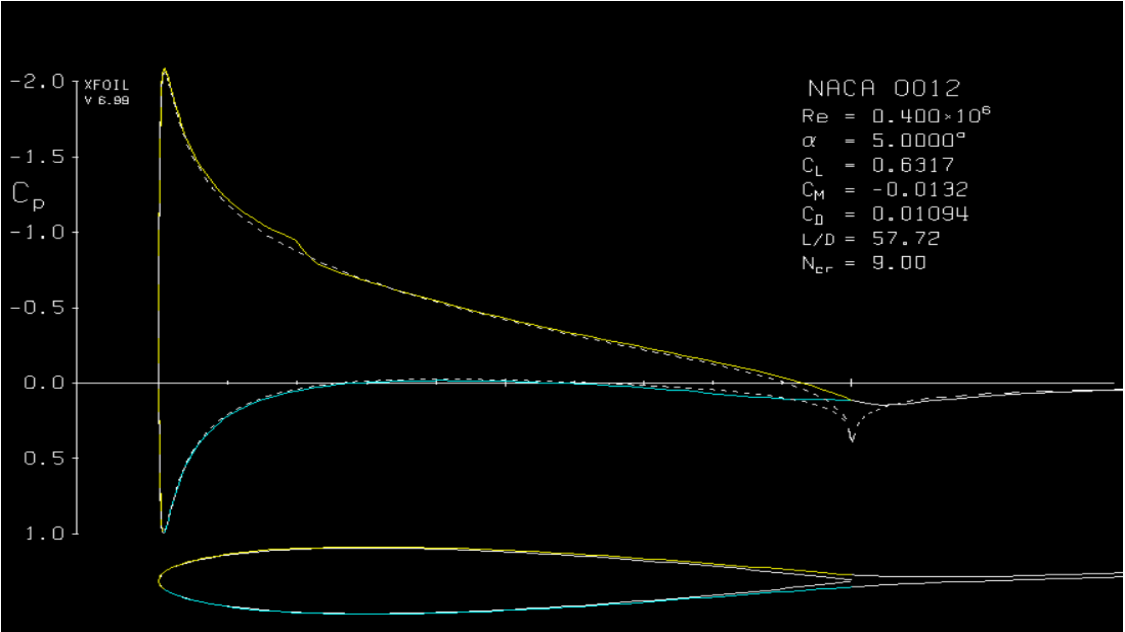


Figure 4.1 : Xfoil Naca 0012 at $Re = 400000$

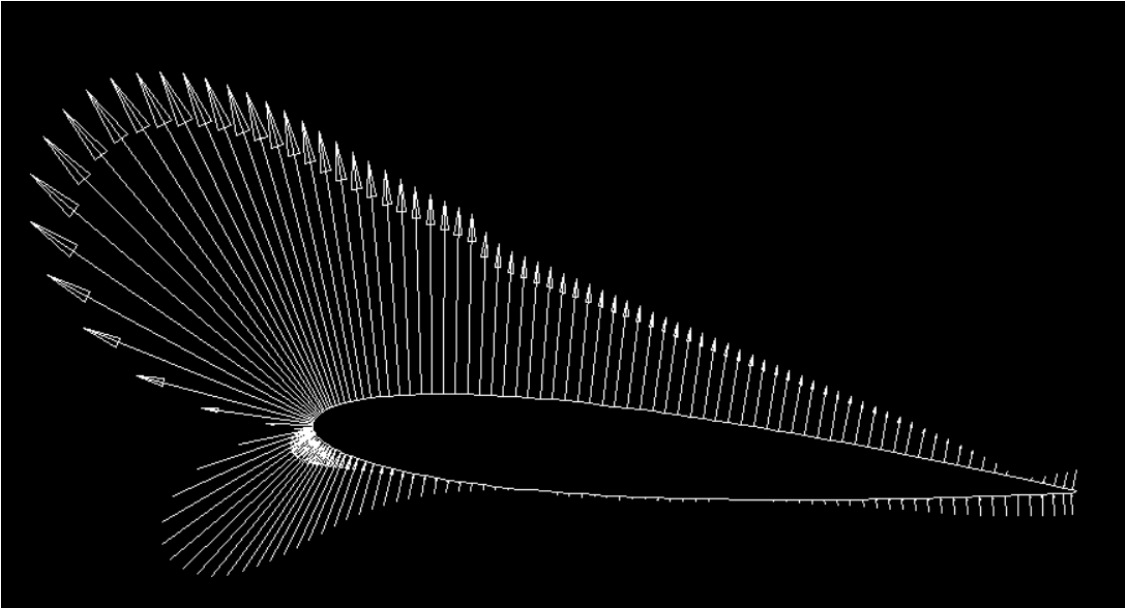


Figure 4.2 : Xfoil Naca 0012 at $Re = 400000$, pressure coefficient vectors

There are numerous factors that has an effect on the rotor aerodynamics. However some of them like we give on the rotor specifications section is decided before for our case. Some parameters are changing over the blade section from root to tip. Main parameter that changes is tangential velocity for every section. It defined as angular velocity times radial distance from the rotation axis. This means that tangential velocity is linearly increasing from root to tip. Because this type of change effects rotor blade sectional properties, rotor balde calculations are needed to be done sectionally. BET calculations requires basically the 2-D aerodynamic characteristics of each airfoil sections of the rotor balde.

At the same environment and nontapered blade the only value is changing is velocity. Changing of the tangential velocity has an effect on the Re.

$$Re = \frac{\rho U_T c}{\mu} \quad (4.1)$$

Changing Re effects the lift and drag polars of the airfoils. This means that for every section these values are changing.

Thus, to make more realistic calculations, a table that has the necessary aerodynamic value for every section can be used. Because, every little change in the radial direction has an impact on the aerodynamic characteristic (Leishman, 2006).

4.2.1 Blade section airfoil polars

While creating the look up table, there are some important points to consider. We are dealing with the blade lift and power characteristics over the rotor blade. Especially in this part of the thesis, we are dealing with the lift and drag polars. Firstly, the balde divided by 6 sections and used the velocity that is beginning and end of that sections to calculate the airfoil polars (see Figure 4.3).

Xfoil program is used to calculate the necessary values. Re and M numbers of every calculation point is given to the Xfoil and polar values are calculated.

The polar values differ from the The polar values are calculated for 7 sections from the angle of attack value of 0 to 12 for twisted blade and for flapped blade. The important value that is caculated from tabulated value is lift curve slope. It is calculated between zero to 8 degrees because this region gives better Cla approximation for long

range of angle of attacks (see Figure 4.4). Furthermore, the lift coefficient values against to angle of attack values are varying largely at the portion that has zero to 4 angle of attack.

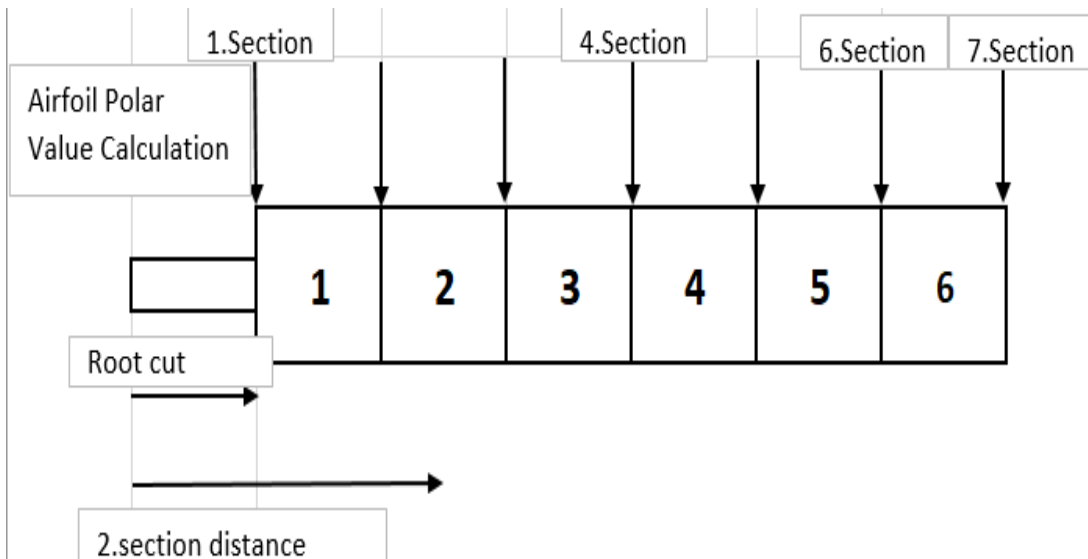


Figure 4.3 : Rotor blade that divided 6 sections

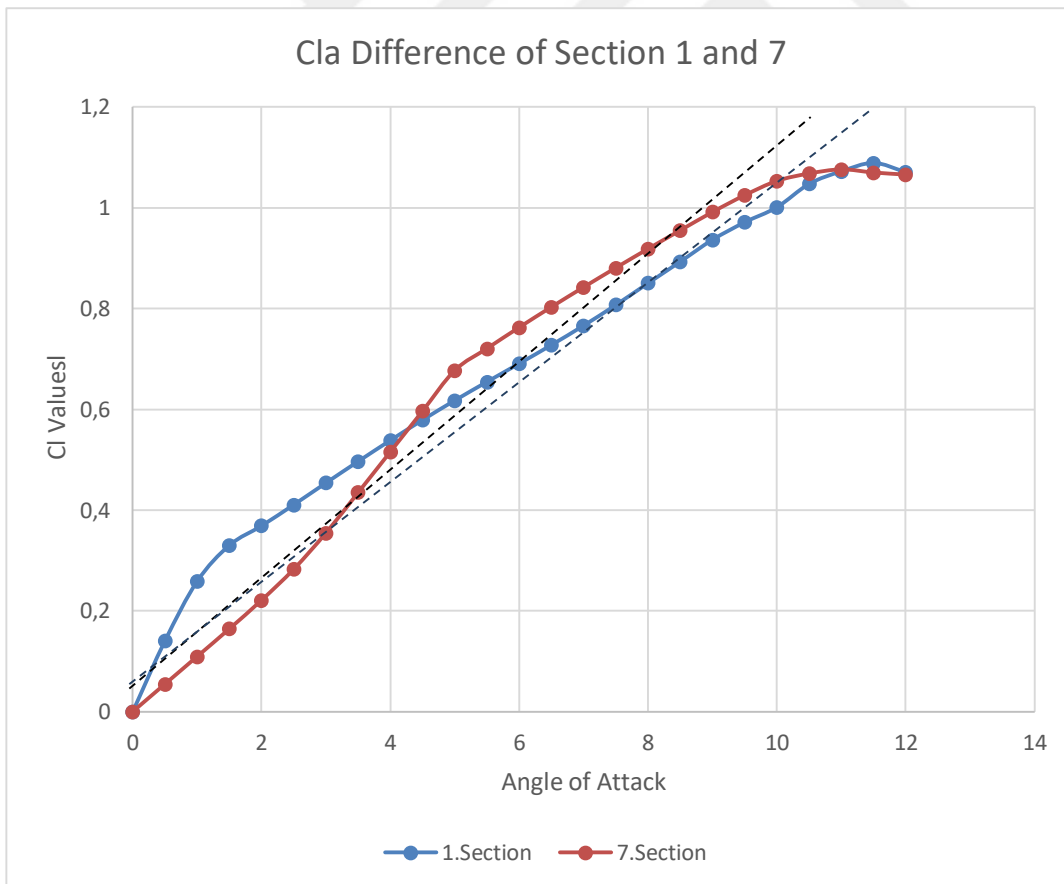


Figure 4.4 : Polar values of 1. and 7. sections

Considering all the informations above, the blade that is divided 240 section to make results more realistic Taking more sections is important to be able to calculate the tip and root section loadings more accurately. The load in the sections changes very rapidly so to see the change for tip portion of the blade needs more blade elements. Dividing the blade as much elements as possible is because to be able to calculate the tip portion tip loss effects. This is shown in Figure 4.5.

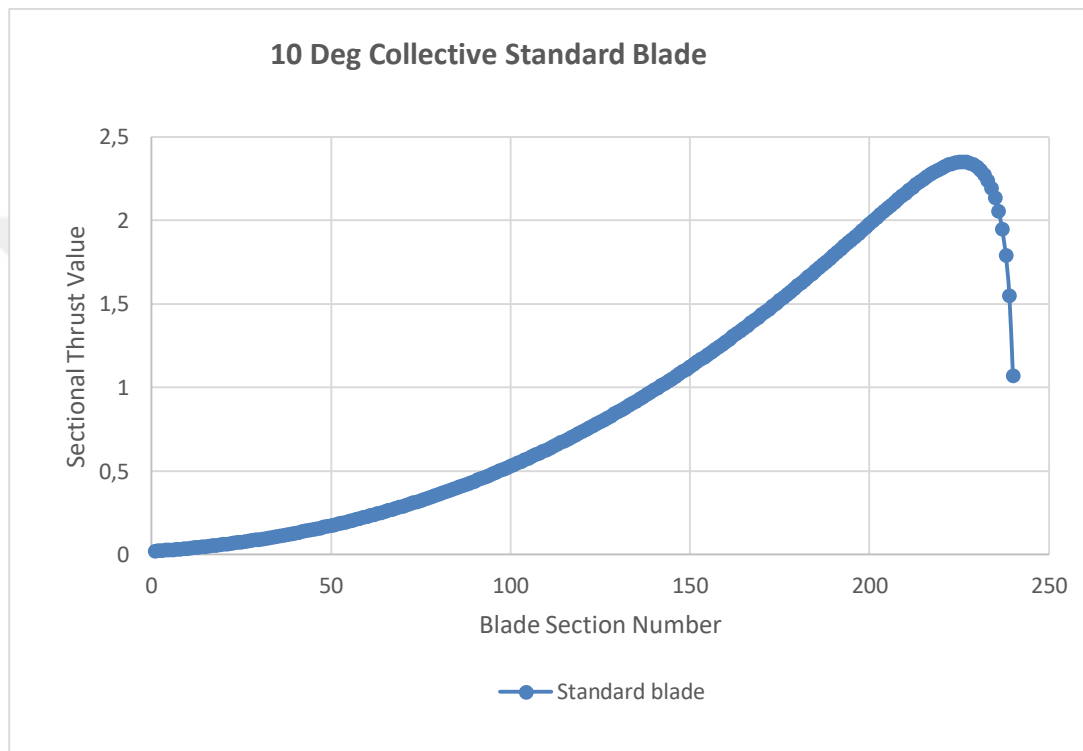


Figure 4.5 : Lift distribution over the rotor blade using BET calculation

4.2.2 C_{la} calculation for more specificity

Generally there are 4 parameters to calculate the inflow ratio and thrust on the blade. Those are solidity, lift curve slope, r and pitch angle of the blade. If blade is not tapered which is in our solution, then solidity is constant. Pitch angle and r is changing over the blade and for each blade section those values are known. Lift curve slope value is generally taken between 5.7-6.3. However, before section we said that airfoil polar specifications are changing radially over the rotor blade because Re is changing. Thus, radial velocity change effects the C_{la} . This specifications can be seen in the Figure 4.6. Airfoil polars are calculated for 7 blade section as it is mentioned.

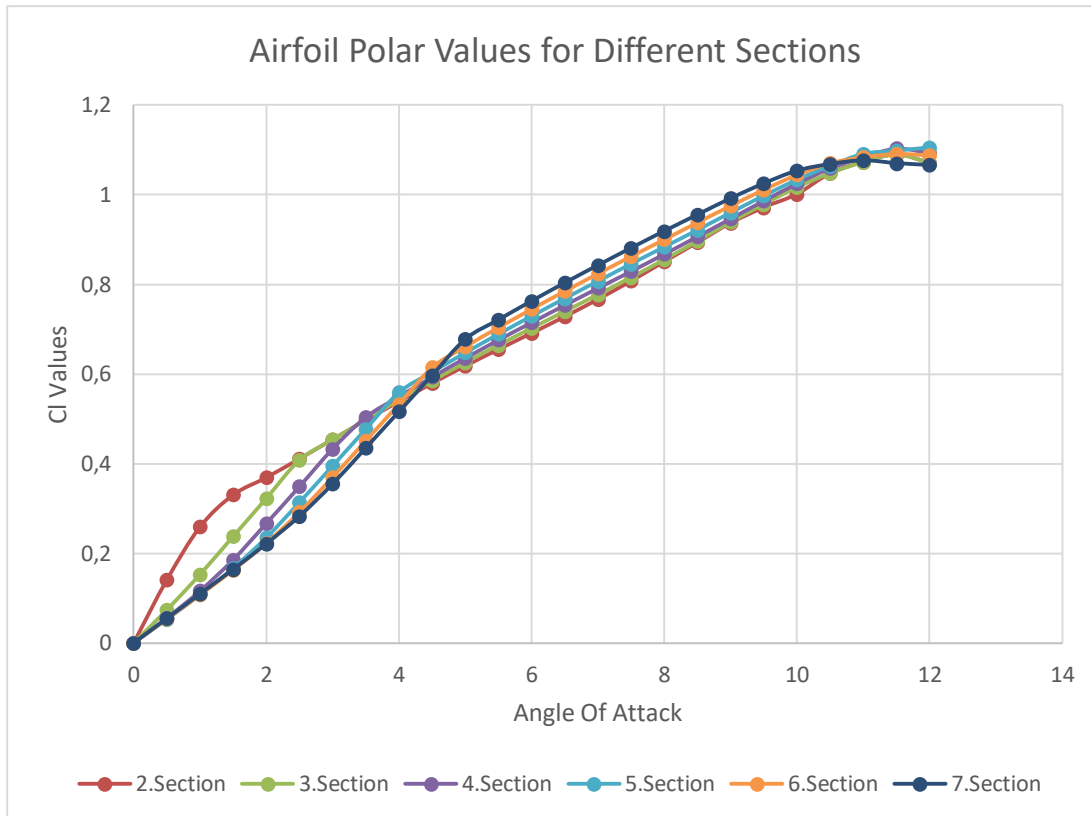


Figure 4.6 : Sectional polar values for all sections

Calculating induced velocity and Cl values for every section based on the constant C_{la} value can be a basic and fast approach. However, for different blade sections that prespecified C_{la} value can cause errors. In the Figure 4.7, it can be easily seen that linear fit to these graphs gives lines with particularly different slopes. That slopes means C_{la} .

It is shown that for different blade sections C_{la} differs. What about at the same blade section that has different pitch angle cases? In the calculation of induced inflow using BEMT C_{la} is needed to be prespecified. However, taking the C_{la} constant for every pitch angle cases is not optimal for low Re aerodynamics because, the slope is more steep form zero to nearly four degree angles than the part where angle of attack is bigger.

Induced inflow ratio is calculated for every blade section to find the effective angle of attack. To describe the real Cl value of this section and make inflow calculations correctly, C_{la} needed to be calculated according to given blade pitch. C_{la} value needs to be calculated to give proper Cl value at this conditions.

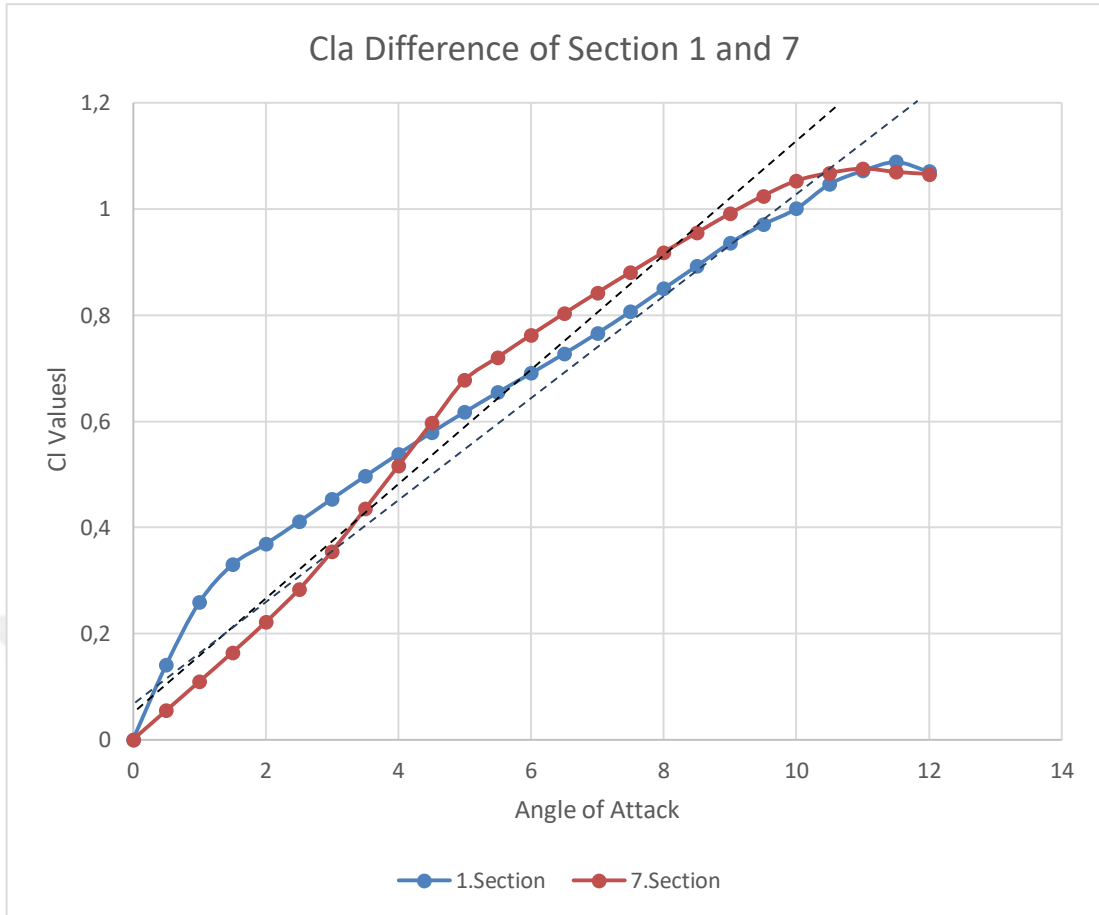


Figure 4.7 : Different Cla values for different pitch angles at a specific section

If we look at the Figure 4.7, let's say we have a 6 degree pitch angle for this section. In that case, if the black line represents the Cla, this would be the most accurate assumption for this particular blade section and particular pitch angle. Rather than some basic line fit we can just use two different points to define Cla. First point is zero lift angle and second point is the blade sectional pitch angle and its corresponding C_l value.

$$C_{l_a} = \frac{C_l(\theta) - C_l(\alpha_0)}{\theta - \alpha_0} \quad (4.2)$$

After Cla is calculated, induced inflow value can be found radially over the rotor blade with using the equation (2.49).

Cd values are also imported from look up table. It is calculated for every blade section like Cl values and polynomial fit applied to the data. However, even in the stall margin there is not much of a difference that affects curve fitting data badly. In the Figure 4.8, there is the drag polars for the nearest section to the root and the nearest section to the tip.

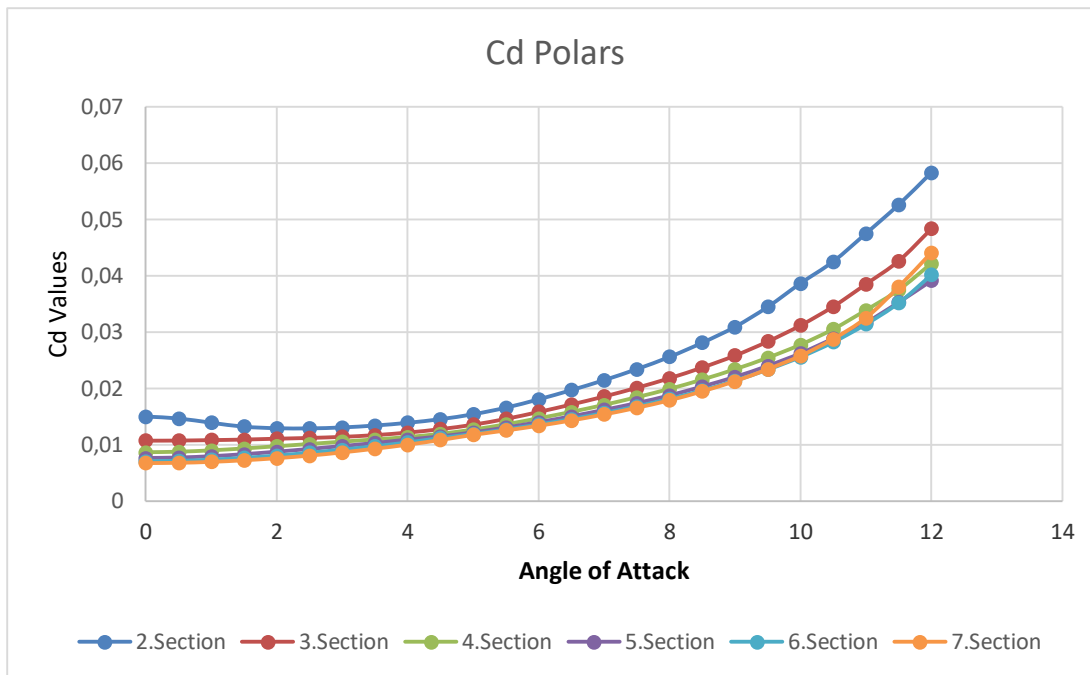


Figure 4.8 : The drag polars for all the section

4.3 Matlab Code Structure

The structure of the code is based on aerodynamic calculation of every section of the helicopter blade. First, atmospheric and geometrical properties of blade and flap section is given to the code. Using these values Re and M numbers are calculated for 7 blade section as shown in Figure 4.3.

To create look up table Xfoil is used to calculate airfoil polar values for these 7 sections. Between these sections airfoil polar values are found by interpolation.

From root to tip blade is divided 240 sections. θ and Cl_a values are specified before the calculations for each section using Xfoil . Twist and flap cases are also included first because they effects the sectional pitch angle. After specifying θ and Cl_a values, BEMT is used to calculate the induced inflow ratio for that section. In the inflow calculations Prandtl tip loss corrections are also included. These calculations gives effective angle of attack for every section of the blade. After calculating effective angle of attack sectional aerodynamic values including thrust, thrust coefficient, power, power coefficient and FM values are calculated using this value. Cl and Cd values are important in the calculations for these values. Look up table that was ready before is used to find those coefficients corresponding to the calculated sectional effective

angle of attack. Lastly, FM value is needed to be calculated to see the aerodynamic efficiency of the rotor blade concepts. Moreover, sectional span is an important parameter. While calculating the 2-D aerodynamics span is not needed, but at some point these calculations are needed to be represented in 3-D. Thus, for every section the sectional 2-D values are multiplied by the sectional span value besides of dimensionless parameters. Sectional span value blade length divided by number of elements that used in calculations which is 240 in our case. The matlab code structure is shown in Figure 4.9.

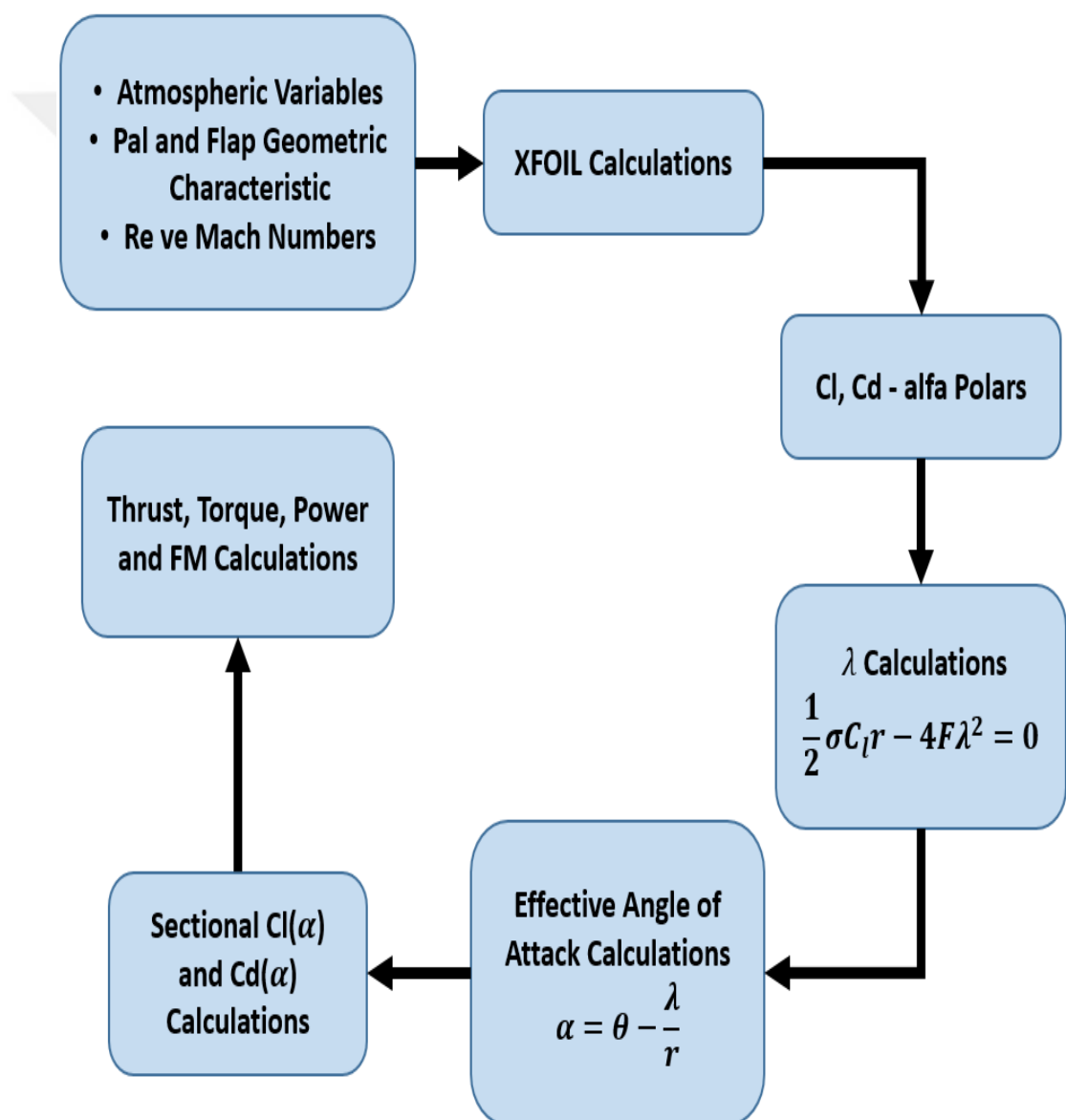


Figure 4.9 : Matlab Code Flow Chart



5. CONCLUSIONS AND RECOMMENDATIONS

5.1 Aerodynamic Properties of the Morphing Blade Concepts

Twist and Flap systems has an effect on the aerodynamic properties of helicopter rotor blade. In this thesis 6 different flapped blade, 1 twisted blade and 1 standard rectangular blade properties are calculated.

The blade specifications in Table 4.1 are used in calculations. All the calculations are done with the collective of $2-10^0$ with 2^0 between them. Linear twisted and flapped blade also has their own specific variables which are linear twist rate and flap deflection angle, respectively.

5.1.1 Flapped blade aerodynamic results

Before giving the results of flapped blade as graphs, this should be known that only the flapped section creates higher thrust values, other sections at the same collective angle creates same sectional thrust. As seen in the Figure 5.1, there are only the blue part of the standart blade is visible because all the section except flapped one has the same sectional thrust and induced inflow ratio values. The invisible blue part is hiding under the red one. While examining the results, it is advisable to keep this explanation in mind.

5.1.1.1 One flap (tip)

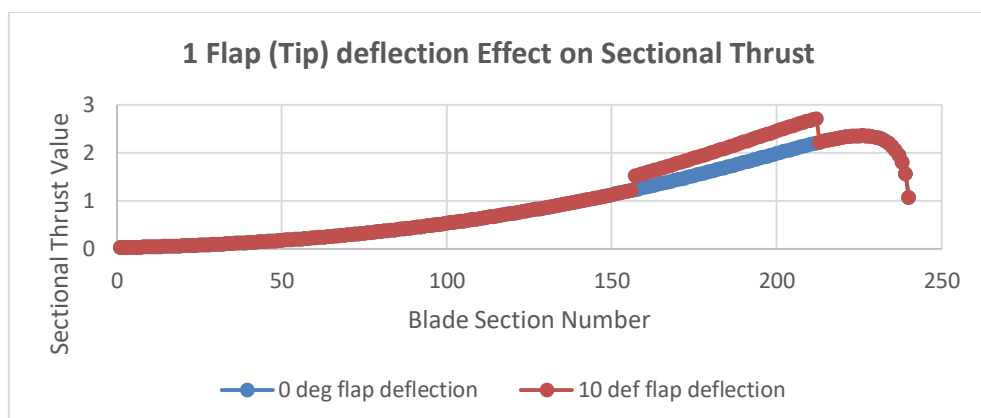


Figure 5.1 : 1 Flap (Tip) deflection Effect on Sectional Thrust

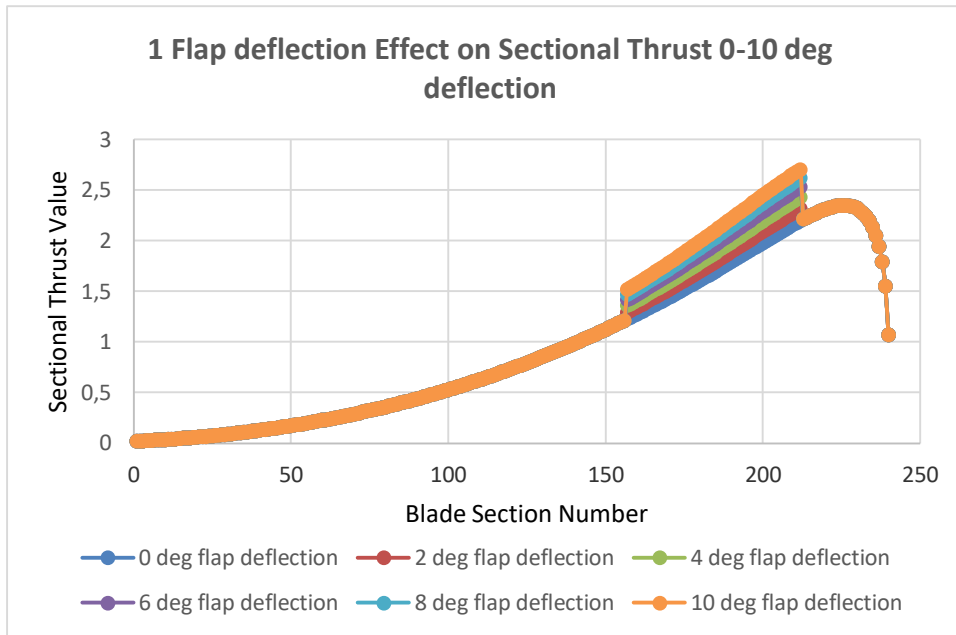


Figure 5.2 : 1 Flap (Tip) deflection Effect on Sectional Thrust 0-10 deg deflection

In the Figure 5.1 unflapped and 10 deg flap deflected blades are compared. The sectional lift of flapped portion is higher than standard blade. In the Figure 5.2 effect of flap deflection of 2 deg is shown.

In the Table 5.1 and Table 5.2 change of aerodynamic values can be seen and it is obvious that flap angle has more effect at higher angle of attack.

Table 5.1 : 1 Flap (Tip) with different flap deflection angles at 4 deg collective

Flap Degree	Thrust	Torque	Power	Ct	Cp
0	60,26	3,36	525,81	0,00159	0,000126
2	61,31	3,43	539,51	0,00162	0,000129
4	62,28	3,51	551,64	0,00165	0,000132
6	63,13	3,58	562,47	0,00167	0,000135
8	63,88	3,66	575,41	0,00169	0,000138
10	64,58	3,77	593,05	0,00171	0,000142

Table 5.2 : 1 Flap (Tip) with different flap deflection angles at 10 deg collective

Flap Degree	Thrust	Torque	Power	Ct	Cp
0	224,96	14,30	2245,46	0,00596	0,000539
2	230,23	14,77	2320,01	0,00610	0,000557
4	235,22	15,23	2391,72	0,00623	0,000574
6	239,68	15,68	2464,51	0,00635	0,000591
8	243,66	16,17	2539,54	0,00646	0,000609
10	247,48	16,64	2613,52	0,00656	0,000627

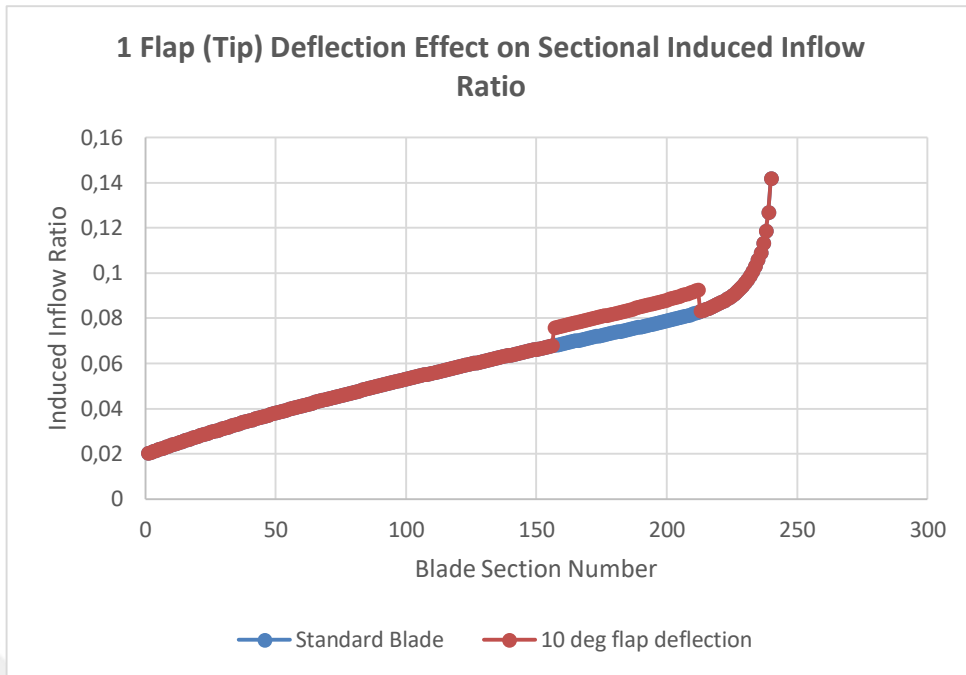


Figure 5.3 : 1 Flap (Tip) Deflection Effect on Sectional Induced Inflow Ratio

As seen in Figure 5.3 the induced inflow ratio of flapped portion of the blade is higher than the standard portion

5.1.1.2 One flap (middle)

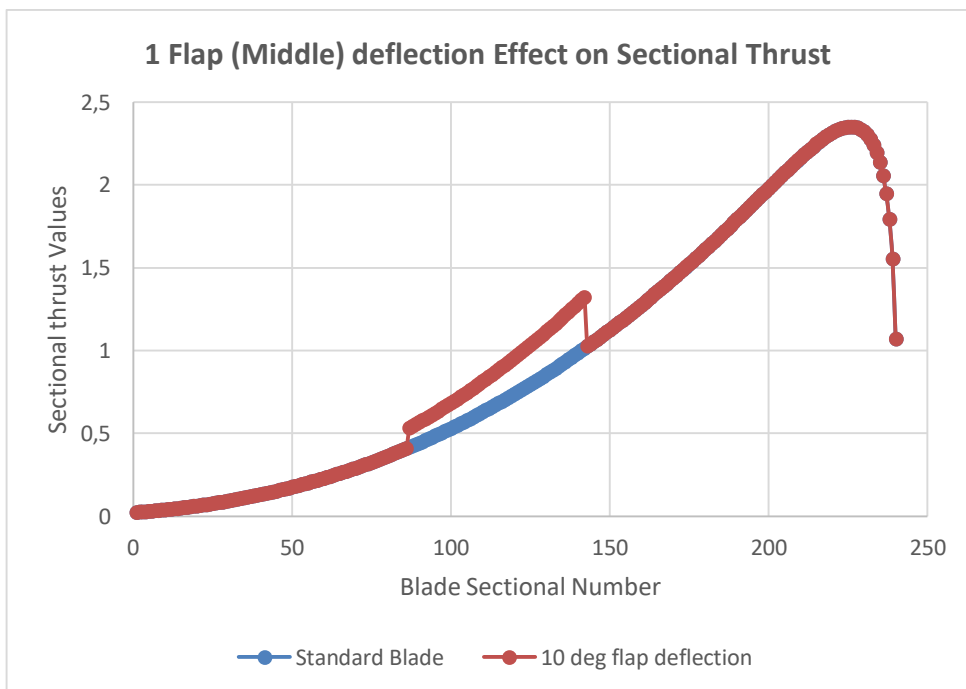


Figure 5.4 : 1 Flap (Middle) deflection Effect on Sectional Thrust

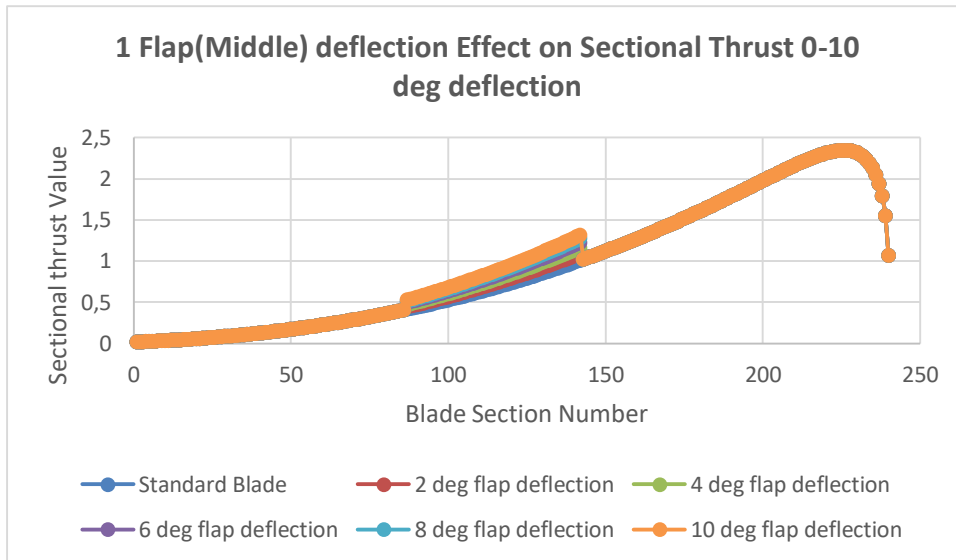


Figure 5.5 : 1 Flap (Middle) deflection Effect on Sectional Thrust 0-10 deg flap deflection

In the Figure 5.4 unflapped and 10 deg flap deflected blades are compared. The sectional lift of flapped portion is higher than standard blade. In the Figure 5.5 effect of flap deflection of 2 deg is shown.

In the Table 5.3 and Table 5.4 change of aerodynamic values can be seen and it is obvious that flap angle has more effect at higher angle of attack

Table 5.3 : 1 Flap (Middle) with different flap deflection angles at 4 deg collective

Flap Degree	Thrust	Torque	Power	Ct	Cp
0	60,26053	3,349555	526,1469	0,001592	0,000126
2	60,78733	3,381256	531,1265	0,001606	0,000127
4	61,2364	3,41817	536,9249	0,001618	0,000129
6	61,61531	3,466447	544,5083	0,001629	0,00013
8	61,89603	3,5658	560,1146	0,001636	0,000134
10	62,12	3,69	579,89	0,001643	0,000139

Table 5.4 : 1 Flap (Middle) with different flap deflection angles at 10 deg collective

Flap Degree	Thrust	Torque	Power	Ct	Cp
0	224,96	14,25	2238,45	0,005962	0,000537
2	227,97	14,45	2270,11	0,006042	0,000545
4	230,65	14,65	2301,25	0,006114	0,000552
6	233,01	14,85	2333,44	0,006177	0,00056
8	234,86	15,05	2364,77	0,006227	0,000567
10	236,43	15,25	2395,77	0,006270	0,000575

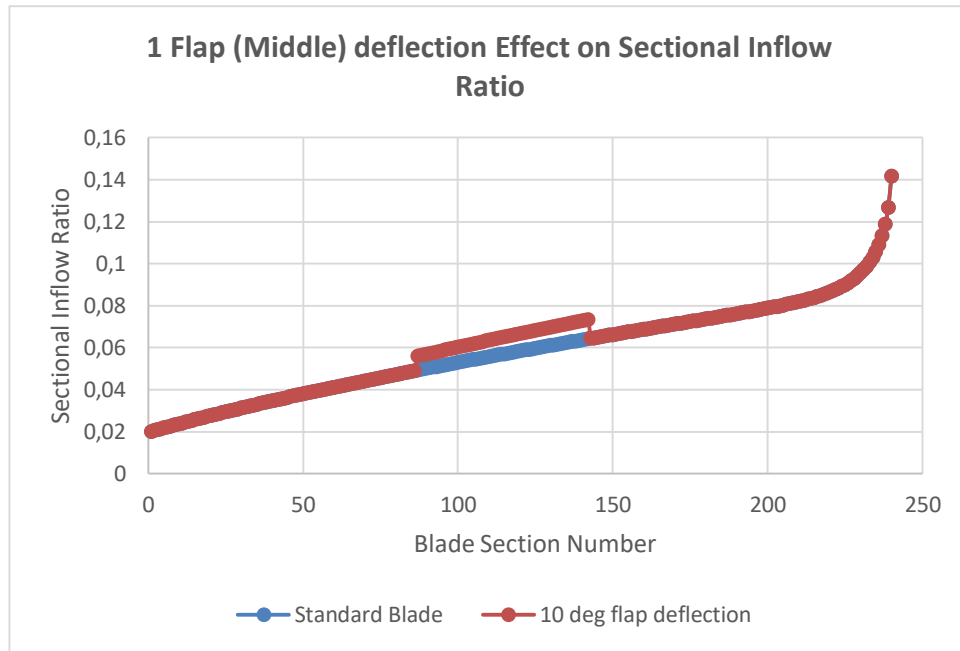


Figure 5.6 : 1 Flap (Middle) deflection Effect on Sectional Inflow Ratio

As seen in Figure 5.6 the induced inflow ratio of flapped portion of the blade is higher than the standard portion

5.1.1.3 One flap (root)

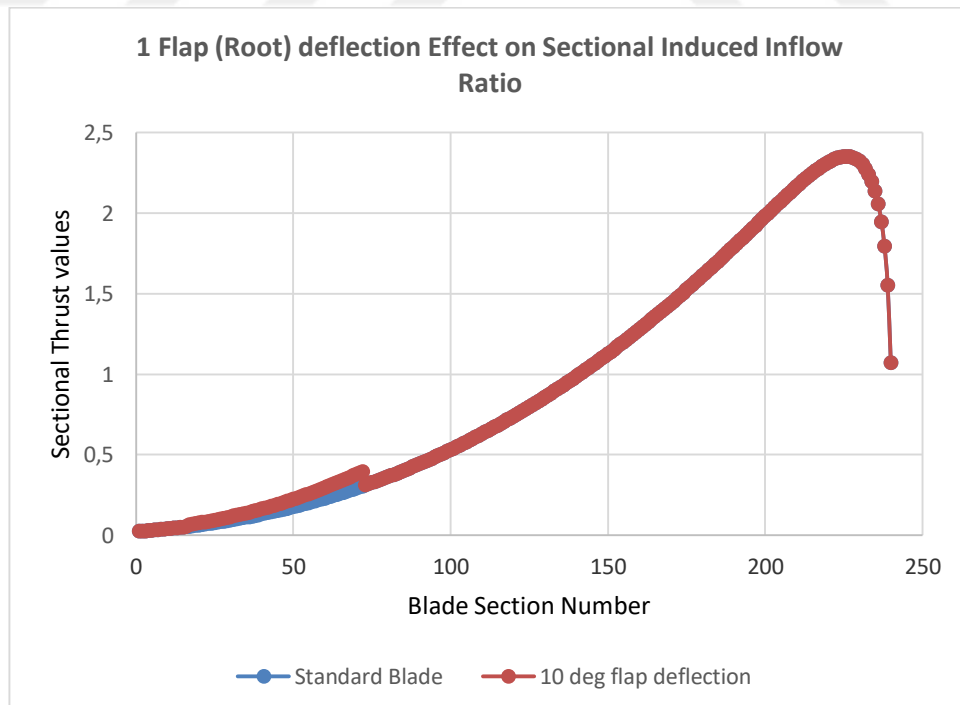


Figure 5.7 : 1 Flap (Root) deflection Effect on Sectional Thrust

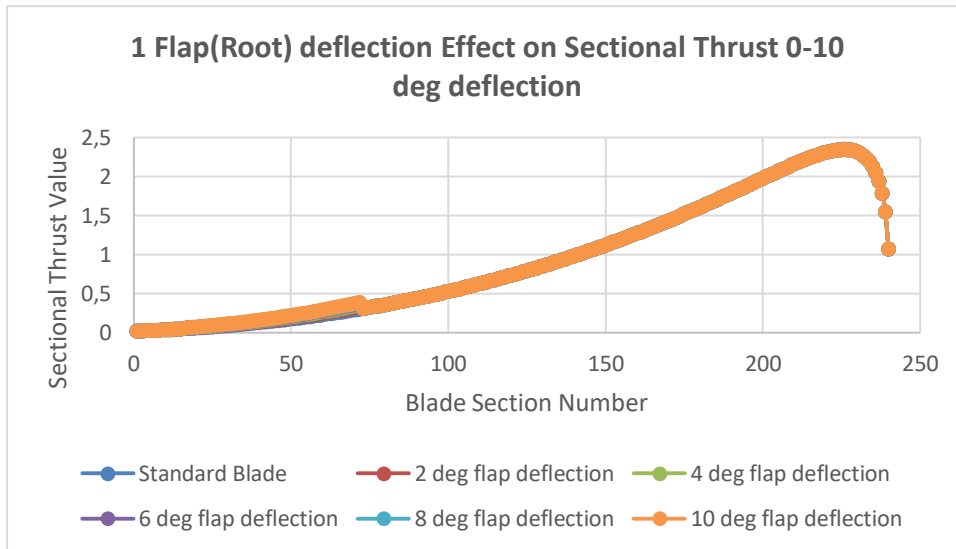


Figure 5.8 : 1 Flap (Root) deflection Effect on Sectional Thrust 0-10 deg flap deflection

In the Figure 5.7 unflapped and 10 deg flap deflected blades are compared. The sectional lift of flapped portion is higher than standard blade. In the Figure 5.8 effect of flap deflection of 2 deg is shown.

In the Table 5.5 and Table 5.6 change of aerodynamic values can be seen and it is obvious that flap angle has more effect at higher angle of attack

Table 5.5 : 1 Flap (Root) with different flap deflection angles at 4 deg collective

Flap Degree	Thrust	Torque	Power	Ct	Cp
0	60,26	3,35	526,14	0,001592	0,000126
2	60,37	3,36	527,17	0,001595	0,000126
4	60,45	3,37	529,70	0,001598	0,000127
6	60,51	3,39	533,66	0,001599	0,000128
8	60,54	3,42	538,39	0,001600	0,000129
10	60,56	3,45	542,42	0,001601	0,00013

Table 5.6 : 1 Flap (Root) with different flap deflection angles at 10 deg collective

Flap Degree	Thrust	Torque	Power	Ct	Cp
0	224,9632	14,25041	2238,45	0,005962	0,000537
2	225,7336	14,28536	2243,94	0,005982	0,000538
4	226,3791	14,32328	2249,895	0,006	0,00054
6	226,8573	14,3572	2255,223	0,006013	0,000541
8	227,1799	14,38933	2260,27	0,006022	0,000542
10	227,38	14,42	2266,38	0,00603	0,000608

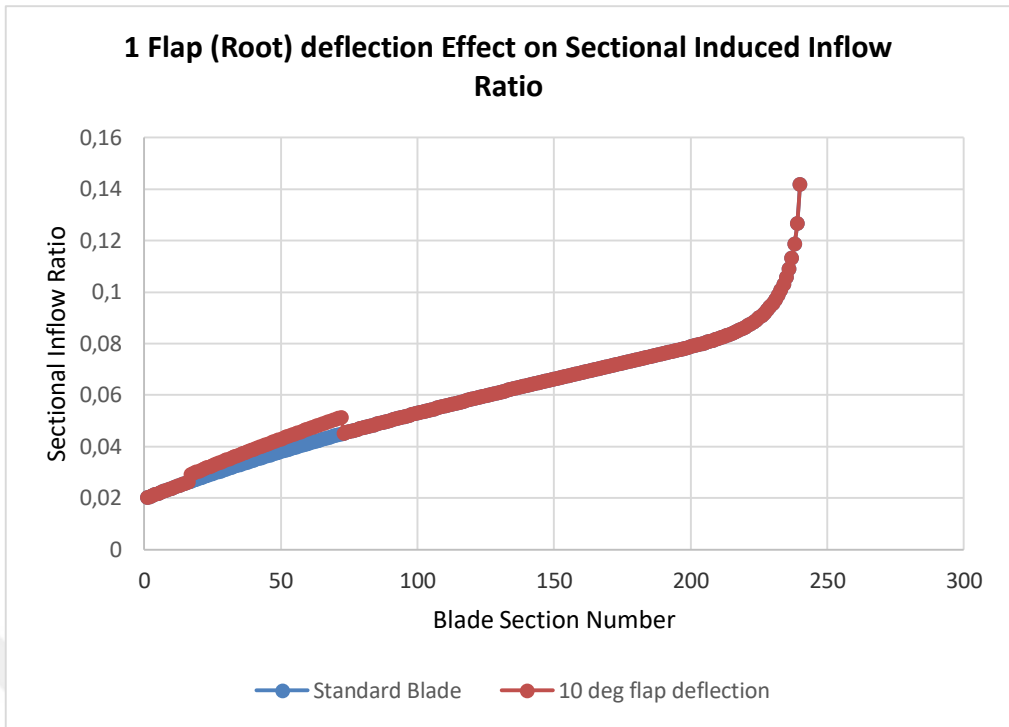


Figure 5.9 : 1 Flap (Root) deflection Effect on Sectional Inflow Ratio

As seen in Figure 5.9 the induced inflow ratio of flapped portion of the blade is higher than the standard portion

5.1.1.4 Two flap (tip, middle)

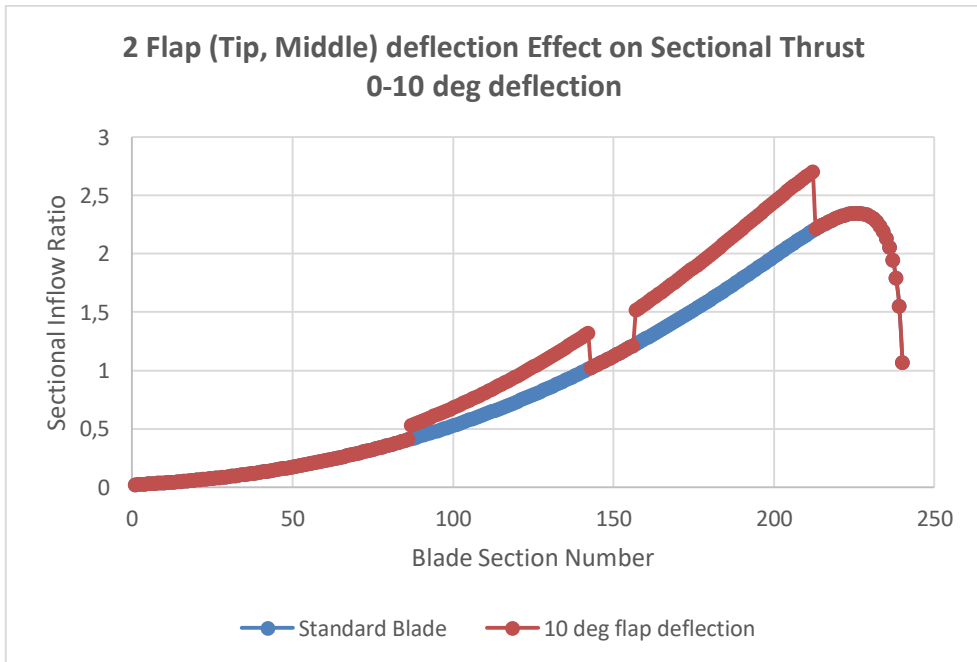


Figure 5.10 : 2 Flap (Tip, Middle) deflection Effect on Sectional Thrust

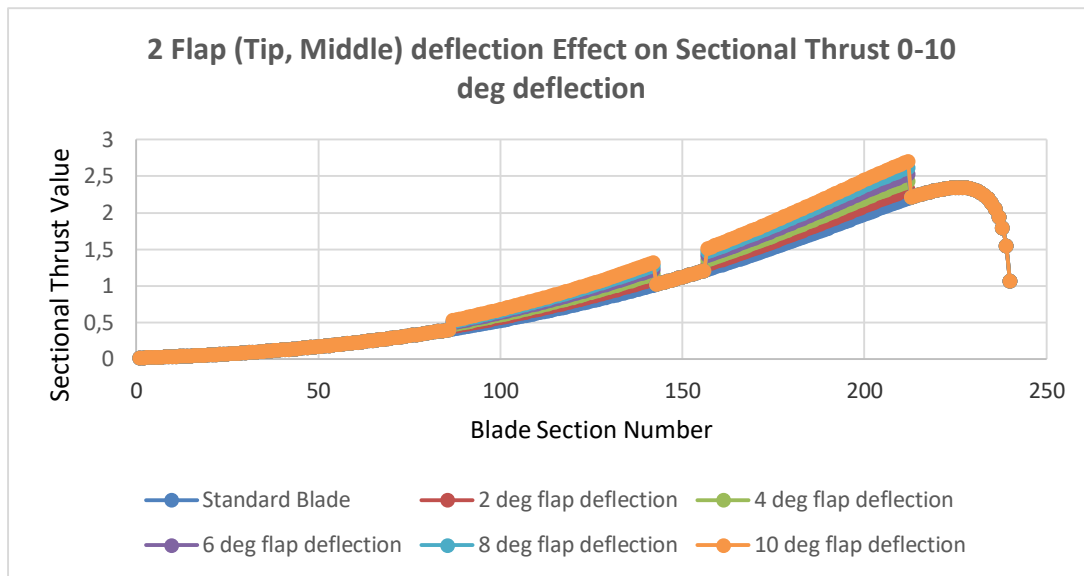


Figure 5.11 : 2 Flap (Tip, Middle) deflection Effect on Sectional Thrust 0-10 deg flap deflection

In the Figure 5.10 unflapped and 10 deg flap deflected blades are compared. The sectional lift of flapped portion is higher than standard blade. In the Figure 5.11 effect of flap deflection of 2 deg is shown.

In the Table 5.7 and Table 5.8 change of aerodynamic values can be seen and it is obvious that flap angle has more effect at higher angle of attack

Table 5.7 : 2 Flap (Tip, Middle) with different flap deflection angles at 4 deg collective

Flap Degree	Thrust	Torque	Power	Ct	Cp
0	60,26	3,36	525,81	0,00159	0,000126
2/3	61,84	3,467949	544,7441	0,001634	0,00013
4/6	63,23	3,585549	563,2167	0,001672	0,000135
6/9	64,49	3,694313	580,3014	0,001705	0,000139
8/12	65,53	3,767	591,719	0,001732	0,000142
10/15	66,48	3,81	598,98	0,001757	0,000143

Table 5.8 : 2 Flap (Tip, Middle) with different flap deflection angles at 10 deg collective

Flap Degree	Thrust	Torque	Power	Ct	Cp
0	224,96	14,30	2245,46	0,00596	0,000539
2/3	233,24	14,97	2351,96	0,006182	0,000564
4/6	240,91	15,63	2454,66	0,006387	0,000589
6/9	247,72	16,29	2559,95	0,006569	0,000614
8/12	253,56	16,98	2667,68	0,006726	0,000640
10/15	258,94	17,66	2774,23	0,006871	0,000666

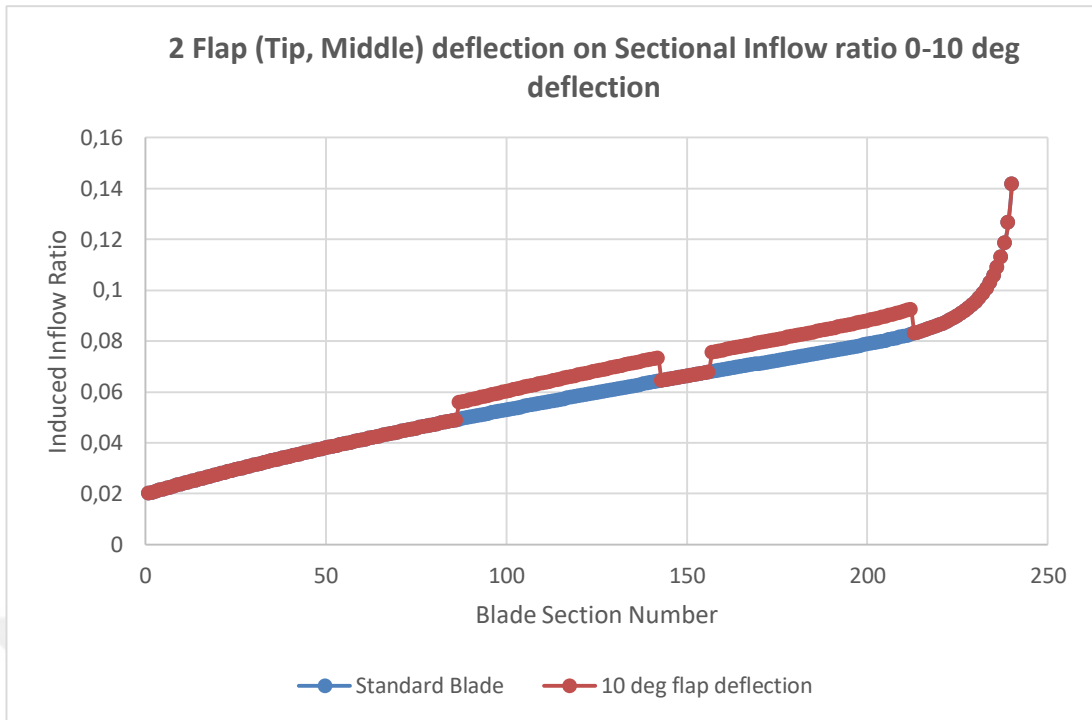


Figure 5.12 : 2 Flap (Tip, Middle) deflection Effect on Sectional Inflow Ratio

As seen in Figure 5.12 the induced inflow ratio of flapped portion of the blade is higher than the standard portion

5.1.1.5 Two flap (middle, root)

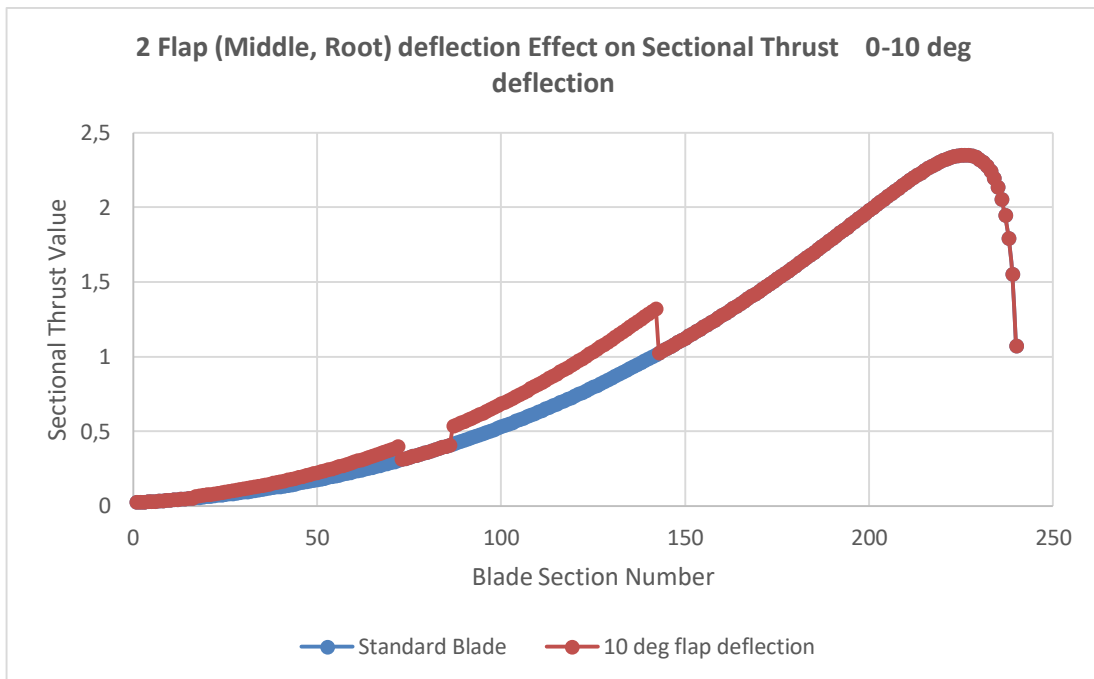


Figure 5.13 : 2 Flap (Middle, Root) deflection Effect on Sectional Thrust

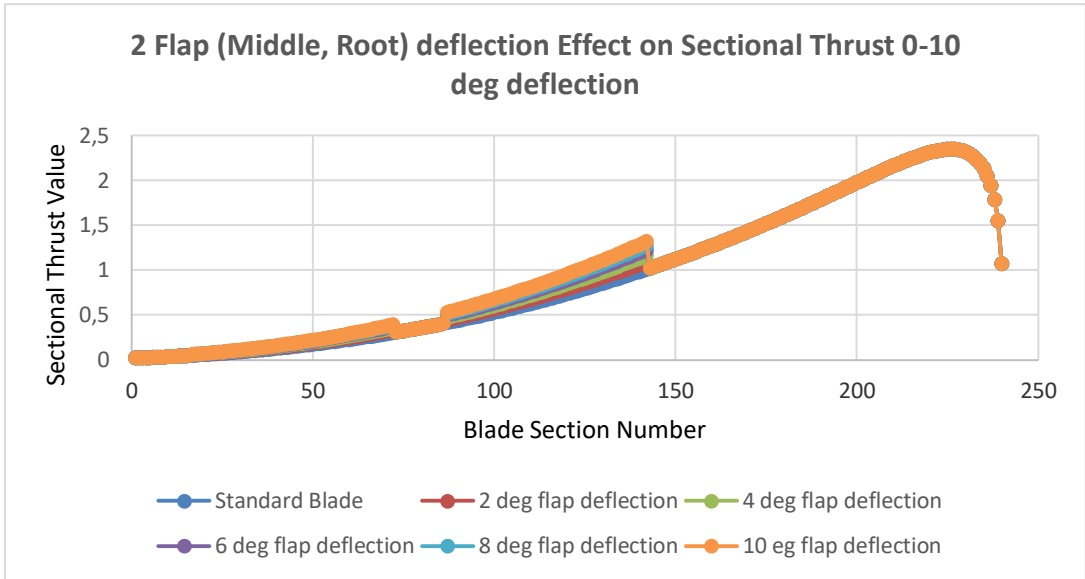


Figure 5.14 : 2 Flap (Middle, Root) deflection Effect on Sectional Thrust 0-10 deg flap deflection

In the Figure 5.13 unflapped and 10 deg flap deflected blades are compared. The sectional lift of flapped portion is higher than standard blade. In the Figure 5.14 effect of flap deflection of 2 deg is shown.

In the Table 5.9 and Table 5.10 change of aerodynamic values can be seen and it is obvious that flap angle has more effect at higher angle of attack

Table 5.9 : 2 Flap (Middle, Root) with different flap deflection angles at 4 deg collective

Flap Degree	Thrust	Torque	Power	Ct	Cp
0	60,26	3,36	525,81	0,001590	0,000126
3/4	60,89	3,39	532,36	0,001609	0,000128
6/8	61,43	3,45	541,76	0,001624	0,00013
9/12	61,86	3,53	555,24	0,001635	0,000133
12/16	62,19	3,56	559,51	0,001644	0,000134
15/20	62,50	3,40	564,87	0,001652	0,000139

Table 5.10 : 2 Flap (Middle, Root) with different flap deflection angles at 10 deg collective

Flap Degree	Thrust	Torque	Power	Ct	Cp
0	224,96	14,30	2245,46	0,00596	0,000539
3/4	228,74	14,53	2282,49	0,006063	0,000548
6/8	232,07	14,76	2318,75	0,006152	0,000556
9/12	234,90	15,02	2356,51	0,006228	0,000565
12/16	237,07	15,24	2394,64	0,006287	0,000574
15/20	258,94	15,49	2774,23	0,006335	0,000584

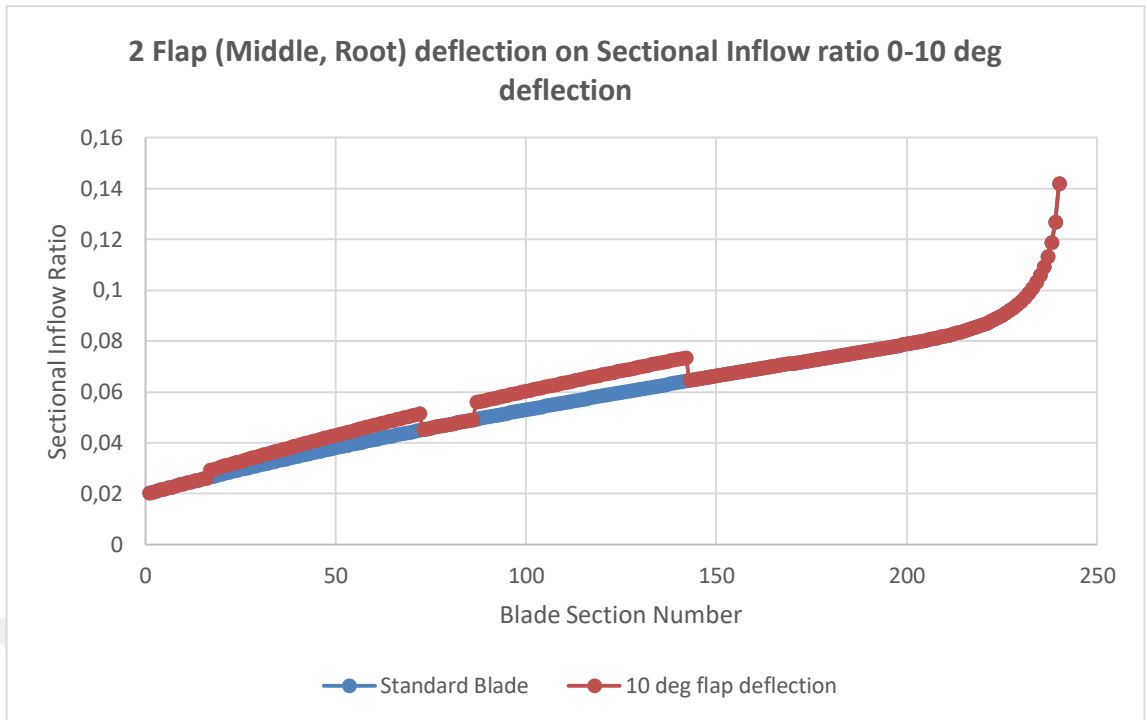


Figure 5.15 : 2 Flap (Middle, Root) deflection Effect on Sectional Inflow Ratio

As seen in Figure 5.15 the induced inflow ratio of flapped portion of the blade is higher than the standard portion

5.1.1.6 Three flap (tip, middle, root)

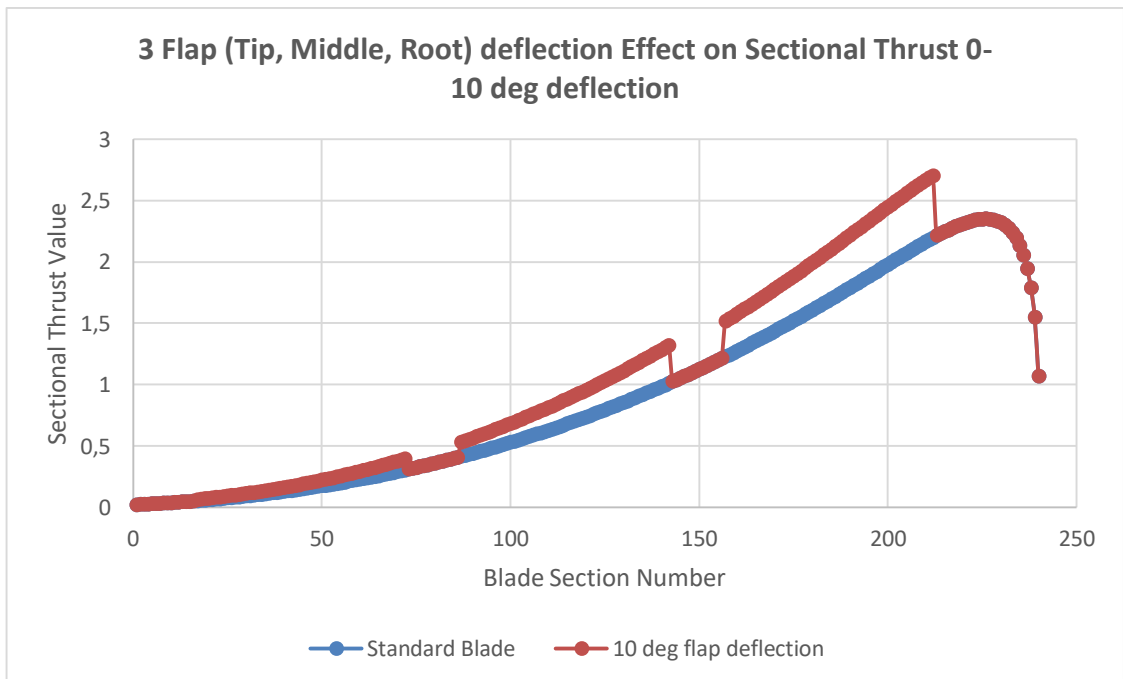


Figure 5.16 : 3 Flap (Tip, Middle, Root) deflection Effect on Sectional Thrust

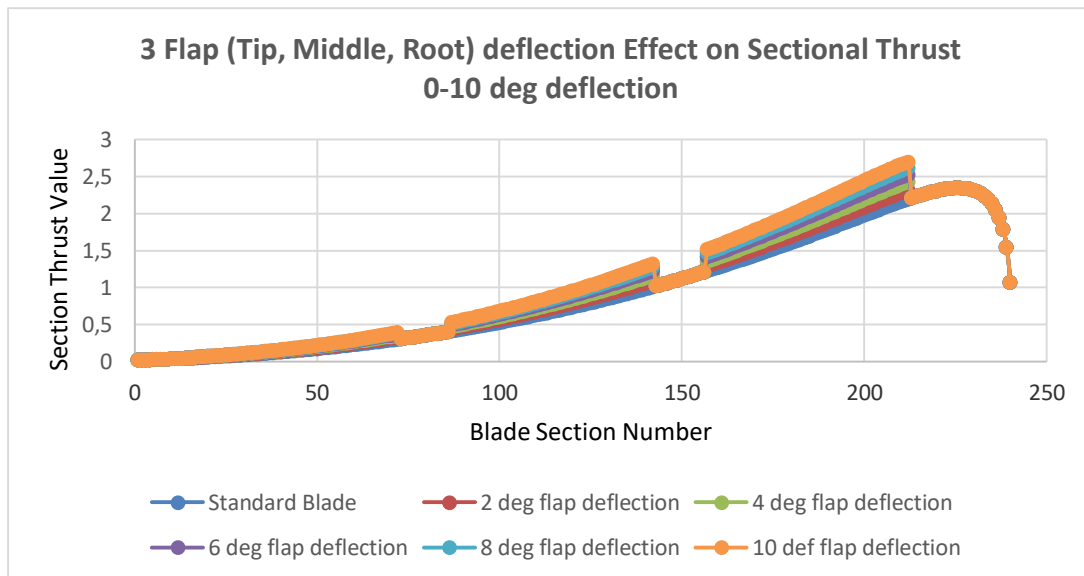


Figure 5.17 : 2 Flap (Tip, Middle, Root) deflection Effect on Sectional Thrust 0-10 deg flap deflection

In the Figure 5.16 unflapped and 10 deg flap deflected blades are compared. The sectional lift of flapped portion is higher than standard blade. In the Figure 5.17 effect of flap deflection of 2 deg is shown.

In the Table 5.11 and Table 5.12 change of aerodynamic values can be seen and it is obvious that flap angle has more effect at higher angle of attack

Table 5.11 : 2 Flap (Tip, Middle, Root) with different flap deflection angles at 4 deg collective

Flap Degree	Thrust	Torque	Power	Ct	Cp
0	60,26	3,36	525,81	0,001590	0,000126
2/3/4	61,95	3,48	546,06	0,001637	0,000131
4/6/8	63,45	3,61	567,59	0,001677	0,000136
6/9/12	64,73	3,77	591,89	0,001712	0,000142
8/12/16	65,81	3,88	609,18	0,001740	0,000146
10/15/20	66,82	4,04	634,03	0,001766	0,000150

Table 5.12 : 2 Flap (Tip, Middle, Root) with different flap deflection angles at 10 deg collective

Flap Degree	Thrust	Torque	Power	Ct	Cp
0	224,96	14,30	2245,46	0,00596	0,000539
2/3/4	234,01	15,01	2357,04	0,006203	0,000565
4/6/8	242,33	15,69	2465,01	0,006425	0,000591
6/9/12	249,62	16,39	2575,55	0,00662	0,000618
8/12/16	255,78	17,12	2688,72	0,006786	0,000645
10/15/20	261,36	17,83	2801,27	0,006937	0,000672

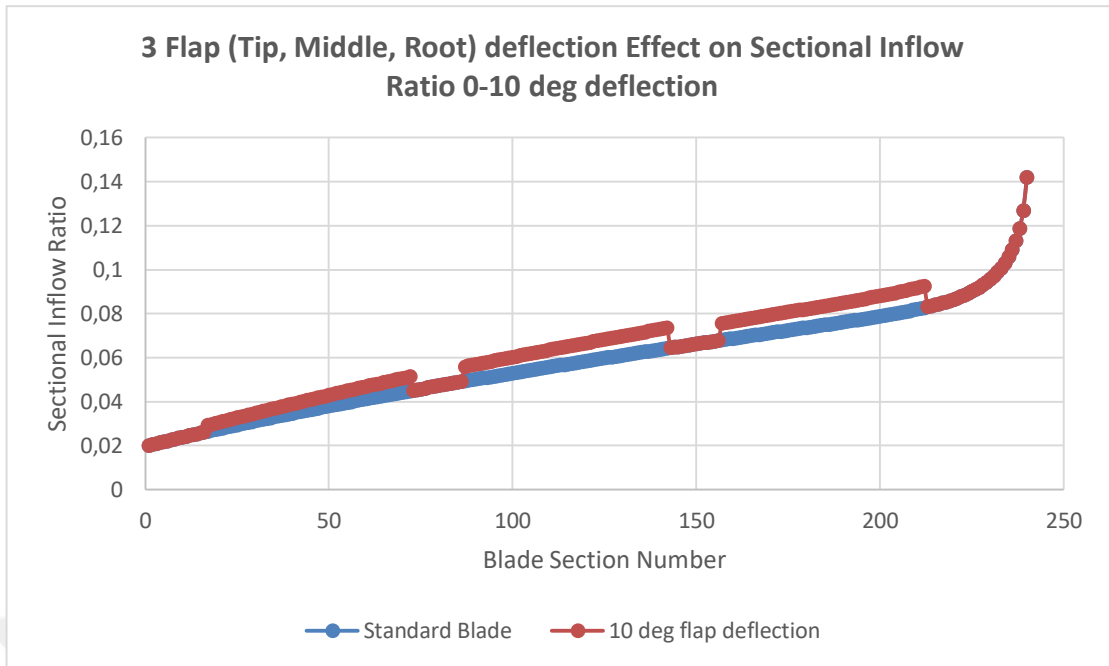


Figure 5.18 : 3 Flap (Tip, Middle, Root) deflection Effect on Sectional Inflow Ratio

As seen in Figure 5.18 the induced inflow ratio of flapped portion of the blade is higher than the standard portion

5.1.1.7 Linear blade twist

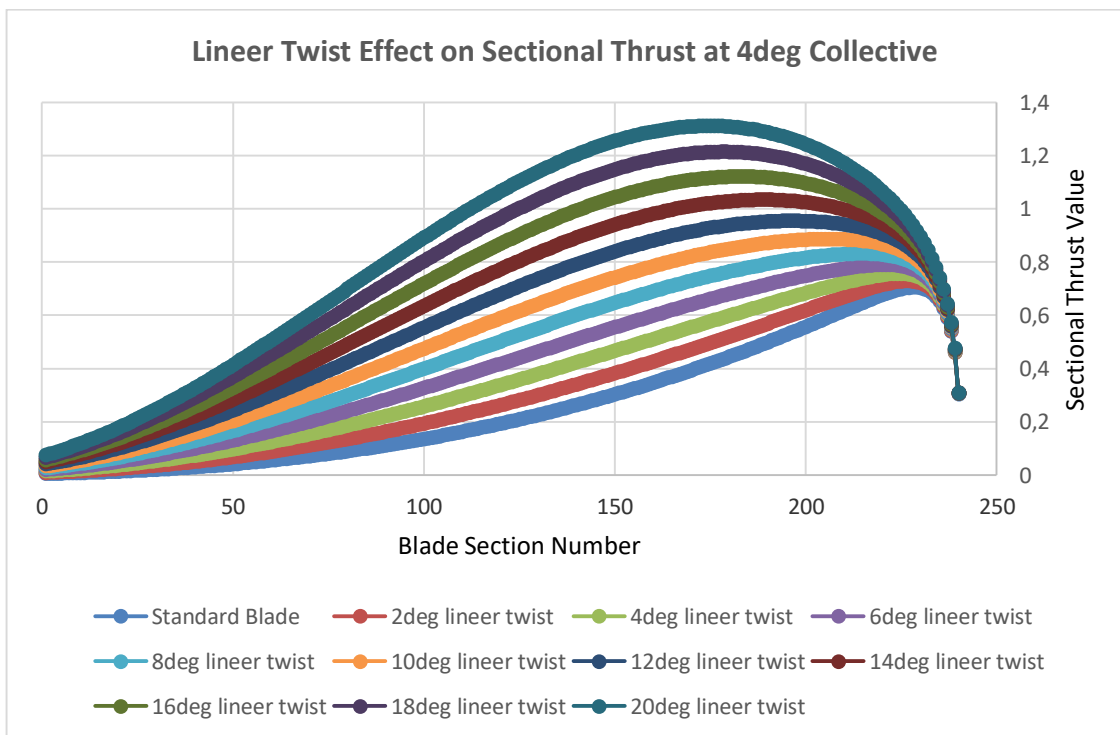


Figure 5.19 : Linear Twist Effect on Sectional Thrust at 4deg Collective

As seen in Figure 5.19 linear twist rate changes the sectional lift distribution and makes it more linear for some optimum twist angle. In table 5.13 aerodynamic the change of aerodynamic values can be seen at the same collective angle.

Table 5.13 : Linear twist with different twist rate values at 4 deg collective

Twist Ratio	Thrust	Torque	Power	Ct	Cp
0	62,29938	3,418765	537,0184	0,001646	0,000129
2	73,78719	3,849596	604,6932	0,00195	0,000145
4	86,0951	4,369332	686,3331	0,002276	0,000164
6	99,09227	4,971008	780,844	0,00262	0,000187
8	112,6784	5,653854	888,1054	0,002981	0,000213
10	126,7748	6,415544	1007,751	0,003355	0,000242
12	141,3173	7,25696	1139,921	0,003742	0,000273
14	156,2532	8,178719	1284,71	0,00414	0,000308
16	171,537	9,183192	1442,492	0,004549	0,000346
18	187,1308	10,27041	1613,273	0,004966	0,000387
20	203,00	11,44	1796,71	0,005391	0,000431

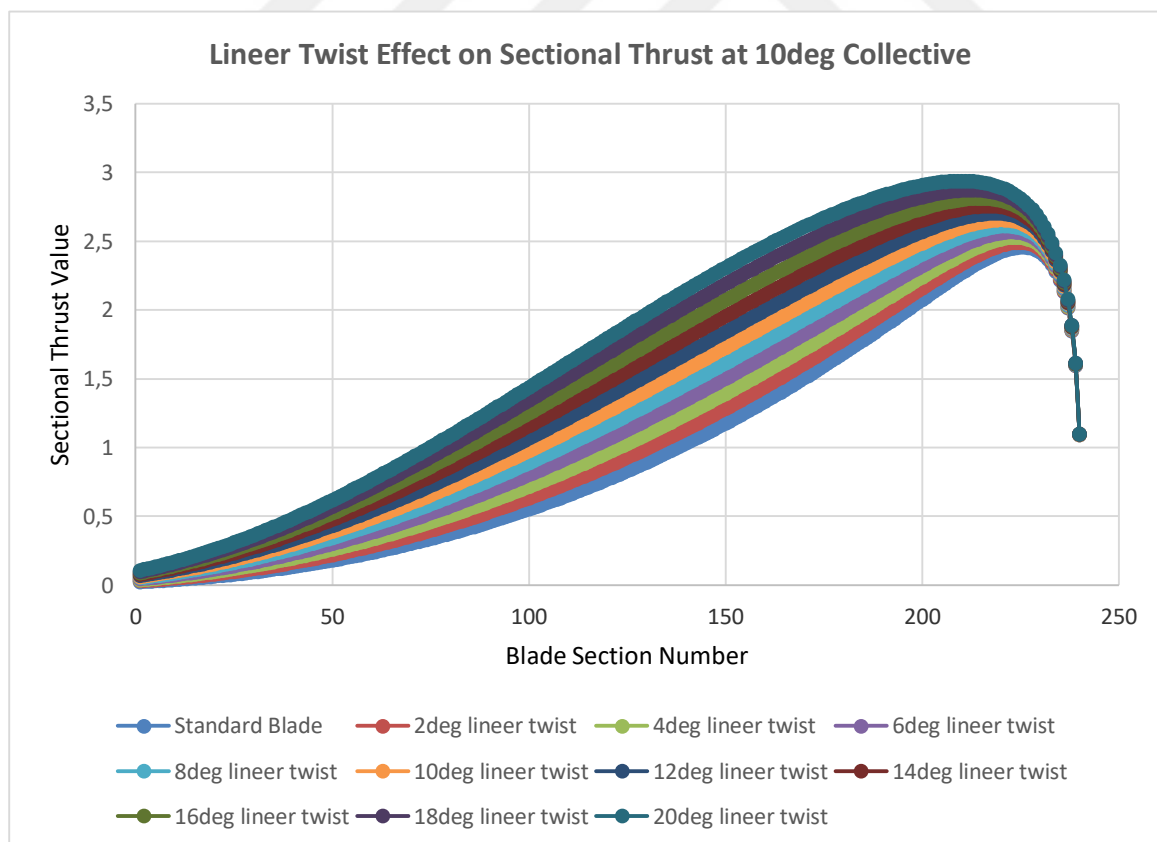


Figure 5.20 : Linear Twist Effect on Sectional Thrust at 10deg Collective

As seen in Figure 5.20 linear twist rate changes the sectional lift distribution and makes it more linear for some optimum twist angle. In table 5.14 aerodynamic the change of aerodynamic values can be seen at the same collective angle.

Table 5.14 : Linear twist with different twist rate values at 10 deg collective

Twist Ratio	Thrust	Torque	Power	Ct	Cp
0	235,1584	15,09151	2370,569	0,00623	0,000569
2	250,8045	16,2459	2551,901	0,00665	0,000612
4	266,7656	17,48209	2746,08	0,00707	0,000659
6	283,0056	18,80067	2953,202	0,00751	0,000709
8	299,4937	20,20056	3173,096	0,00795	0,000762
10	316,2054	21,67753	3405,099	0,00840	0,000817
12	333,1183	23,23046	3649,032	0,00885	0,000876
14	350,2122	24,85978	3904,965	0,00932	0,000938
16	367,4673	26,56774	4173,251	0,00978	0,001003
18	384,862	28,36131	4454,984	0,01026	0,00107
20	402,41	30,21	4745,18	0,01073	0,001141

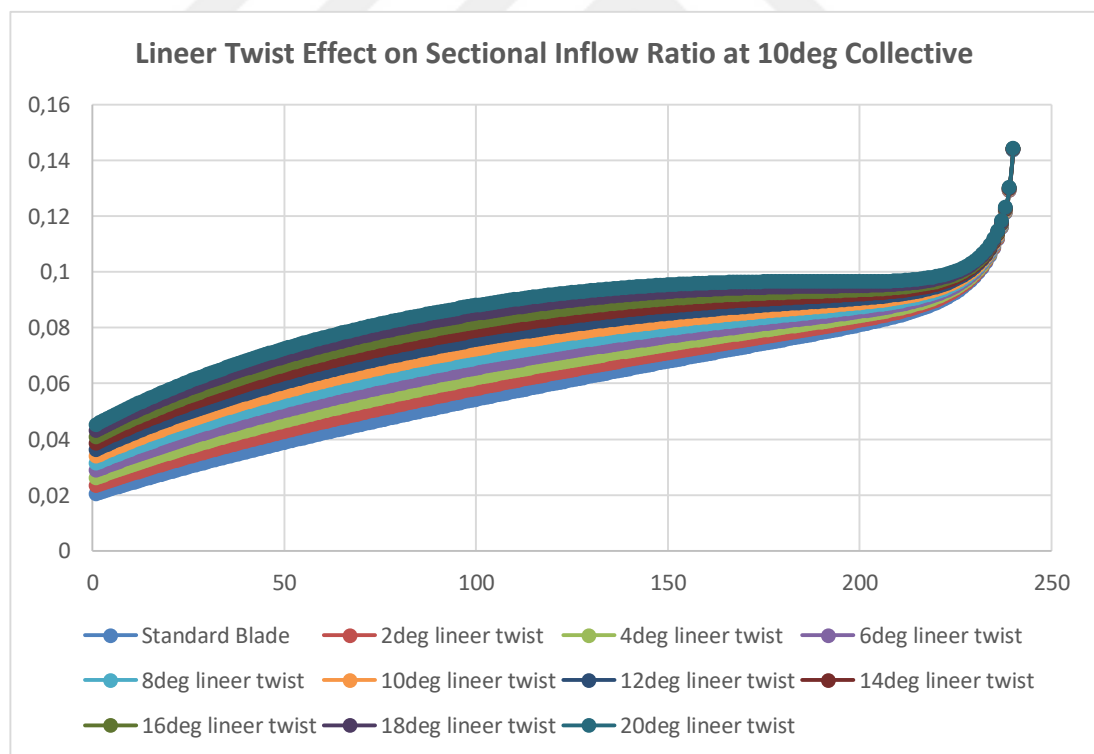


Figure 5.21 : Linear Twist Effect on Sectional Inflow Ratio at 10deg Collective

In the Figure 5.21 the induced inflow ratio can be seen at the same collective angle and different twist ratios.

5.2 Performance Properties of the Morphing Blade Concepts

5.2.1 Flapped blade results

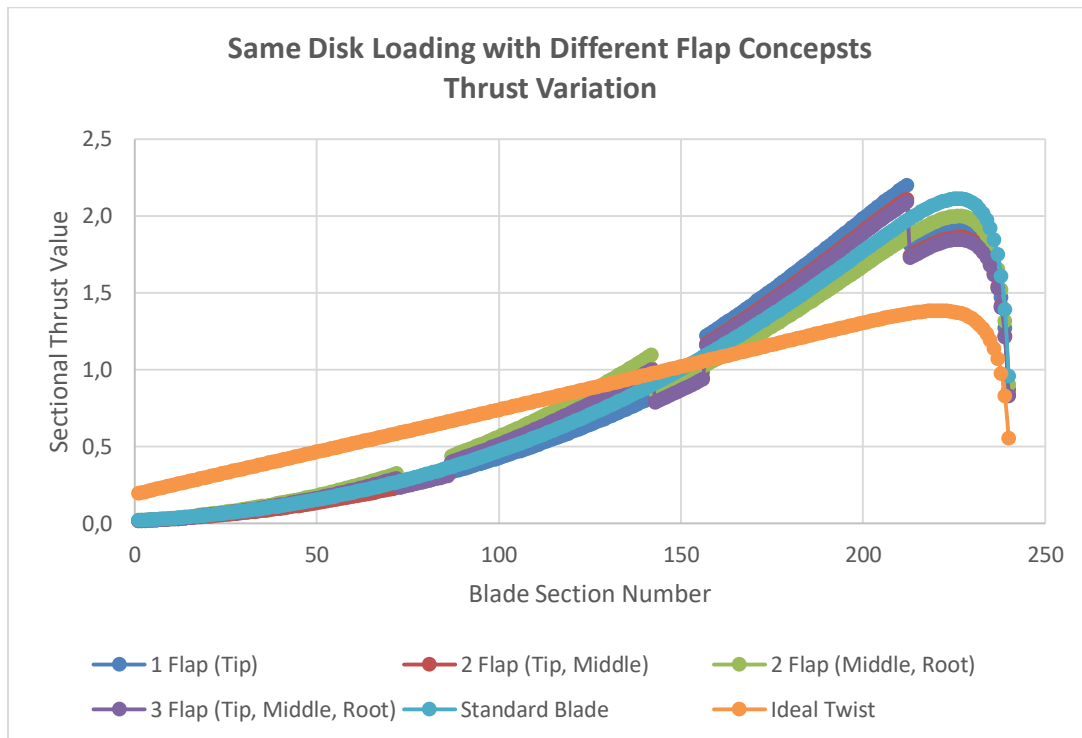


Figure 5.22 : Same Disk Loading with Different Flap Concepts Thrust Variation

In the Figure 5.22 sectional lift distribution at the same disk loading for 6 different flapped blade case is given.

As seen at the Table 5.15 for the same disk loading except thrust all the values differs from each other.

Table 5.15 : Same Disk Loading with Different Flap Concepts Performance Comparison

Flapped Blade Concept	Thrust	Torque	Power	Ct	Cp	FM
Standard Blade	201	12	1910,9	0,0053	0,000462	0,5957
1 Flap (Tip)	200,53	12,59	1978,2	0,0053	0,000474	0,5819
1 Flap (Middle)	200,19	12,22	1920	0,0053	0,00046	0,5932
1 Flap (Root)	200,40	12,17	1921,22	0,0053	0,000458	0,5965
2 Flap (Tip, Middle)	200,60	12,65	1987,7	0,0053	0,000461	0,5793
2 Flap (Middle, Root)	200,47	12,29	1930,9	0,0053	0,000463	0,5913
3 Flap (Tip, Middle, Root)	200,53	12,64	1985,8	0,0053	0,000476	0,5753

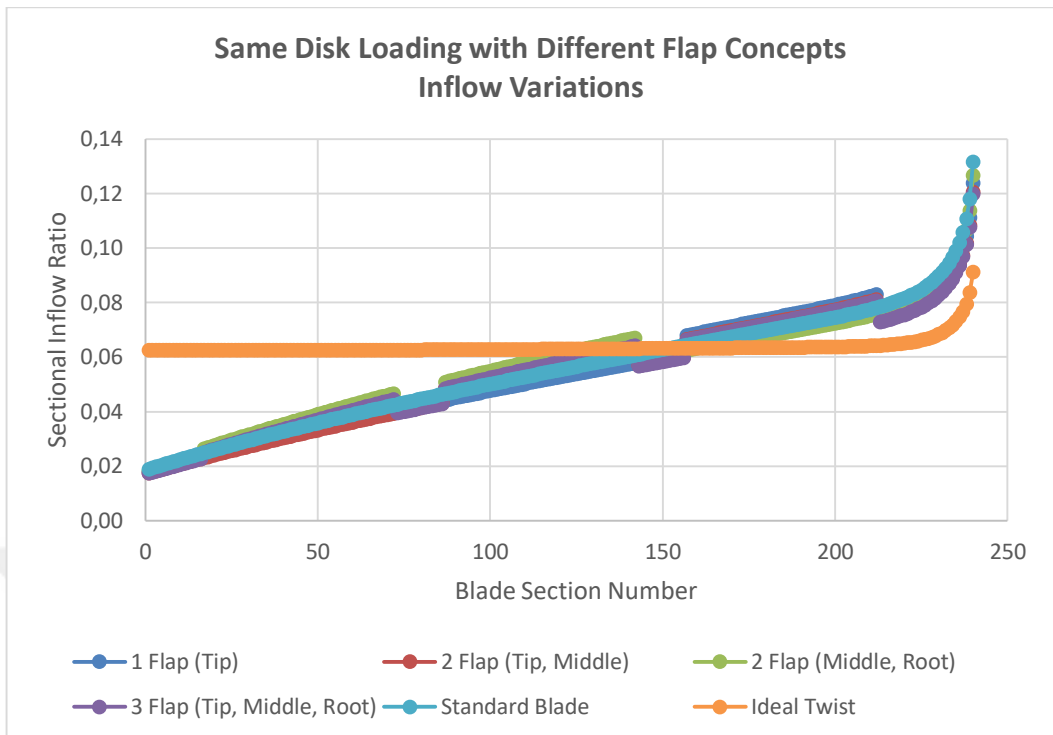


Figure 5.23 : Same Disk Loading with Different Flap Concepts Inflow Variations

In the Figure 5.23 the induced inflow ratio is shown for the same disk loading values.

5.2.2 Twisted blade performance results

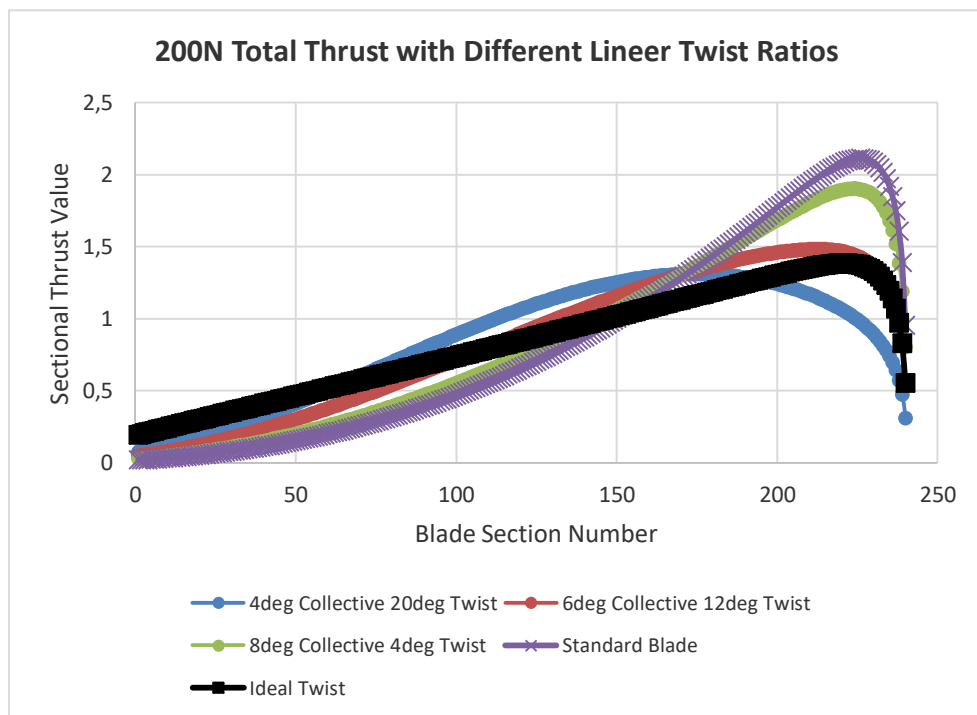


Figure 5.24 : Same Disk Loading with Different Twist Ratio

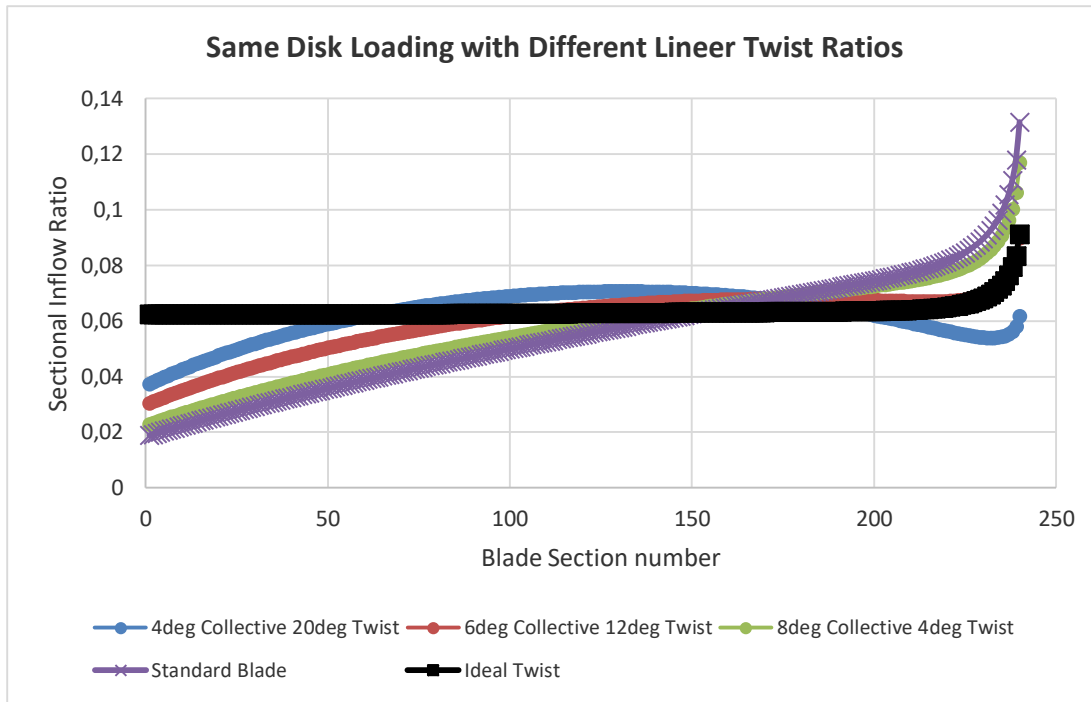


Figure 5.25 : Same Disk Loading with Different Twist Ratios Inflow Variations

In the Figure 5.24 and Figure 5.25, the sectional lift distribution and induced inflow ratio is given for the twisted blade at the same disk loading

As seen at the Table 5.16 for the same disk loading except thrust all the values differs from each other.

Table 5.16 : Same Disk Loading with Different Twist Ratios Performance Comparison

Twisted Blade Concept	Thrust	Torque	Power	Ct	Cp	FM
Standard Blade	201	12	1910,9	0,0053	0,00046	0,5957
8/4(Collective/Twist)	202,38	11,93	1874,01	0,0053	0,00045	0,6175
6/12(Collective/Twist)	201,77	11,40	1790,80	0,0053	0,00043	0,6440
4/20(Collective/Twist)	203,0	11,44	1796,71	0,0053	0,00043	0,6491
6.1(Collective) Ideal twist	201	11,0387	1734	0,0053	0,00042	0,6593

5.3 Conclusions of Aerodynamic and Performance Calculations

There are several aerodynamic and performance results that can be deduced from the graphs and tables in sections 5.1 and 5.2.

First of all let's begin with the aerodynamic results. 2 mainly different blade morphing concept are calculated. For the flapped concept, there are 6 cases with 3 flapped on the blade. All the combinations of the flaps are examined. Only tip and tip and middle flapped cases has the potential to create higher lift with the added flapped sections which is good for the operation which need more lift (Figure 5.1, 5.2, 5.10, 5.11). Moreover the sectional lift is increased at the tip section more which creates more nonlinear lift distribution. In the case of 3 flap deflected, the total lift is increased for all the blade even though the flap deflection is higher through the root.(Figure 5.16, 5.17) This case also creates the more nonlinear lift distribution over the blade. However, the sectional lift become more linear in the case of 1 flap at the root (Figure 5.7, 5.8).

Twisted blade also has number of important results in terms of aerodynamics. At the same collective the sectional lift is getting more linear with the twist ratio increment. Furthermore, this effect is more pronounced at the small collective angles. The maximum lift produced section is shifted thorough the middle section of the blade. At the lower collective angles the total lift is more effected from linear twist rate proportionally than the higher collectives (Figure 5.19, 5.20).

Second of all performance results seen in the calculations are also important because they gives a knowledge about FM rate of rotor blades. It is known form the section 3 that there is an ideal lift and induced inflow distribution for a rotor blade to operate minimum power condition. For flapped and twisted blade at the same disk loading, the performance parameter is FM value. It shown for flapped blade that for 1 flap tip, 2 flap tip, middle and 3 flapped values Fm value is smaller than standardblade which means that these flap cases makes the blade more ineffective. It is because these flap cases makes the blade sectional lift more nonlinear (Figure 5.22). However for the case of 1 flap at the root, it seems that FM value is higher than other flap cases and standard blade cases which is because the lift is higher at the root and this makes the lift more linear and makes the inflow more prone to the ideal case (Figure 5.22,5.23 and Table 5.15). For the twist results, the increment of FM values for the same disk

loading at different twist rates are more visible (Table 5.16). The ideal twist case is written to the graphs to compare the sectional twist and induced inflow ratio values. The more the thrust or inflow values are similar to this ideal case the more they are effective. This is seen if we look at the Figure 5.24, 5.25 and then compare the results with the Table 5.16. If the twist rate is increase then the blade is become more effective. There is one thing that is to know about twist calculations, all the calculations are done using lift curve slope value which means that stall calculations are not added for twisted blades. This assumption is creates some imbalance between flapped and twisted blade calculations. Because of that, we can not directly compare the twist and flapped case effectiveness with each other at the scope of this thesis. However, even if they are seen seperately they gives us numerous important insights abuot morphing balde aerodynamics and performance.

5.4 Future Work

For future work, there are some aspects to consider, those are different blade geometries, more precise aerodynamic models and interaction between aerodynamic and structural forces.

Blade geometry has 3 main variables, those are blade radius, blade cord and airfoil type. In this thesis, the calculations are conducted for only one blade geometry. However, those three variables can be changed to calculate different blade geometry effects on aerodynamics of rotor.

Blade element geometry is a basic but effective tool to see the aerodynamic effects on the blade. It uses 2-D aerodynamics to calculate every blade section and add tip loss effect. However, more adveced techniques can be used to see the real 3-D effects more accurately, like CFD methods.

Aerodynamçc forces has an effect on the blade structure and blade structure affects the aerodynamic forces. Thus, to make the calculations more realistic aeroelastic effects can be added to the computer code.

REFERENCES

- Abbot, I. H., & van Doenhoeff, A. E.** (1959). Theory of Wing sections. including airfoil data Dover Publications. *Inc., New York.*
- Anderson Jr, J. D.** (2010). *Fundamentals of aerodynamics.* Tata McGraw-Hill Education.
- Chen, P. C., & Chopra, I.** (1997). Hover Testing of Smart Rotor with Induced-Strain Actuation of Blade Twist. *AIAA Journal*, 35(1), 6-16.
- Johnson, W.** (2012). *Helicopter theory.* Courier Corporation.
- Koratkar, N. A., & Chopra, I.** (2000). Analysis and Testing of Mach-Scaled Rotor with Trailing-Edge Flaps. *AIAA Journal*, 38(7), 1113-1124.
- Krishnan, V. G.** (2017). Aerodynamic and Performance Analysis of a Morphing Helicopter Rotor System.
- Leishman, G. J.** (2006). *Principles of helicopter aerodynamics with CD extra.* Cambridge university press.
- Miller, M., Narkiewicz, J., Kania, W., & Czechyra, T.** (2006). The application of helicopter rotor blade active control systems for noise and vibration reduction and performance improvement. *Prace Instytutu Lotnictwa*, 164-180.
- Mueller, T. J. (Ed.)**. (2013). *Low Reynolds Number Aerodynamics: Proceedings of the Conference Notre Dame, Indiana, USA, 5–7 June 1989* (Vol. 54). Springer Science & Business Media.
- Rauleder, J., van der Wall, B. G., Abdelmoula, A., Komp, D., Kumar, S., Ondra, V., ... & Woods, B. K.** (2018, May). Aerodynamic performance of morphing blades and rotor systems. In *AHS International 74th Annual Forum & Technology Display, Phoenix, Arizona.*

- Ravichandran, K., Chopra, I., Wake, B. E., & Hein, B.** (2013). Trailing-edge flaps for rotor performance enhancement and vibration reduction. *Journal of the American Helicopter Society*, 58(2), 1-13.
- Spencer, B. T., & Chopra, I.** (1996, May). Design and testing of a helicopter trailing edge flap with piezoelectric stack actuators. In *Smart Structures and Materials 1996: Smart Structures and Integrated Systems* (Vol. 2717, pp. 120-131). International Society for Optics and Photonics.
- Walz, C., & Chopra, I.** (1994). Design and testing of a helicopter rotor model with smart trailing edge flaps. In *Adaptive Structures Forum* (p. 1767).
- Weisshaar, T. A.** (2013). Morphing aircraft systems: historical perspectives and future challenges. *Journal of Aircraft*, 50(2), 337-353.
- Wilbur, M. L., Mistry, M. P., Lorber, P. F., Blackwell Jr, R., Barbarino, S., Lawrence, T. H., & Arnold, U. T.** (2018). Rotary Wings Morphing Technologies: State of the Art and Perspectives. In *Morphing Wing Technologies* (pp. 759-797). Butterworth-Heinemann.

CURRICULUM VITAE



Name Surname : Hüseyin Ural
Place and Date of Birth : Selçuk/ İzmir 01/09/1993
E-Mail : uralhuseyin@outlook.com

EDUCATION

- **B.Sc.** : 2016, Istanbul Technical University, Aeronautical and Aerospace Engineering Faculty, Aeronautical and Aerospace Engineering Department
- **M.Sc.** : 2019, Istanbul Technical University, Aeronautical and Aerospace Engineering Faculty, Aeronautical and Aerospace Engineering Department

PROFESSIONAL EXPERIENCE AND REWARDS:

PUBLICATIONS, PRESENTATIONS AND PATENTS ON THE THESIS:

OTHER PUBLICATIONS, PRESENTATIONS AND PATENTS: